IMPROVEMENT OF THE ENVIRONMENTAL AND ECONOMIC CHARACTERISTICS OF COOLING TOWERS

THE PERIODIC COOLING TOWER - SMALL SCALE, FULL SCALE, AND SURFACE ROUGHENING TESTS

by

Pou Cheong Hon
Je-Chin Han
Paul F. Pilger
David A. Fink
Bruce R. Andeen
Leon R. Glicksman
Warren M. Rohsenow

Energy Laboratory
in association with
Heat Transfer Laboratory
Department of Mechanical Engineering
MASSACHUSETTS INSTITUTE OF TECHNOLOGY

Sponsored by:
Empire State Electric Energy Research Corporation
New York

Energy Lab Report No. MIT-EL 75-018
Heat Transfer Lab Report No. 80047-95
June 30, 1975

ABSTRACT

This report describes research for the past year on methods to enhance the environmental and economic performance of dry cooling towers.

The work has concentrated on dry cooling towers utilizing periodic water to air heat exchangers. Periodic towers have sheet metal discs partially submerged in hot, power plant condenser effluent. As the discs rotate, the discs alternately absorb heat from the effluent and discharge heat to the air. The means of heat transfer on the air side can be either evaporative and/or convective, depending upon the amount of effluent carried into the air side on the surface of the plates. An oil layer, floated on the water's surface, has been shown to be effective in eliminating water carry-over to the air side.

The advantages of the periodic tower lie in the low cost of the discs and the ability to operate dry . A periodic tower should be significantly less expensive than a conventional dry tower fabricated with finned tubes. Further, since the periodic tower can also operate wet, by removing the oil film, the high capacity losses incurred during warm months by conventional dry towers can be eliminated.

In the past year, tests on a 20 inch model of the periodic tower indicated that at operational speeds of the full sized disc, no noticeable churning of the oil layer ocurred. Heat transfer rates measured with the 20 inch model were 20 percent higher than predicted by an approximate analysis. Finally, silicone oils' low vapor pressure make them superior to hydrocarbon oils on the basis of evaporation rates, but their higher costs and possible ecological impact necessitates a closer look at hydrocarbon oils.

Construction of the full scale test facility is complete. Shaped, rigid five foot diameter discs have been designed, fabricated, and assembled into an initial test module. Instrumentation for heat transfer tests is also complete; including instrumentation for measuring disc temperatures, and both air and water flow rates and temperatures. A parametric study of the oil film

thickness on the air side of the test module has been completed. Measured thicknesses were 20 percent less than that previously predicted. This thinner oil layer means an increase in the disc heat transfer.

A test apparatus to study the further enhancement of disc performance by surface roughening has been constructed, instrumented and calibrated. The apparatus has reproduced experimental friction factor and heat transfer coefficient curves for flat plates, and will be used to evaluate enhancement as a function of rib shape, size, spacings and Reynold's number.

Visits to several architectural engineers across the country were made with representatives of Air Preheater Company to gage their acceptance of the rotary concept. All felt that if the reliability of the rotary concept could be demonstrated and the costs were less than equivalent conventional dry towers, the rotary desing would be the preferred choice. Based on these findings, Air Preheater is planning to do design and cost studies of the rotary concept for the coming year.

ACKNOWLEDGEMENTS

This study was sponsored by the Empire State Electric Energy Research Corporation (ESEERCO). Their support is gratefully acknowledged.

Special thanks are due Paul Torpey, Art Sugden, Howard Philipp, and other members of the ESEERCO technical committee. Their active interest and suggestions were an asset to the program.

Table of Contents

LIST OF FIGURES

NOMENCLATURE

A	Area
C_{ao}	Concentration of oil in air near oil surface
C_{a*}	Concentration of oil in ambient air
C_p	Specific heat
D	Spacing between discs
D	Tube diameter
De	Hydraulic diameter
d'	Diffusivity of mass transfer
e	Rib height
F	Shear force
f	Friction factor
g	Gravitational constant
H	Maximum vertical height of flow channel
h	Heat transfer coefficient
h_d	Mass transfer coefficient
k	Thermal conductivity
L	Length
ℓ	Wiper length
M	Molecular weight
m	Mass
$\dot{m}$	Flow rate
$\hat{n}$	Unit normal vector
P	Space between ribs
P	Pressure

Pr	Prandtl number
P_v	Vapor pressure
Q	Volume flow
Q_T	Total volume flow on one side of disc
q	Heat transfer
$\dot{q}$	Rate of heat transfer
R	Gas constant
Re	Reynold's number
R_f	Heat transfer resistance
r	Radius
St	Stanton number
T	Temperature
t	Time
t_p	Plate (disc) thickness
V	Velocity
V_a	Molecular volume of air
V_b	Molecular volume of compound b
V_D	Velocity of any point on disc
$\overline{V}_o$	Average oil velocity relative to ground
$\overline{V}_r$	Average oil velocity relative to disc
v_o	Plate velocity in vertical direction
$\overline{v}_n$	Component of $\overline{V}_o$ normal to pickup
v_y	Oil velocity down flat plate
$\overline{v}_y$	Average oil velocity down flat plate relative to ground
y	Radial distance from tube wall

Greek Symbols:

α	Flow angle of attack
δ	Oil film thickness
δ	Boundary layer thickness
ε	Heat exchanger effectiveness
θ	Angle of rotation
μ	Absolute viscosity
ν	Kinetmatic viscosity
ρ	Density
σ	Surface tension
τ_o	Shear stress at wall
ω	Angular velocity

Subscripts:

a	Air
B	Buffer layer
b	Compound 'b'
f	Fluid, water
f	Fully developed
i	Initial
L	Laminar sublayer
m	Mean
o	Final
p	Plate, disc
t	Total
w	Water

x	In the horizontal direction
y	In the vertical direction
1	Inlet
2	Outlet

Superscripts:

-	Average

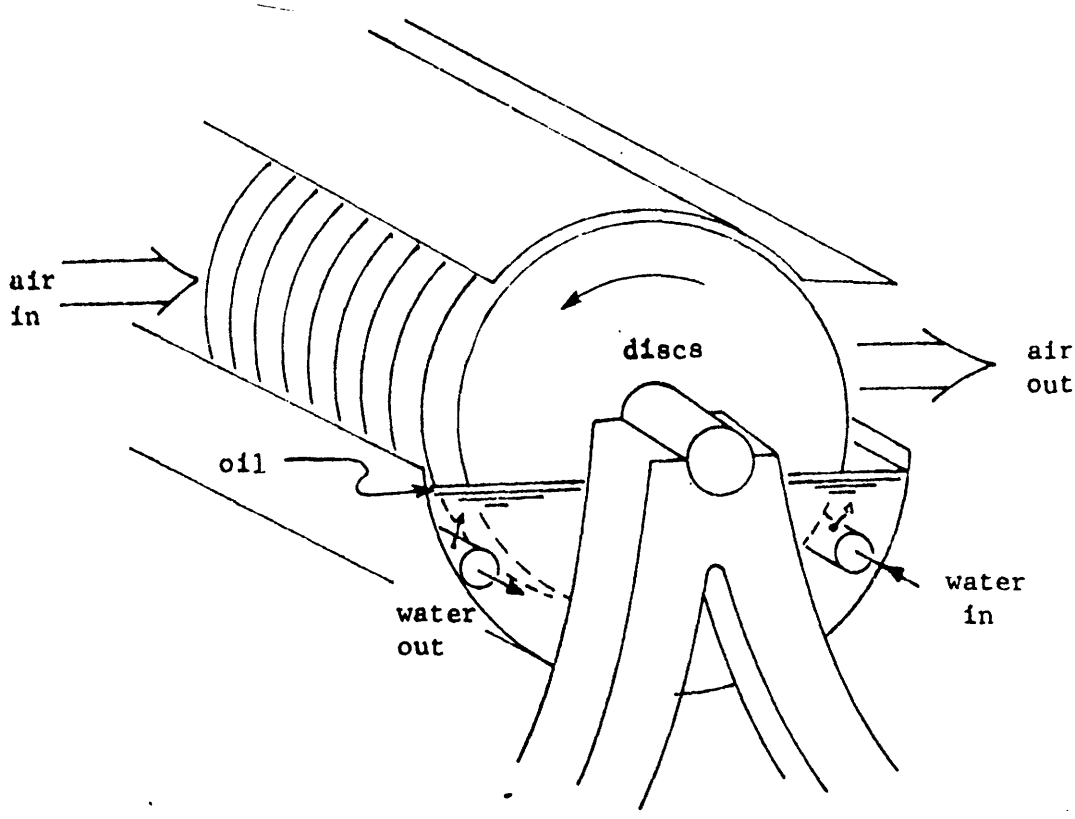

Conceptual design of periodic heat exchanger

Figure 1

I. INTRODUCTION

This report summarizes the results of the 3rd year of investigation on the improvement of the environmental and economic characteristics of cooling towers.

Steam-turbine electric power plants operate with a thermal efficiency of about 40%. Thus for every 4 units of energy generated as electricity, 6 units of energy have to be rejected as waste heat. In the past, this waste heat was rejected to the environment by circulating large quantity of water to cool the condenser. The water after cooling the condenser is simply discarded. This is the so-called once-through cooling system. An electric power plant with a once-through cooling system has to be located near a river or a lake where a large quantity of water is available.

There are occasions when an electric power plant has to be built in a location where the water supply is not abundant, or the protection of the ecology of water bodies such as rivers and lakes from thermal pollution prevents the use of the once-through cooling system. Evaporative cooling can sometimes provide a cheap alternative to once-through cooling. However, evaporative cooling also has its drawbacks. In evaporative cooling, the tower circulating water is heated up as it cools the condenser. This hot circulating water is cooled by splashing it down through a wet cooling tower. The water evaporated to the air in the process carries with it the waste heat to the atmosphere. The cooled water collected at the basin of the wet cooling tower is then circulated back to cool the condenser again. Usually about 1.5% of the circulating water in the wet cooling tower is lost to the atmosphere in the form of water vapor, and drift adds another 0.2% loss [1]. Evaporative cooling makes a significant improvement towards reducing the requirement of water supply. However, for a large electric power plant, the consumption of 1.7% of the circulating water is still a significant amount.*

Let us consider as an example of an electric power plant of, say 1000 megawatts. Assuming the most efficient heat transfer performance now in practice, it requires 0.38 GPM of circulating water to generate 1 kilowatt of electricity [2]. For an electric power plant of 1000 megawatts, the amount

*The rate of water loss is approximately equal to the water flow rate through the boiler.

of water lost to the atmosphere in evaporative cooling can be as much as 9.3 million gallons per day. Apart from the problem of getting an adequate water supply, of more significance is the possible detrimental effects on the environment by the rejection of such a large quantity of water vapor to the atmosphere. With cold ambient air and a high relative humidity, the water vapor rejected by the wet cooling tower may form a fog plume. The fog plume, besides being aesthetically unpleasing, may also impair the visibility on highways and in airports.

A dry cooling tower can handle the waste heat rejection without any one of the aforementioned problems. But unfortunately, in many circumstances the dry cooling tower costs three or four times more than a conventional wet cooling tower [3]. This high cost of dry cooling is a direct result of the relatively poor heat transport properties of air. Rejecting a given heat rate to air rather than water requires more surface area, and dry surface costs more per unit area than wet fill does. To minimize the cost of a dry tower, one must find a surface with a low ratio of cost to performance and optimize the interaction of the cooling tower with the power plant. One surface which has such a low ratio is the periodic cooling tower developed during this program.

I.1. The Periodic Concept

The periodic cooling tower consists of a number of properly spaced steel discs which are mounted on a rotating shaft. The lower half of the discs is immersed in a trough of hot water. On the upper half of the discs, air is drawn through the spacings between the discs. Therefore as the discs rotate, heat is transferred from the hot water in the trough to the air by means of the periodic convective cooling and heating of the steel discs on the air side and on the water side respectively. The water after cooling the condenser is circulated through the trough. Hot water enters the trough at an inlet and, after being cooled by the rotating discs, it leaves the trough through an outlet. On top of the hot water in the trough floats a thin layer of oil. The oil, by covering the water in the trough and by coating the rotating discs, has the function of eliminating any water evaporation. The cooled water leaving the trough is circulated to cool the condenser again. Figure [1] shows a conceptual design of the periodic cooling tower.

The periodic cooling tower has the following advantages:

1. The cooling system of the periodic cooling tower is a closed system. It has a very low water consumption rate and hence it does not require a continuous supply of a large quantity of water.
2. The periodic cooling tower has no detrimental effects on the environment because there is no rejection of hot water into the rivers or lakes.
3. The periodic cooling tower has the advantages of a dry cooling tower. But the cost of construction of a periodic cooling tower should be much cheaper than that of a conventional dry cooling tower of finned-surface with the same heat transfer performance.

I.2 Brief Summary of the First Two Years of Study

During the first year of study on the periodic tower, the initial assessment of the concept was made. A model with 12 inch discs rotating through heated, but stagnant, water was constructed and tested. Its performance was within 10% of theoretical predictions. A slow leak through the shaft support bearings prevented an accurate assessment of the model's ability to operate totally dry. However, ignoring the leak and assuming all water losses were due to evaporation, less than .4% of the heat load was borne by evaporation. This compares to a figure of about 80% for conventional wet towers.

The oil used for the separation of water and air in these tests was a parafinic hydrocarbon oil, but initial calculations based upon projected operating temperatures, surface areas, and available information on vapor pressures indicated that hydrocarbons would have a significant depletion due to evaporation. It was therefore recommended that silicon oils be used to reduce evaporation losses of the oil.

An economic optimization was also performed on the periodic tower during the first year. Results indicated that with five foot diameter discs the periodic tower held a significant cost advantage over dry towers using conventional finned surfaces.

During the second year, work progressed on three fronts:

1. Scale model tests. A larger scale, 20" model was constructed. This model included a water circulation system to study circulation patterns in the disc trough and determine the most desireable locations of water input and drain ports in the trough. Further, the 20 inch model was used to show that the churning effect of the discs on a layer of silicone oils was well within acceptable limits for the proposed 5 foot full sized disc.
2. Surface roughening. The greatest resistance to heat transfer is on the air side of the discs. A means of decreasing this resistance (and thereby increasing the disc performance) by roughening the surface with ribs was analytically examined. Using existing correlations

for the surface roughening effect and a modification of the optimization program, a parametric study of characteristic rib dimensions was performed. Results indicated that under optimum conditions, the resistance to heat transfer is 20% less than that of a smooth plate.

3. Full scale test facility. Construction was begun on a test facility large enough to test a one foot module of the full sized 5 foot discs. The test facility required the design and construction of: a contraction cone to deliver air with a uniform velocity profile to the test section, a test section to contain the discs and both air and water systems, a fan to drive air through the test section, and a hot water supply system to simulate hot power plant effulent.

For more details regarding the first two years of study, see references 4 and 5.

1.3 Areas of Study Covered in Third Year.

This report is on the third year of study, which was again centered in three main efforts:

1. Small scale testing. The 20 inch model was employed to make heat transfer tests, and further study on oil churning caused by various disc designs.
2. Full scale testing. The full scale test facility was completed, and fully instrumented. A module of 5 foot discs was constructed and tests run on it to determine the thickness of the oil layer on the discs.
3. Disc performance enhancement by surface roughening with ribs. Previous correlations on heat transfer augmentation by use of ribs are based upon high Reynolds' number flows and square rib profiles. Under actual operating conditions, the rib shape will be altered by the presence of an oil film, and will experience lower Reynolds' number flows. A test facility has been built and calibrated to evaluate the effect of rib shape in Reynolds' numbers representative of the periodic tower.

The following sections describe in detail the investigation of the prior year.

II. PERIODIC COOLING TOWER

II.1 Small Scale Testing.

A model of the periodic cooling tower was constructed. The objective of this project was two-fold:

1. To test the heat transfer performance of the periodic cooling tower and to experiment with various means to improve its heat transfer performance.
2. To locate any problems in the implementation of the periodic cooling tower and subsequently to find solutions for these problems. Some of the key problems investigated included the flow patterns of water circulating through the trough of the periodic cooling tower, the churning of the oil layer by the rotating discs, and the heat transfer resistance of the oil film that coats the rotating discs.

Part of the small scale testing was discussed in last year's annual report. Those sections include the description of the rotary plates system, the circulating water and air flow systems, and the results of the flow visualization tests ascertaining the dependence of water circulation on the location of water inlet and outlet ports.

Briefly summerizing those sections, the model was fabricated out of 15 20 inch discs spaced 1/3 inch apart. Proper spacing was assured by using spacers placed at four locations near the perifery of the discs. Fourteen of the discs were made of 40 mil galvanized steel, and one outer disc was made of 66 mil plexiglas. The plexiglas disc facilitated the viewing of the fluid flow between the discs. The shaft on which the discs were mounted was driven by a variable speed/reversible motor.

The water circulation system included a controlable immersion heater, and the water flow could be controlled and measured.

The air delivery system was comprised of an inlet channel, including a flow straightening section, a shroud to prevent most of the air from passing through the top of the plates, and an exhaust fan. Local air velocities were

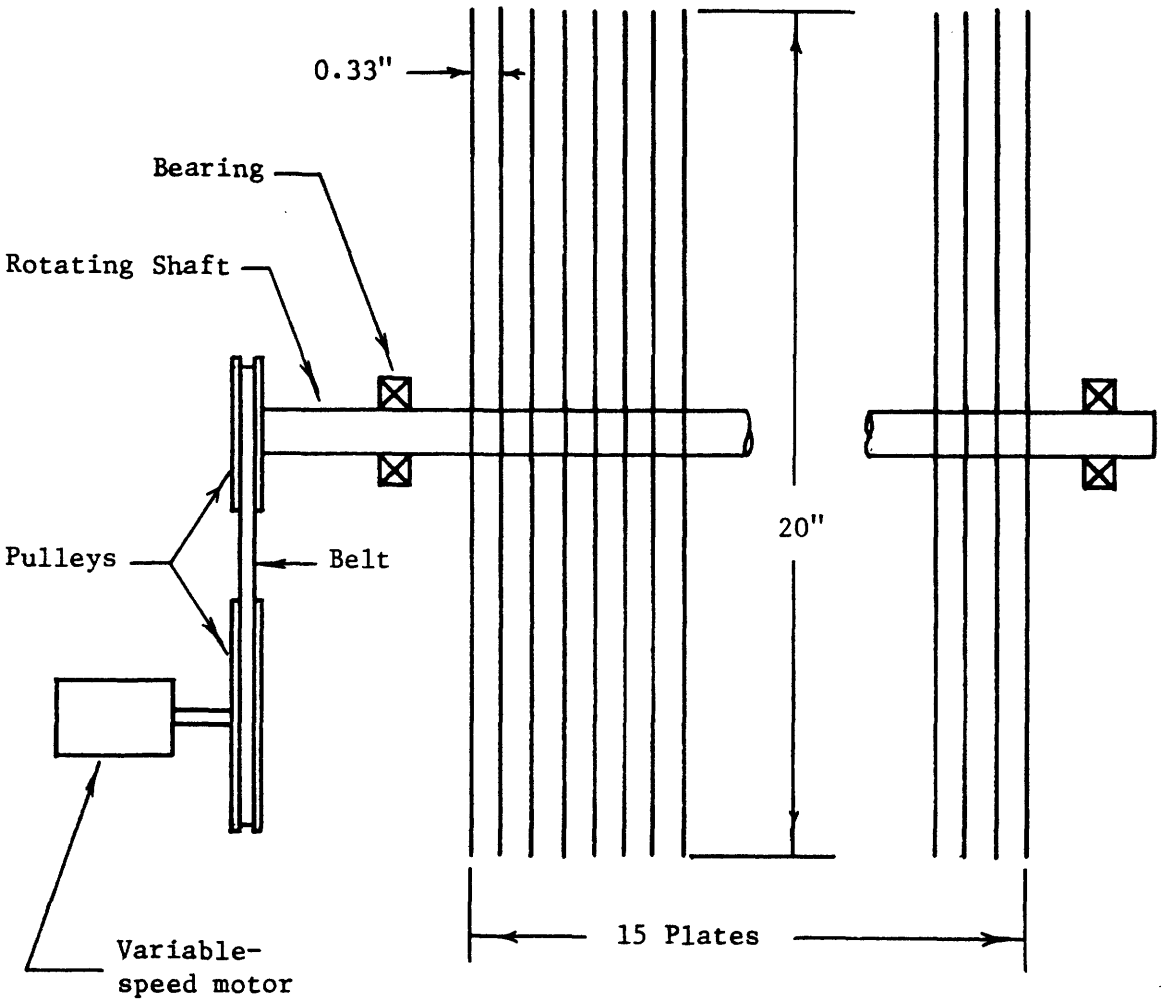

Rotary Heat Exchanger Model Schema

Figure 2

measured by a traversing pitot tube. Figures 2, 3, and 4 are schematics of the 20 inch model.

The flow visualization tests showed that the flow in the water trough was dominated by the disc rotation. Inlet and outlet ports should be located such that the flow conditions accomplish the following two objectives: (1) the plates should make contact with the hottest water just before entering the air stream so that they are heated to the highest possible temperature, (2) the residence time of the water must be sufficiently long for adequate water cooling.

Two port locations tested by dye injection and found acceptable are illustrated in figures 5 and 6. In both cases,the plates rotate in a direction counter to the water jet. In figure 5, the ports are located 3" below the water level, while in figure 6 they are 6 3/4" below the water level. The location of the jets in figure 6 allows the fluid to enter more into the central circular path than in figure 5, becoming more dispersed and covering a larger area of the plates. However, a portion of the hot water entering the trough travels only half of the plate diameter to get to the outlet. Further, the discs leave the water immediately after being exposed to the hottest water, but due to the dispersed nature of the water, the temperature may not be as high as in figure 5. Visual observations cannot ascertain the superiority of figure 5 or figure 6. The final results must be determined by actual heat transfer tests.

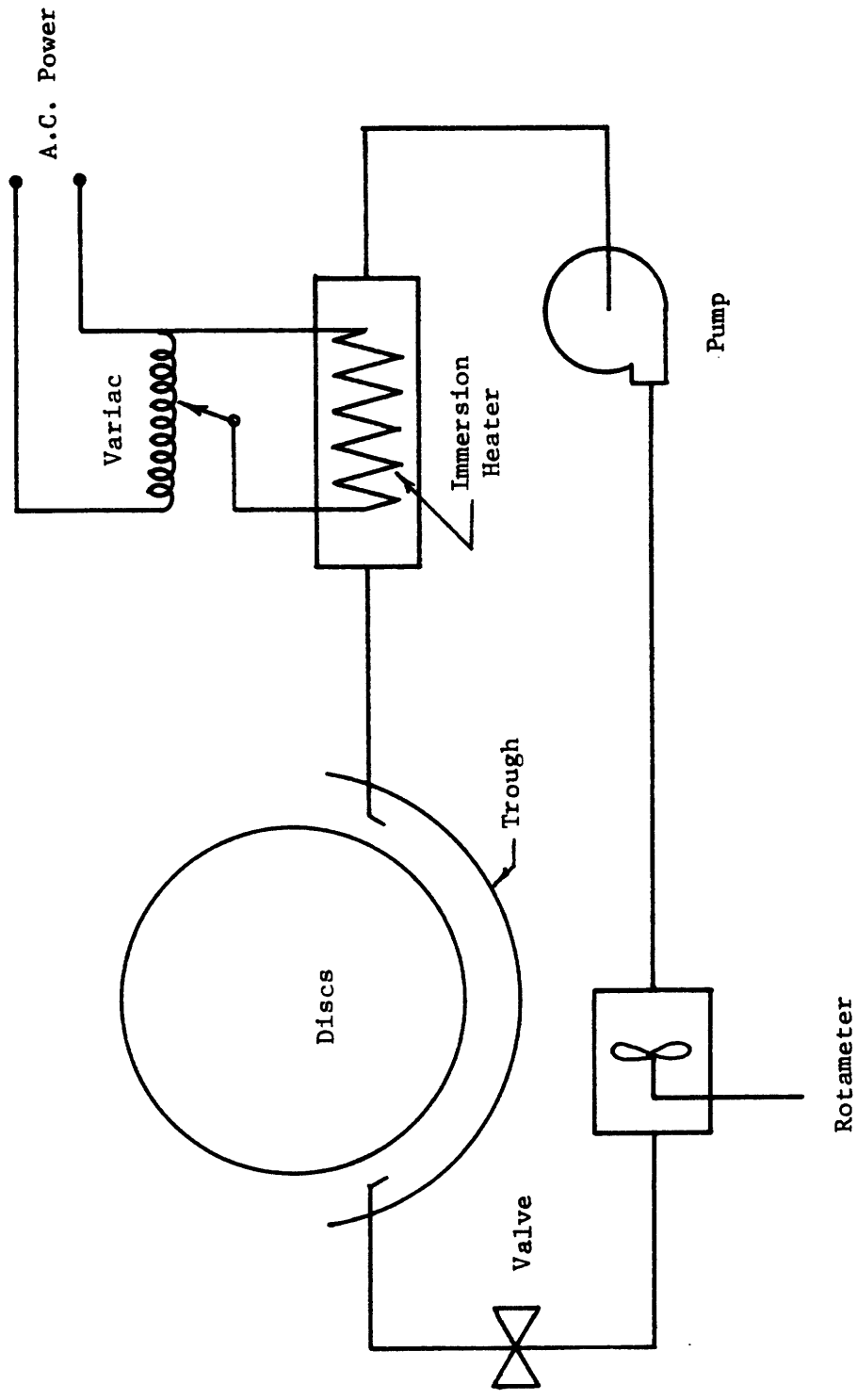

Fluid Circuit Schema

Figure 3

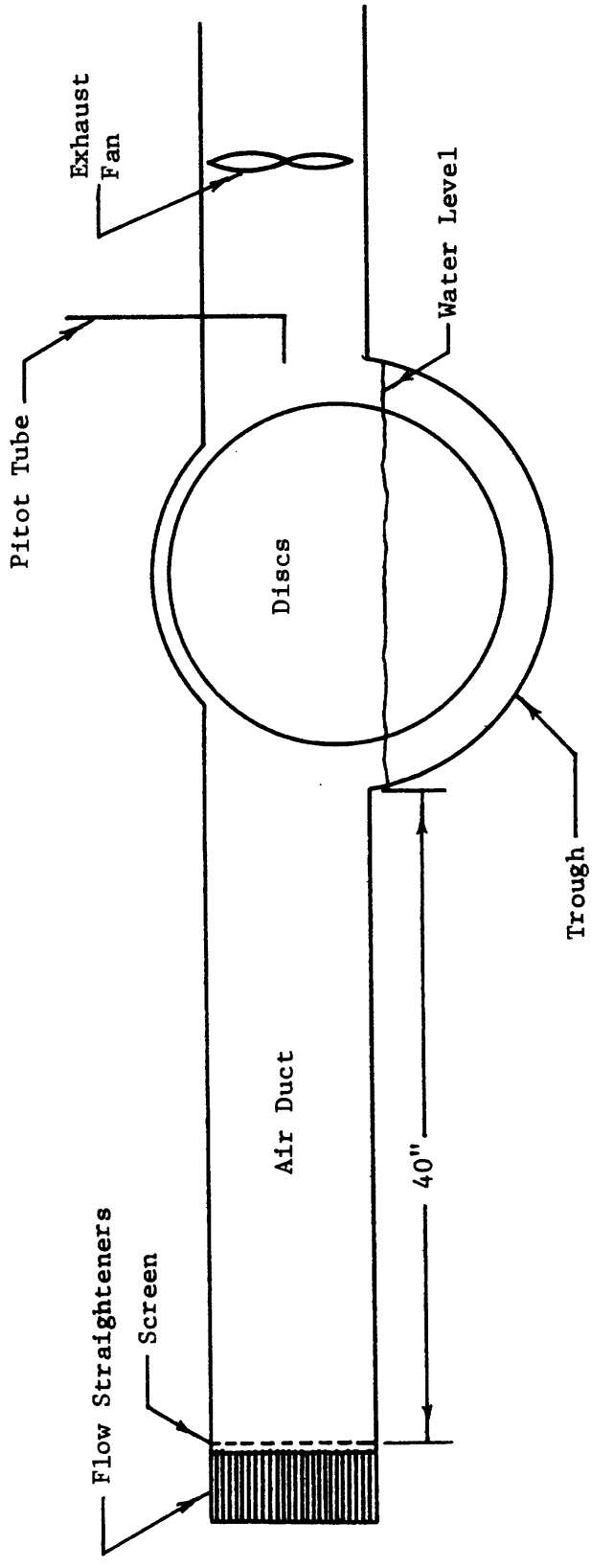

Air Duct - Disc Design

Figure 4

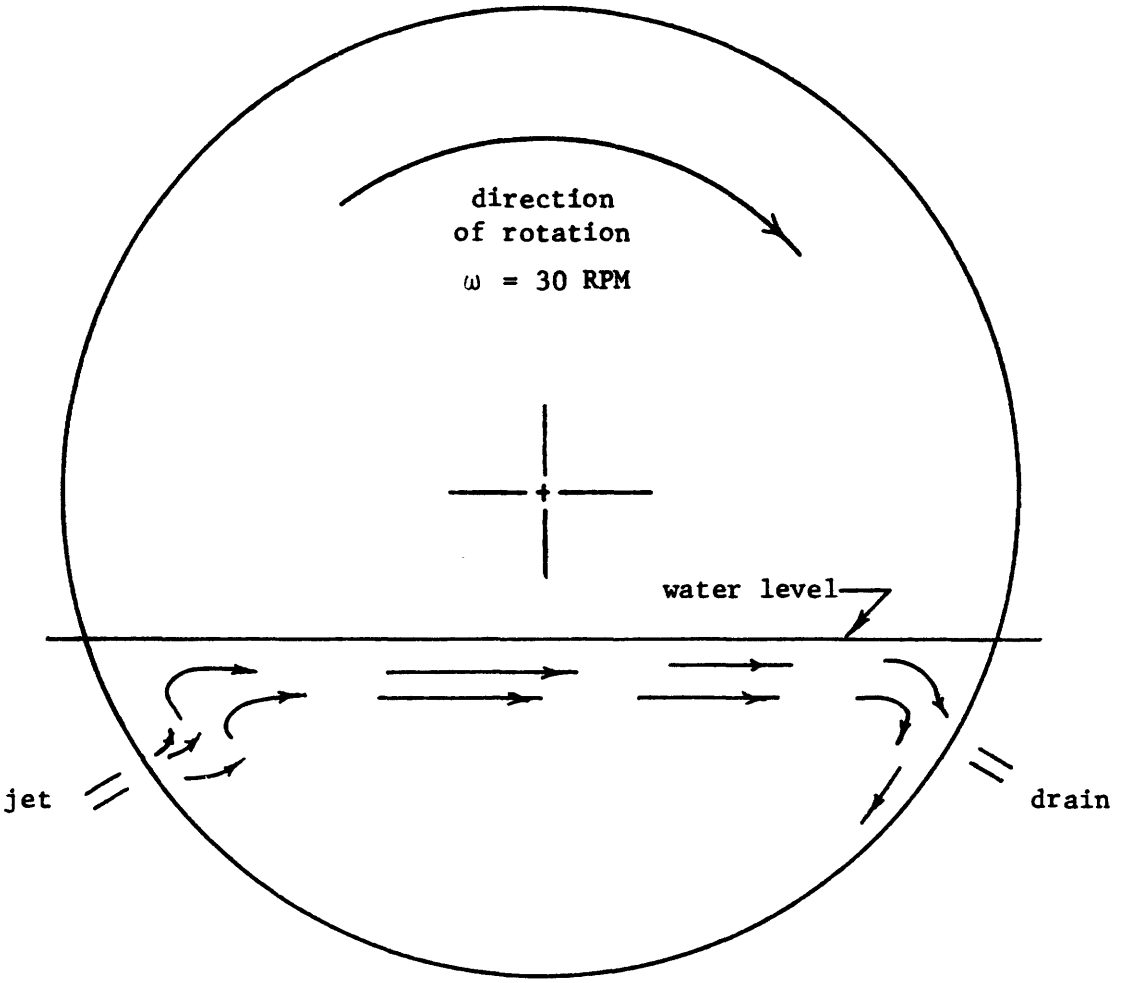

FLOW PATTERN WITH WATER CIRCULATION THROUGH THE TROUGH
Counter flow - with jet 3 inches below water level

Figure 5

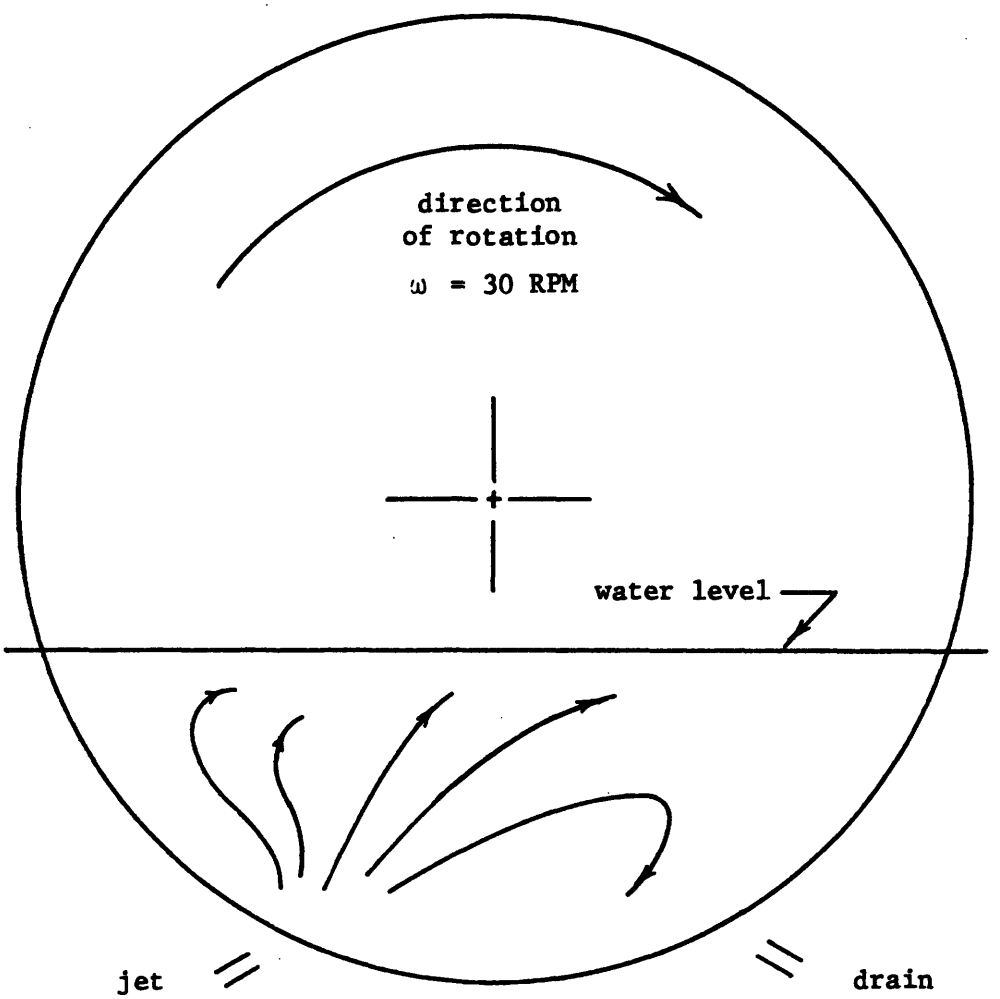

FLOW PATTERN WITH WATER CIRCULATION THROUGH THE TROUGH
Counter flow - with jet 6 3/4 inches below water level

Figure 6

II.1.1 Small Scale Periodic Cooling Tower Tests

The performance of a periodic cooling tower is determined by two factors:

1. Its ability to eliminate any water evaporation.
2. Its heat transfer effectiveness.

These two factors will be discussed in detail in the following sections.

It has been mentioned that a layer of oil floats on top of the hot water contained in the trough. As the discs rotate either into the air side or into the water side,they cut across the oil layer. Because the oil preferentially wets the metal with respect to water, the rotating discs are always coated with an oil film so that no water is exposed to the air stream. This eliminates any water evaporation. For this scheme to work successfully, the kind of oil must meet certain criteria. The choice of oil must take into account the following considerations:

1. The specific gravity of the oil.
2. The evaporation rate of the oil under the operating conditions of the periodic cooling tower.
3. The heat transfer resistance of the oil film that coats the rotating discs.

The heat transfer effectiveness of the periodic cooling tower depends on many factors, namely:

1. The air velocity.
2. The thickness of the oil film that coats the disc surface.
3. The air temperature.
4. The rotational speed of the discs.
5. The temperature profile of the hot water in the trough.

Of the five factors mentioned above, the effects on heat transfer of the first two factors are known. The effect on heat transfer of the air velocity can be determined by existing experimental correlations. The thickness of the oil film coating the rotating discs, and hence its heat transfer resistance, can also be estimated by existing correlations. The third factor, the air temperature, is fixed by the environment and is not a variable that we can control. The fourth factor, the rotational speed of the discs, is limited by a consider-

ation of oil churning. However, no information can be found in the literature to give the temperature profile of the water in the trough of the periodic cooling tower. This fifth factor was investigated experimentally.

II.1.1.1 Selection of Oil

In the periodic cooling tower it is necessary to cover the water contained in the trough with a layer of oil to eliminate any water evaporation. There are four criteria in the selection of the oil:

1. As the oil must float on the water, the oil must have a specific gravity less than one.
2. The oil, like water, when exposed to the forced convection of an air stream, undergoes a mass transfer of oil to the air stream. If the oil has a high mass transfer rate, the environmental questions raised by the rejection of a quantity of oil vapor into the atmosphere may well exceed the possible environmental drawbacks of a wet cooling tower. Besides, the high cost of continuously replacing a large quantity of oil lost by evaporation may well render the periodic cooling tower economically impractical. Therefore, a negligible evaporation rate of the oil under the operating conditions of the periodic cooling tower is essential.
3. The oil film coating the rotating discs adds an additional resistance to heat transfer. This added heat transfer resistance is directly proportional to the oil film thickness. The oil film thickness is directly proportional to the square root of the oil viscosity (6). An oil with a very low viscosity, therefore, would give a very thin oil film with a very small heat transfer resistance.
4. As it is desireable to avoid oil and water mixing, it is preferred to have an oil with a low specific gravity so that the time for seperation by settling is small, and/or an oil that is highly immissible with water and does not form a stable emulsion with water.

II.1.1.1.1 Oil Evaporation

The evaporation rate of an oil surface exposed to a turbulent stream of air can be estimated with existing experimental correlations. These correlations can be found in standard textbooks on mass transfer. The equations used in this section can be found in reference [7].

Mass evaporation rate per unit area is given by

$$\dot{m}/A = h_d(C_{ao} - C_{a*}) \qquad [1]$$

Assuming that the oil concentration at infinity in the atmosphere is zero, $C_{a*} = 0$. The oil concentration at the oil surface is related to its vapor pressure and temperature by the ideal gas equation:

$$C_{ao} = \frac{P_v}{RT} \qquad [2]$$

The mass transfer coefficient h_d is given by the Gilliland correlation:

$$h_d = 0.023 \frac{d'}{2D} \left(\frac{2DV}{\nu}\right)^{.83} \left(\frac{\mu}{\rho d'}\right)^{.44} \qquad [3]$$

where the diffusivity d' is given by another Gilliland correlation:

$$d' = 0.0069 \frac{T^{1.5}}{P\,(V_a^{.33} + V_b^{.33})^2} \left[\frac{1}{M_a} + \frac{1}{M_b}\right]^{1/2} \qquad [4]$$

Equations [1] to [4] indicate an oil with a very low vapor pressure has a very low evaporation rate. Silicone oils are well-known for their low vapor pressures and neglibible evaporation rate. The vapor pressure of high molecular weight silicone oils as measured by Mennicken [8] is shown in Table 1.

TABLE 1

Temperature, ^{o}C	Vapor pressure (torr)
140	1×10^{-5}
170	1×10^{-4}
200	8×10^{-4}

When the above data is extrapolated to 135 degrees F, the operating temperature of the silicone oil in the periodic cooling tower, the vapor pressure is approximately 10^{-8} torr. With a vapor pressure of 10^{-8} torr, an estimate of the oil evaporation rate by Equations [1] to [4] for a 1000 megawatts power plant shows an insignificant value of less than 2 lbm/hr. It thus shows the silicone oils can satisfy the neglibible evaporation requirement. However, the cost of silicon oils are significantly greater than hydrocarbon oils. It may be necessary or desirable to accept a higher make-up rate (200-250 lbm/hr) and operate with a less expensive hydrocarbon oil.

Table 2 lists 4 silicone oils which can satisfy the negligible evaporation requirement. These silicone oils are manufactured by the General Electric Company and have relatively low viscosities. All four of these silicone oils have specific gravity less than one.

TABLE 2

Commercial names	Nominal viscosity centistokes at 25 C	Specific gravity at 25 C
SF-96	20	0.953
SF-1147	50	0.890
SF-96*	50	0.963
SF-81	50	0.972

* SF-96 is available in several viscosities.

II.1.1.1.2 Oil Film Thickness

Equations for estimating the thickness of the liquid film adhering to a flat plate that is being drawn from the liquid were formulated by Levich [6]. The equations are reproduced here:

$$\delta = \left(\frac{\mu V}{\rho g}\right)^{.5} \quad f\left(\frac{\mu V}{\sigma}\right) \qquad [5]$$

where $f\left(\frac{\mu V}{\sigma}\right) = 0.93 \left(\frac{\mu V}{\sigma}\right)^{\frac{1}{6}}$ for $\frac{\mu V}{\sigma} < 1$

$f\left(\frac{\mu V}{\sigma}\right) = 1$ for $\frac{\mu V}{\sigma} \gg 1$

Equation [5] was formulated by Levich for the following conditions:

1. A clean flat plate was pulled away vertically from a liquid with a constant velocity V.
2. Assuming the thickness of the liquid film on the plate surface reaches a constant value as the plate recedes to infinity from the liquid surface, the analytic formulation yields this thickness(δ) at infinity as given by Equation [5]. It is clear that the thickness δ is the minimum liquid film thickness over the entire plate.

In a periodic cooling tower, the lower half of the rotating discs is immersed in a trough of water which is covered with a layer of oil. Every time a disc cuts across the oil layer either when it rotates into the air side or into the water side, it picks up a certain amount of oil. But the thickness of this oil film coating the rotating discs cannot be accurately estimated by simply applying Equation [5] because of the following two reasons:

1. The region of the disc near its center never moves far away from the surface of the oil layer and hence it might not satisfy the condition of attaining a limiting constant value for the oil film thickness. The oil film in the region near the disc center might therefore be thicker than that would be indicated by Equation [5].

2. It was observed in the experiments that when a disc rotated into the air side, the disc edge and a small region around it brought up a much thicker film of oil than other parts of the disc. As the disc rotated further, this thick oil film sticking around the disc edge began to fall down due to gravity, covering the whole disc surface that was exposed to the air side. It thus appeared the amount of oil brought up by the disc edge and the small region around it contributed significantly to the oil film thickness of the entire disc if the disc is small. However, for a very big disc, this disc edge effect on the overall oil film thickness of the entire disc might be minimal. Observations of oil film thickness on the water side were hard to make, but it is expected that phenomena similar to the air side exist on the water side. The only difference is that instead of gravity pulling down the oil film on the air side, there was a buoyancy force pulling up the oil film on the water side.

It thus appears that to evaluate the oil film thickness on the rotating discs with Equation [5] would result an underestimation of the true oil film thickness. However, in view of lacking a better formulation of this complicated problem, prior to the oil thickness measurements, a conservative estimate is that the oil film thickness on the rotating discs is two times the δ in Equation [5] for discs with a radius of 10 inches. The heat transfer resistance of the oil film is then given by:

$$R_{oil} = \frac{\text{Oil film thickness}}{\text{Oil Conductivity}} = \frac{2\delta}{k} \qquad [6]$$

Actual measurements of oil film thickness were made on the full sized five foot diameter discs after the small scale tests and are discussed in Section II.2.2.

II.1.1.1.3 Oil Churning

A high rotational speed of the discs has the advantage of allowing thinner discs to be used, but it also has the disadvantage of increasing the thickness of the oil film coating the rotating discs and thereby increasing the heat transfer resistance. Besides, when the discs rotate with a very high speed, they churn the oil layer into the water so much that they can cause a thorough mixing of the oil with the water. The mixing of oil with water is unacceptable because of the following four reasons:

1. Besides the amount of oil that coats the discs and covers the water in the trough, additional amounts of oil get mixed with the water. This adds to the capital costs of the periodic cooling tower.
2. Some water will be exposed to the air stream and carried off by the air stream into the atmosphere.
3. When the circulating water cooling the condenser gets mixed with oil, the condenser might be coated with an oil film that reduces the heat transfer.
4. With the presence of oil in the condenser, the possibility exists for oil to pass through leaks in the condenser and enter the boiler feed water loop.

Tests were run with the small model to study the churning of the oil by the rotating discs. In one test, 15 discs of diameter 20 inches, spaced 0.33 inch apart, were assembled on a steel shaft. The discs were made of 0.040 inch thick galvanized steel with a smooth surface. The discs were immersed to three inches below their centers in a trough of water. On top of the water in the trough floated a layer of silicone oil which was about 1/2 inch thick. There was no water circulation through the trough. The rotational speed of the discs was gradually increased. With rotational speeds less than 15 RPM, no distinct oil globules were observed being brought down below the oil layer by the rotating discs. As the rotational speed was increased beyond 15 RPM, more oil globules were observed to be brought down into the water. Some of these oil globules stuck to the rotating discs and were brought back to the oil layer when the discs rotated into the air side. Some of these oil glob-

ules moved up quickly back into the oil layer by the buoyancy force. No thorough mixing of oil with water was observed for rotational speed up to 20 rpm. At 20 rpm, the oil still stayed as a separate layer on top of the water, but with many oil globules moving up and down just beneath the oil layer. At this high rotational speed, it was observed that more oil churning occurred on the side where the discs left the water. On the other side where the discs rotated into the water, less oil agitation was observed. This phenomenon was understandable. The oil globules generated by the discs rotation, following the direction of the disc circumferential velocity, tend to accumulate on the one side where the discs left the water, giving the appearance of more severe oil agitation on that side.

Those observations described above indicate the model periodic cooling tower can be operated with smooth discs at 15 rpm without churning the oil layer. The model is 1/3 of the full-scale size, and taking the disc circumferential velocity as the dominant factor in this oil churning, it is concluded that operating the full-scale periodic cooling tower with smooth discs at 5 rpm would not have any problem of oil churning.

It should also be noted that the 20 inch model has spacers between the discs near the disc perifery. These four spacers strike each oil/water interface a total of four times per revolution, and are responsible for a significant proportion of the oil churning. Elimination of these spacers would increase the acceptable operating speed of the discs.

In another test to study the oil churning problem, discs with radial ribs were used. Six radial ribs, equally spaced, were formed on a disc by pressing the disc between two dies. Figure [7] shows such a disc. The ribs on the disc have the advantage of increasing the disc rigidity so as to eliminate any buckling. These ribbed discs are sufficiently stiff so they can be properly spaced without using spacers along the disc circumference, and this greatly simplifies the assembly of the discs. On the other hand, the ribs on the disc may cause more agitation to the oil layer.

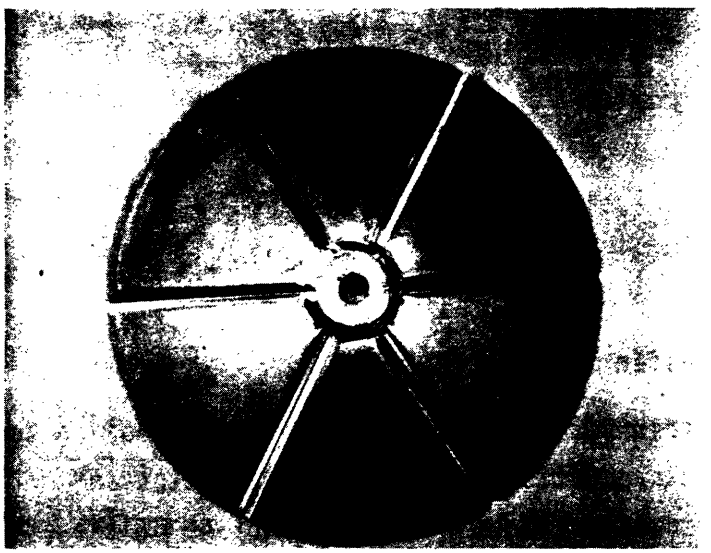

20 Inch Disc with Radial Ribs

Figure 7

Four discs of diameter 20 inches, each with six radial ribs, were assembled onto a shaft. These discs were made of 26 gauge cold rolled steel sheet and were spaced 3/4 inch apart. As in the previous test, the discs were immersed to 3 inches below their centers in a trough of water. The water was covered with a layer of silicone oil 1/2 inch thick. The rotational speed of the discs was gradually increased. Again, not until the rotational speed reached about 15 rpm, were any distinct oil globules brought down below the oil layer. Further increased in rotational speed resulted similar oil churning phenomenon as in the case with smooth discs. It thus appeared the radial ribs on the discs had a small effect on the oil churning.

II.1.1.2 Heat Transfer Test

The heat transfer performance of the periodic cooling tower can be predicted with the basic equation of energy conservation and certain experimental correlations. Some assumptions or simplifications of the actual complex situation are, however, necessary to reduce the energy conservation equation into a manageable form. These assumptions or simplifications, plus some deviations from the experimental correlations employed, may cause some discrepency between the theoretical estimate and the results observed experimentally.

A theoretical analysis of heat transfer is given in the next section. This is followed by the description of an experiment to test the heat transfer of the model periodic cooling tower. A comparison will then be made between the theoretical estimate and the experimental results to determine the validity of the theoretical analysis.

II.1.1.2.1 Heat Transfer Analysis

A heat transfer analysis for the periodic heat exchanger was presented in the first annual report [4]. There it was assumed that the plate temperature remained constant, and that the fluid temperature varied. That analysis yielded a relation between ε_a or ε_w and NTU*, and is shown in figures 8 and 9.

Where,

$$NTU^* = \frac{4\ r\ h_f}{\rho_f v_f\ C_{pf}\ D} \qquad [7]$$

$$\varepsilon_a = \frac{T_{a2} - T_{a1}}{T_p - T_{a1}} \qquad [8]$$

and

$$\varepsilon_w = \frac{T_{w1} - T_{w2}}{T_{w1} - T_p} \qquad [9]$$

The rate of heat transfer from one plate is given by any of the following equations:

$$\dot{q} = B(T_p - T_{a1}) \qquad [10]$$

$$\dot{q} = C(T_{w1} - T_p) \qquad [11]$$

$$\dot{q} = \frac{BC}{B + C}(T_{w1} - T_{a1}) \qquad [12]$$

where $B = \rho_a\ V_a\ C_{pa}\ D\ H_a\ \varepsilon_a$

$C = \rho_w\ V_w\ C_{pw}\ D\ H_w\ \varepsilon_w$

For further details of the derivation, see reference [4].

However, temperature variations in the disc do occur. An analysis based upon variations in disc temperatures follows.

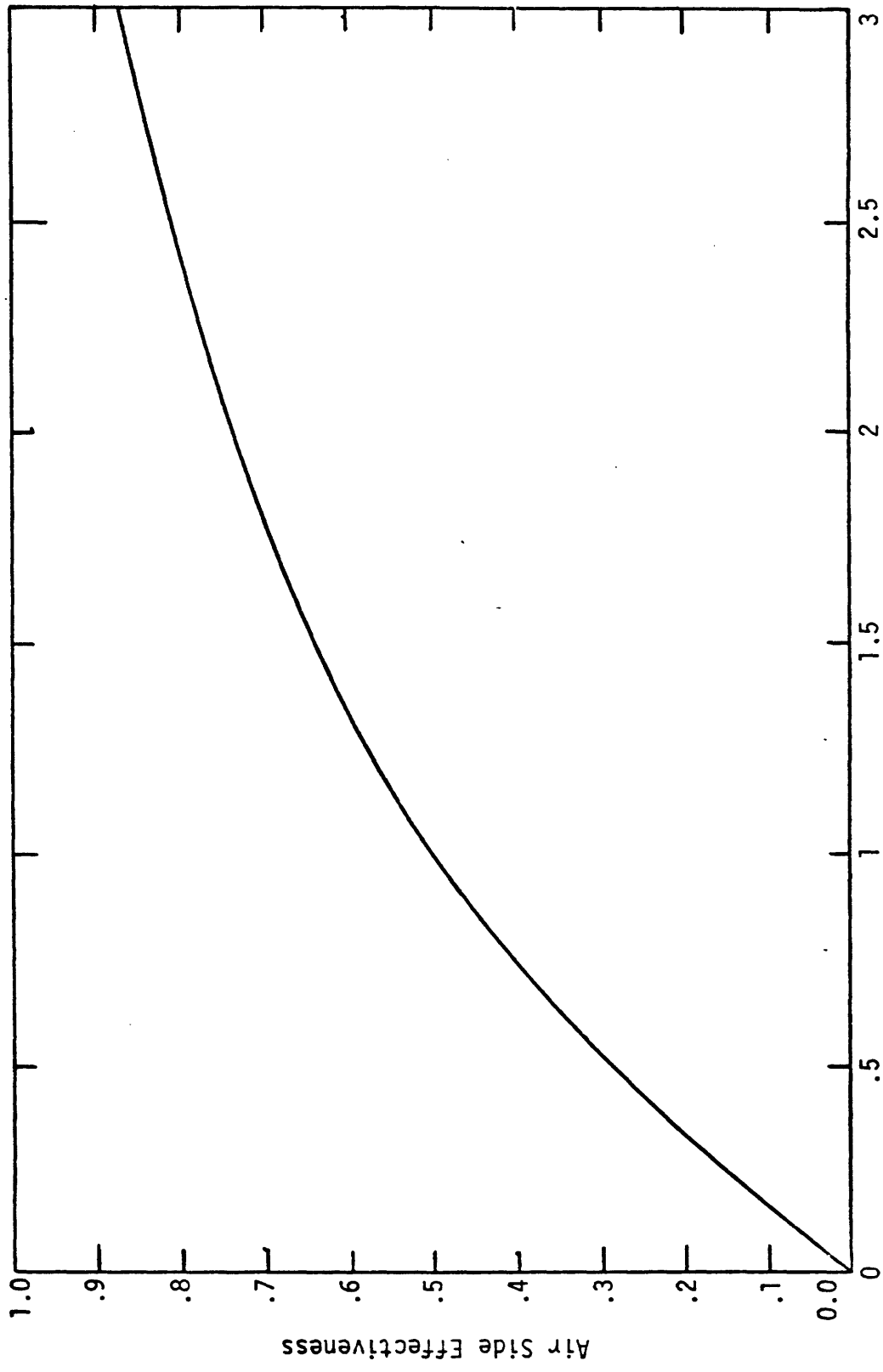

AIR SIDE EFFECTIVENESS VS. NTU*

Figure 8

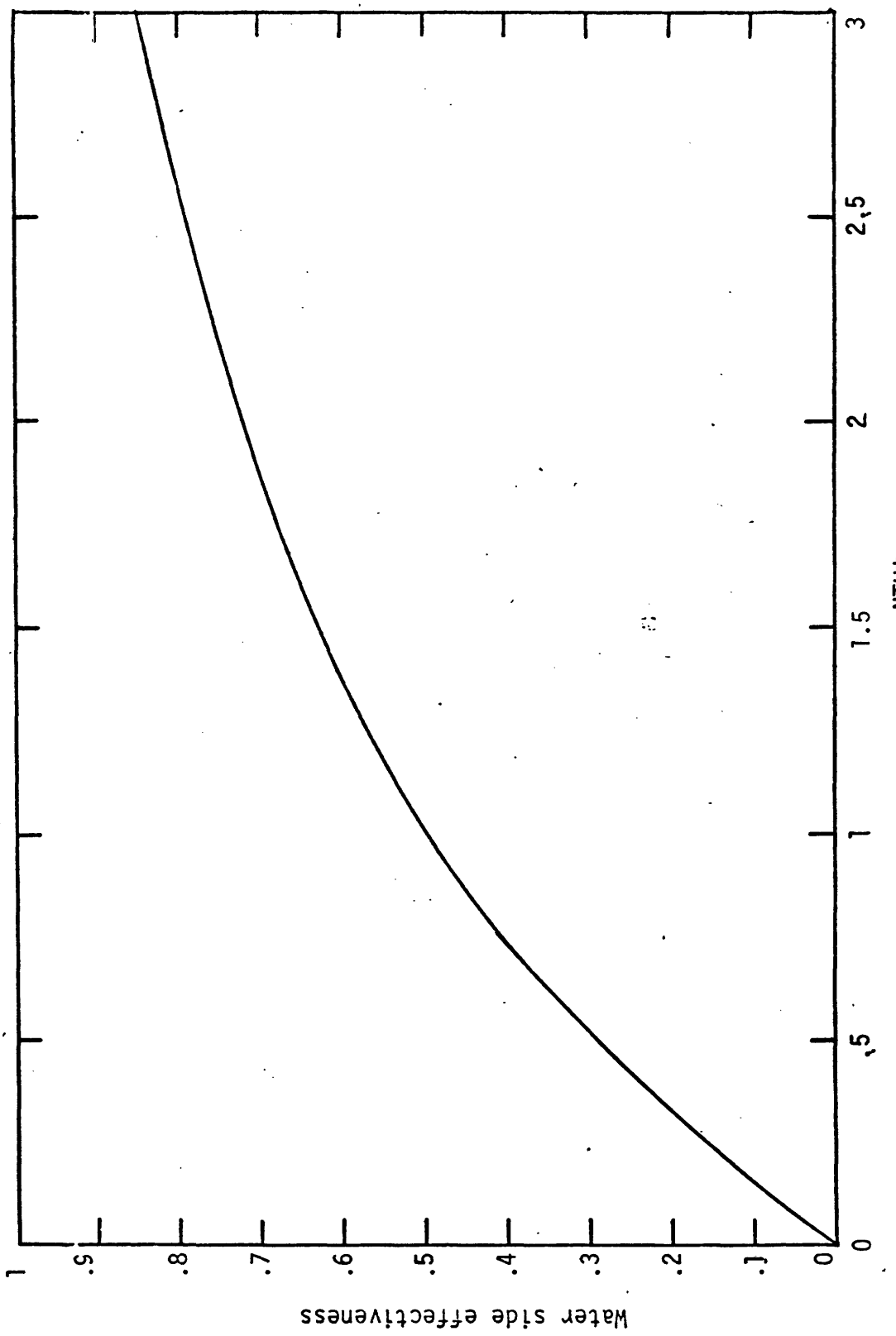

WATER SIDE EFFECTIVENESS VS. NTU*
Figure 9

Consider a small element of area dA of a rotating disc as in Figure 10. Neglecting any radial and angular heat conduction of the disc element, and assuming there is no temperature variation across the disc thickness, the energy balance gives:

$$2h(T_f - T_p)\, dA\, dt = t_p C_p \rho_p\, dA\, dT_p \qquad [13]$$

Let $$B = \frac{2h}{t_p C_p \rho_p \omega} \qquad [14]$$

and $$dt = \frac{d\Theta}{\omega} \qquad [15]$$

Substituting Equations [15] and [14] into Equation [13] gives

$$B\, d\Theta = \frac{dT_p}{(T_f - T_p)} \qquad [16]$$

Equation [16] can easily be integrated if T_f and B are constants. So assume

1. T_f= constant. This is a good assumption since the temperature drop of the water across the trough is only about 6 degrees F. Take $T_f = 1/2(T_{fi} + T_{fo})$.
2. h = constant. This is also a good assumption and hence B = constant.

Integrate Equation [16] from Θ=o to $\theta = \theta_o$ to give

$$T_{po} = T_f(1-e^{-B\theta_o}) + T_{pi}e^{-B\theta_o} \qquad [17]$$

Equation [17] is derived for the water side. A similar equation for the air side is given as follows:

$$T_{pi} = T_a(1-e^{-B'\Theta'_o}) + T_{po}e^{-B'\Theta'_o} \qquad [18]$$

where B' is defined similar to B but replacing the water side heat transfer coefficient by the air side heat transfer coefficient, and $\Theta_o + \Theta'_o = 2\pi$.

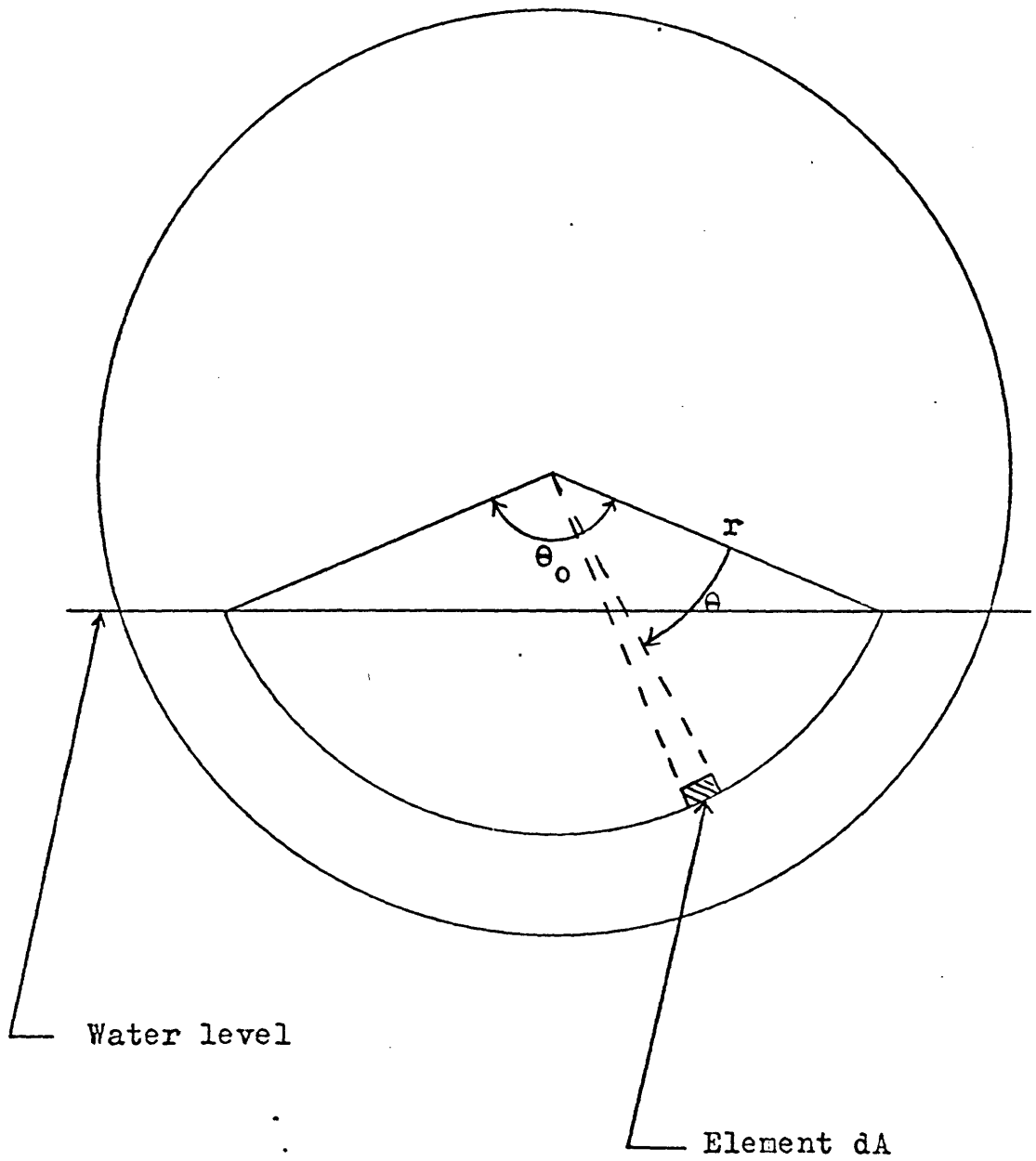

Disc Element

Figure 10

It should be pointed out the assumption of a constant T_a in deriving Equation [18] is not as good as the assumption of a constant T_f, since the variation of T_a on the air side is relatively large, e.g., about 15 degrees F.

Now the two Equations [17] and [18] enable us to evaluate the two unknowns T_{pi} and T_{po}. With the temperature variation $(T_{po} - T_{pi})$ as a function of the disc radius r known, the heat transfer per disc per revolution is then given by:

$$q/REV = \int_0^r (T_{po} - T_{pi})\, 2\pi r t_p C_p \rho_p dr \qquad [19]$$

It should be noted that the two analyses apply to different extremes of operating conditions. The assumption of constant fluid temperature would only be approached under the conditions of high fluid flow rates. Conversely, the assumption of constant plate temperatures is approximated with high disc RPM. True operating conditions will yield temperature changes in both the disc and the fluids.

II.1.1.2.2 Heat Transfer Coefficients

The evaluation of NTU* in Equation [7] or of T_{pi} and T_{po} in Equations [17] and [18] requires a knowledge of the heat transfer coefficients on both the air side and the water side.

II.1.1.2.2.1 Air Side Heat Transfer Coefficient

The resistance to disc-to-air heat transfer consists of two terms, the air film resistance $R_{f,air}$ and the oil film resistance $R_{f,oil}$. The air film resistance is given by:

$$R_{f,air} = \frac{1}{h_m} \qquad [20]$$

where the mean air film heat transfer coefficient, h_m, is related to the heat transfer coefficient in the fully developed region, h_f, by the following correlation [9]. This is a correction due to the entrance affect.

$$h_m = h_f \left(1 + \frac{6D_e}{L}\right) \qquad [21]$$

The heat transfer coefficient in the fully developed region can be obtained by McAdams correlation: [7]

$$\frac{h_f D_e}{k} = 0.023 \, (Re)^{.8} \, (Pr)^{.4} \qquad [22]$$

The oil film resistance $R_{f,oil}$, following the suggestion mentioned in section II.1.1.1.2 to evaluate the oil film thickness, is given by:

$$R_{f,oil} = \frac{2\delta}{k} \qquad [23]$$

where δ can be obtained from Equation [5].

Therefore the overall heat transfer coefficient h for the air side is as follows:

$$h = \frac{1}{R_{f,\,air} + R_{f,oil}} \qquad [24]$$

On the air side, the air film heat transfer resistance is much larger than the oil film heat transfer resistance. For example, with an air velocity of 20 ft per sec. and a disc rotational speed of 6 rpm, the estimated value for $R_{f,air}$ is 0.111 hr ft^2F/BTU while $r_{f,oil}$ is equal to 0.025 hr ft^2F/BTU at a 10 inch radius.

II.1.1.2.2.2 Water Side heat transfer coefficient

The resistance to water-to-disc heat transfer also consists of two terms, the water film resistance $R_{f,water}$ and the oil film resistance $R_{f,oil}$. These two terms are evaluated in exactly the same procedures as that in section II.1.1.2.2.1 for the air side. On the water side, the oil film heat transfer resistance dominates. For example, with a disc rotational speed of 6 rpm, the estimated value for $R_{f,water}$ is 0.003 hr ft^2 F/BTU while $R_{f,oil}$ is equal to 0.025 hr ft^2 F/BTU at a radius of 10 inches.

II.1.1.2.3 Experimental Heat Transfer Measurements.

The small model of the periodic cooling tower was tested for its heat transfer. Thirteen galvanized steel discs, 0.040 inch thick and 20 inches in diameter, were assembled onto a steel shaft. The discs were spaced 0.33 inch apart, and were immersed in a trough of water to three inches below their centers. The water in the trough was covered with a layer of silicone oil about 1/2 inch thick. The rotary discs system, the water circulation system and the air flow system were as described briefly in Section II.1, Figs. 2, 3, & 4 and in more detail in last years Annual Report [5].

To measure the disc temperature, 30 gauge (0.010 inch diameter) copper-constantan thermocouple wire was used. Thermocouples were fixed at five locations onto the center disc and onto one side disc. These five locations of thermocouples are shown in Figure 11. The temperature measurements of the side disc were compared with that of the center disc to determine if there was any edge effect due to the plexiglass air duct and water trough. To fix a thermocouple onto the disc,a 0.030 inch diameter hole, about 0.030 inch deep, was drilled on one side of the disc. The head of the thermocouple junction was pressed into the hole and was covered with a little soft solder to ensure a good contact between the thermocouple and the disc. The other end of the thermocouple was drawn outside the air duct through a hole drilled along the shaft axis, and was connected via a switch to a copper slip ring (Figure 12). Both the switch and the copper slip ring were fixed to the end of the steel shaft so that they rotated together with the shaft. Two brushes, made of copper-graphite mixture and each with a copper lead, were held against the copper slip ring by two small springs. The two brushes were pressed tightly against the rotating slip ring by the tensions in the two springs to ensure a good connection. The outputs of the ten thermocouples on the discs were measured with a X-Y chart recorder, in the range of 5 millivolts per inch.

Copper-constantan thermocouples were also used to measure the water and air temperatures. The outputs of these thermocouples were measured with a X-Y chart recorder.

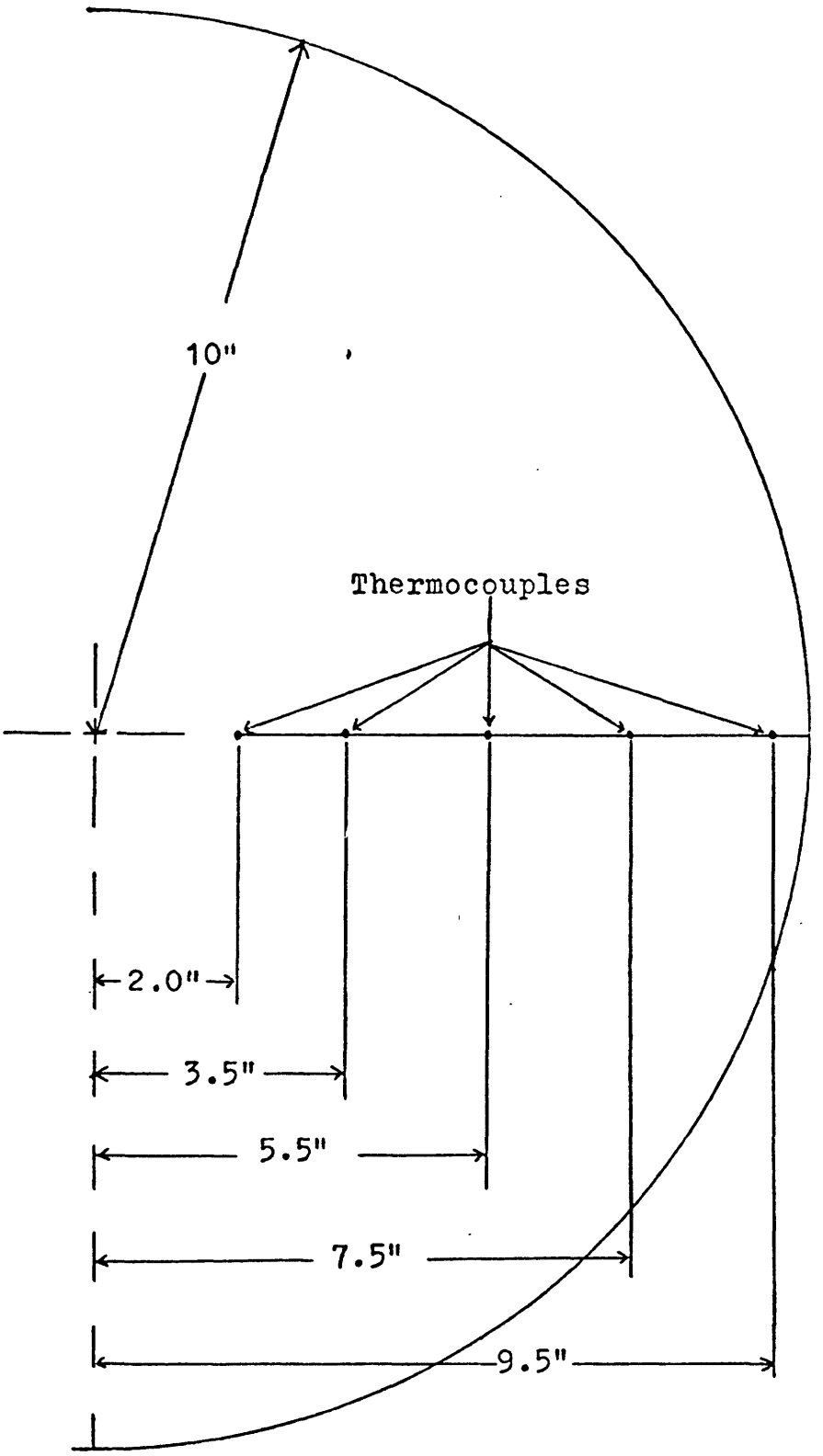

Locations of Thermocouples on Disc

Figure 11

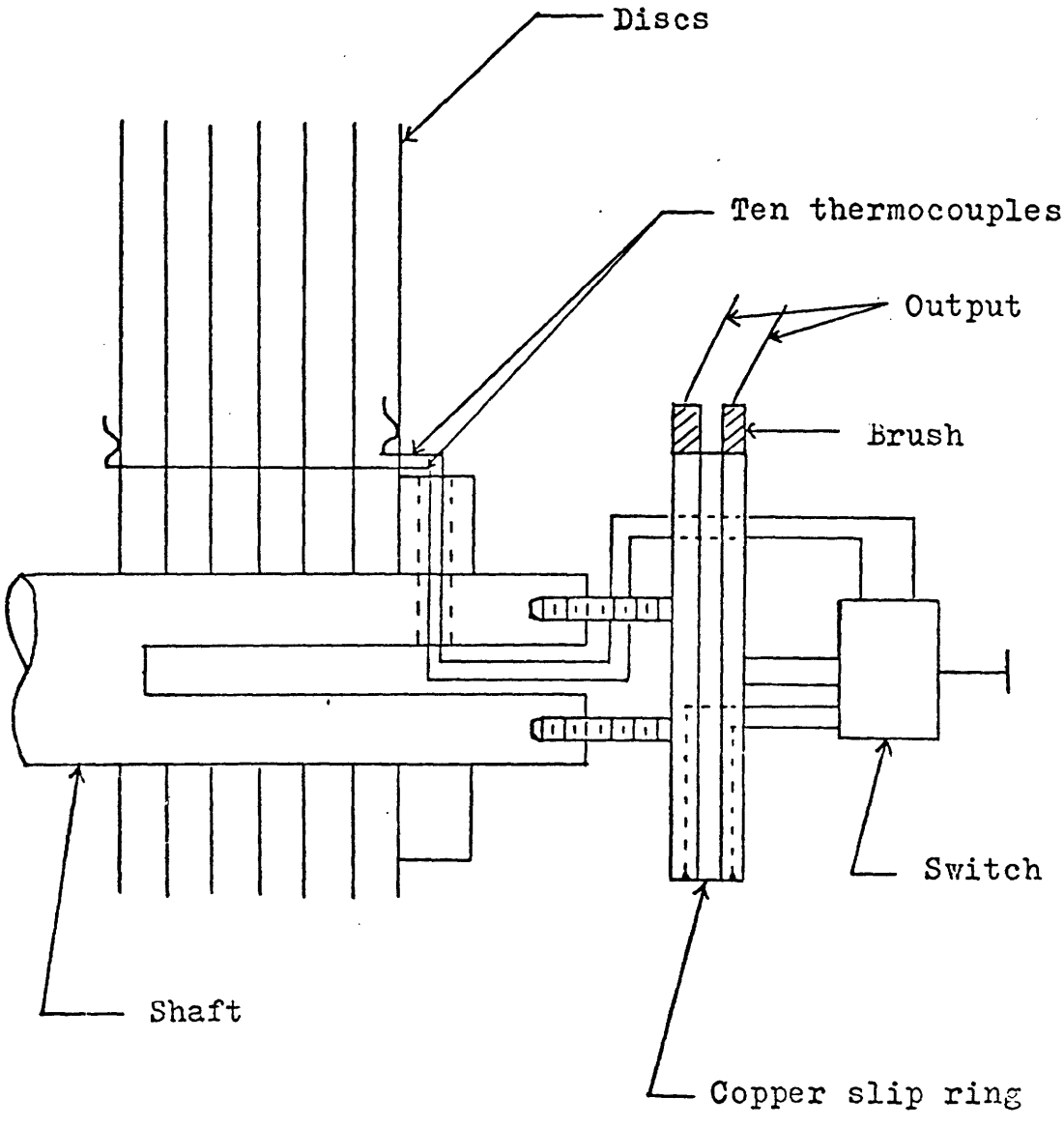

Connection of Thermocouples on Disc

Figure 12

II.1.1.2.4 Experimental Heat Transfer Results

Figure 13 shows the temperature data recorded in one test. The curves traced on the left-hand side of Figure 13 recorded the temperature profile of the center disc while the curves on the right-hand side recorded the temperature profile of the side disc. Different curves correspond to different locations on the rotating disc. The wavy curves indicate the temperature variations experienced by the disc as the disc rotated between the air side and the water side. A comparison of these temperature data between the center disc and the side disc indicates that in this experimental set-up there was negligible side effect due to the plexiglass air duct and water trough. The test data of the center disc is thus representative of a periodic cooling tower with a very large number of rotating discs.

In this test, the inlet water temperature was 125 degrees F and the outlet water temperature was 116 degrees F. The inlet air temperature was 73 degrees F and the temperature profile of the air immediately downstream of the rotating discs is shown in Figure 14 . The temperature of the air leaving the rotating discs was not uniform, and its temperature profile as shown in Figure 14 was expected. The air passing across the top of the rotating discs had a shorter time for heat transfer from the hot discs, so its temperature on leaving the discs was lower. The air passing across the center portion of the discs, being heated longer by the hot discs, had a higher temperature downstream of the rotating discs.

The temperature of the rotating disc was plotted against the disc radius in Figure 15. For radii greater than 3 inches, the disc experiences a cyclic heating and cooling on the water side and on the air side respectively, and so the disc temperature varied between a peak and a trough. The crest of the wavy curve shown in Figure 13 indicates the peak temperature of the disc while the bottom of the wavy curve indicates the trough temperature of the disc. In figure 15, curve (1) is the peak temperature and curve (2) is the trough temperature. For radii less than 3 inches, the disc never touched the water and hence there was no temperature variation. Therefore as the radius gets smaller, the two curves (1) and (2) converge into one single curve.

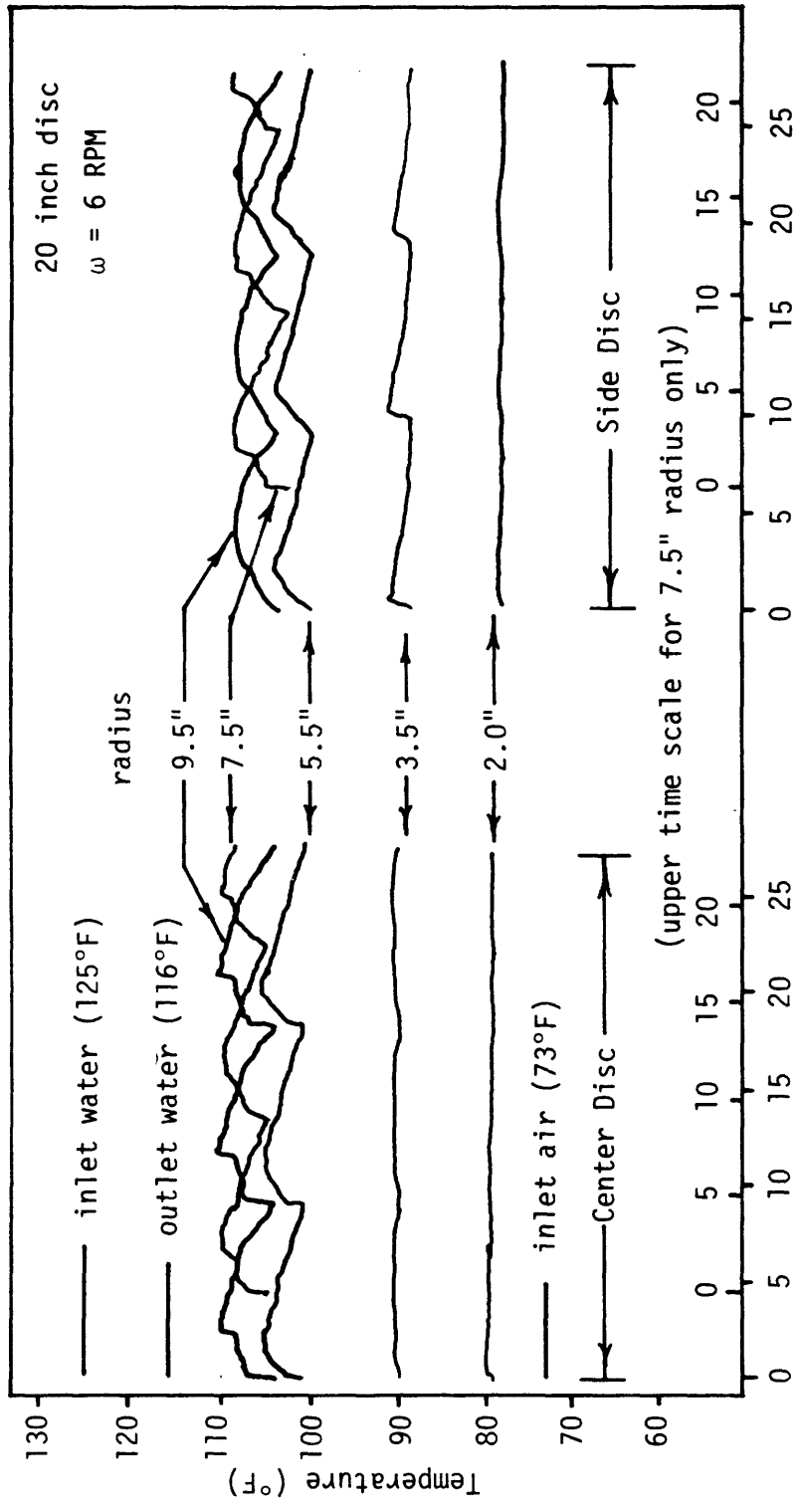

EXPERIMENTAL DISC TEMPERATURES

Figure 13

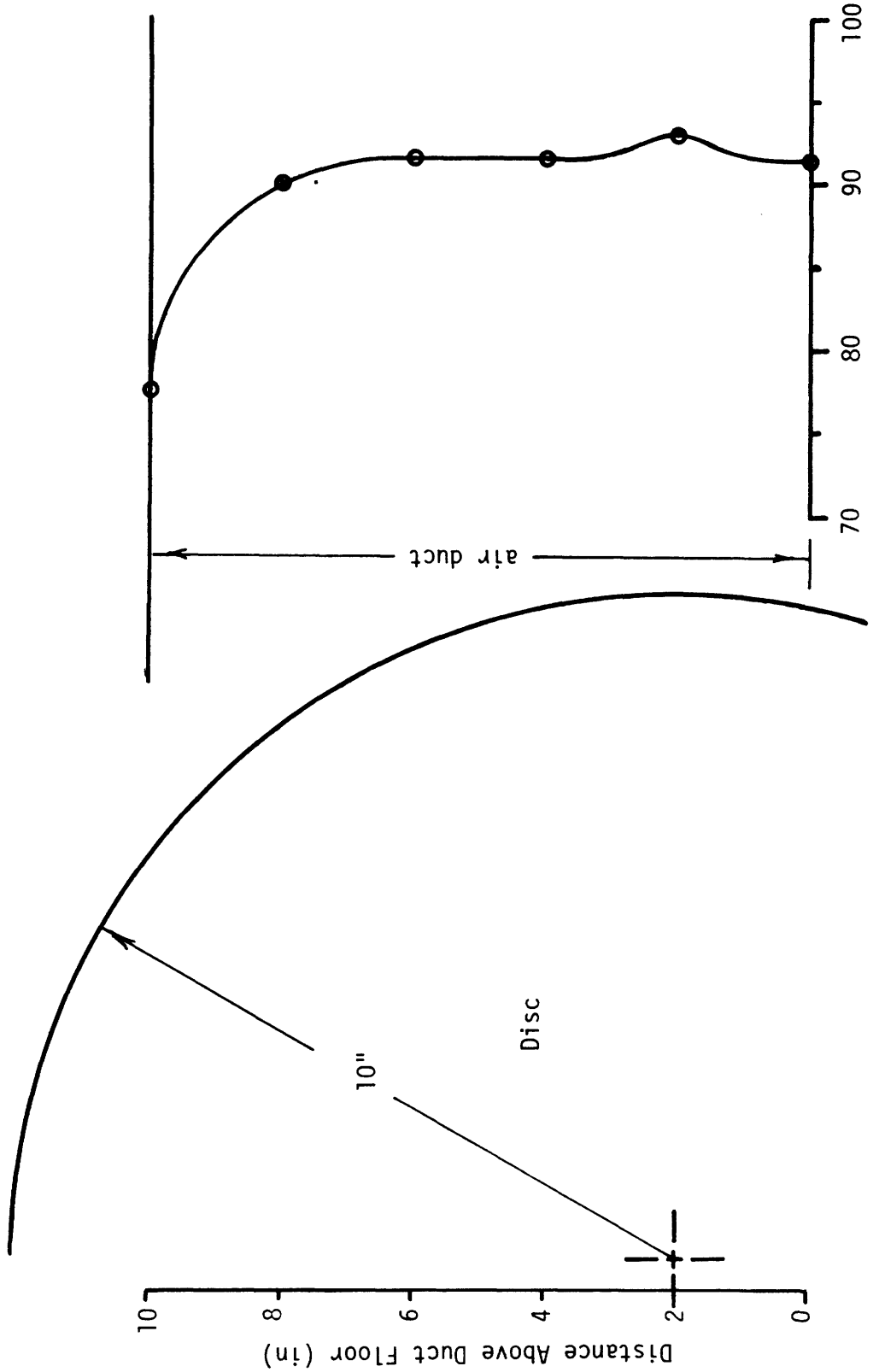

TEMPERATURE PROFILE OF AIR DOWNSTREAM OF ROTATING DISCS

Figure 14

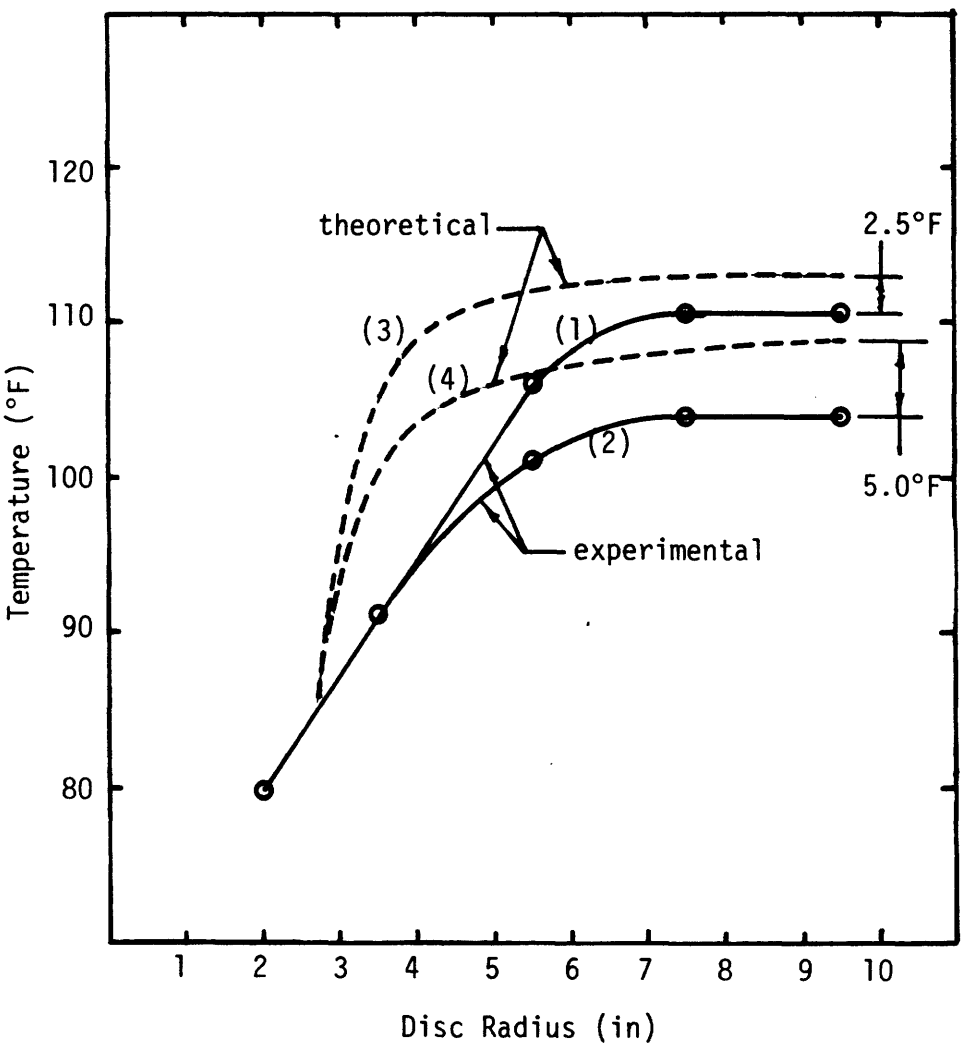

DISC TEMPERATURE PROFILE OF
1/3 FULL SCALE PERIODIC COOLING TOWER

Figure 15

The temperature of the disc increased with the radius relatively rapidly at small radii. At a radius equal to 6 inches, both the peak and the trough temperatures began to level off. For radii greater than 6 inches, the very small radial temperature gradient indicates it is a good assumption to neglect the radial heat conduction in the derivation of Equations 17 and 18. For small radii, say less that 6 inches, the radial heat conduction term may not be negligible in the energy equation due to the presence of the radial temperature gradient.

Following the procedures outlined in the theoretical analysis developed in section II.1.1.2.1 and section II.1.1.2.2, the temperature of the disc was evaluated for the same conditions as in the experiment. The results were plotted in Figure 15 for comparison with the the experimental data. Curve (3) is the peak temperature and curve (4) is the trough temperature. For radius greater than 6 inches, the theoretical predictions of both the peak and the trough temperatures of the disc are fairly good. The theory overestimates both the peak and the trough temperatures of the disc. This overestimation can be attributed to either one, or a combination of, the following three factors:

1. On the water side, the oil film heat transfer resistance dominates the water film heat transfer resistance. As it was pointed out in section II.1.1.1.2, the oil film resistance to heat transfer cannot be very accurately estimated due to the complexity of the problem. An underestimation of this oil film resistance leads to a higher estimation of the disk peak temperature as the disc leaves the water side. On the air side, the air film heat transfer resistance dominates the oil film heat transfer resistance. An underestimation of the oil film resistance would have very little effect on the overall heat transfer coefficient on the air side. Consequently the drop of the disc temperature on the air side remains essentially the same. An underestimation of the oil film resistance to heat transfer therefore leads to an overestimation of the disc trough temperature as well.
2. On the air side, the dominant air film heat transfer resistance was evaluated with experimental correlations. If we overestimate this air film resistance because of any deviation from the experimental corre-

lations, we would have a smaller drop in disc temperature on the air side. Similar to the previous explanation for the water side, a smaller drop of disc temperature on the air side leads to a higher disc trough temperature, which in turn pushes up the disc peak temperature.

3. The theoretical fluid temperature, by this analysis, is assumed constant. Fluid temperatures do vary, and in fact, for the experiment run, vary more than the temperature of the disc.

At the radius that barely touches the water, the prediction of the disc temperature is surprisingly good. However, for small radii, the theory gives a much steeper radial temperature gradient than that was observed in the experiment. This discrepency is thought to be the result of neglecting the radial heat conduction in the derivation of Equations 17 and 18 . In the actual situation, the radial heat conduction tends to lower the disc temperature and the temperature gradient.

Table 3 compares the experimental values of the heat transfer coefficients on the water side and on the air side and of the heat transfer per disc with the theoretical predictions.

TABLE 3

	Heat transfer coefficient on water side, BUT/hr.ft.^{2}F	Heat transfer coefficient on air side BTU/hr.ft.^{2}F	Heat transfer rate per disc BTU/hr.
Experimental measurement	36.0	9.0	706
Theoretical prediction	39.6	7.5	566 (with T_p Const.) 561 (with T_f Const.)
Deviation from experimental measurement %	10	16.7	20.5

The equation defining the heat transfer coefficient is

$$h = \frac{\dot{q}}{A\,(T - T_p)} \qquad [25]$$

where q is the heat transfer rate per disc, A is the heat transfer area of the disc, T_p is the disc temperature, and T is either the water temperature or the air temperature. To evaluate the heat transfer coefficients, we encounter the problem of a varying disc temperature and non-uniform air and water temperatures. Average values for the disc, air and water temperatures have to be assumed. If the variation and non-uniformity of the temperatures are small, an arithmetic average is sufficiently good. Since most of the heat transfer takes place at large radii, the disc temperature is taken as the average of the peak and trough temperatures at radii of 5.5, 7.5 and 9.5 inches. The water temperature is assumed to be the average of the inlet and outlet temperatures. The air temperature is taken to be 1/2 (inlet temperature + average of outlet temperatures).

The predicted heat transfer coefficient on the water side compares favorably with the experimental value. Since the oil film is the dominant resistance to heat transfer on the water side, it thus indicates Equation (6) gives a good estimate of the oil film thickness.

On the air side, the theoretical estimate for the heat transfer is a little lower than the experimental value. This may be attributed to an over estimation of the oil thickness deviations from the correlations used, or some undetected evaporative heat transfer of water drops that were carried over to the air side. The first and last factors may also be responsible for the larger experimental value of heat transfer per disc. As will be seen in section II.2.2, measured oil thicknesses on the 5' disc was less than that predicted by the method used to estimate the oil thickness on the 20" model.

It should be pointed out that all the temperatures were measured with copper-constantan thermocouples, and these temperature measurements were accurate to 1 degree F. A small drop in temperature in certain cases may lead to some uncertainty in the interpretation of experimental results.

As it was stated previously, the theoretical analysis of heat transfer was based upon a number of assumptions. Deviations from these assumptions in the actual situation may cause discrepancy between experimental results and theoretical predictions as well. More accurate predictions of the heat transfer coefficients and heat transfer can be obtained by a more accurate and realistic modeling of the problem.

One improvement to the theory is, instead of assuming either constant values for both the air and the water temperatures or constant plate temperatures, determine the air and the water temperature profiles as a function of the disc radius r and angle θ. Then Equation [16] can be integrated numerically to give the disc temperature. Another improvement is to divide the disc into two zones, an outer zone that neglects the radial heat conduction, and an inner zone that included the radial heat conduction term in the energy equation. Solutions from these two zones are then patched together at the dividing boundary.

Finally, Figure 16 shows the predicted disc temperature distribution for a full-scale model of the periodic cooling tower. The diameter of the disc in the full-scale model is 5 feet. The average air temperature is 85 degrees F, and the average water temperature is 135 degrees F. The discs rotate at 5 rpm. Equation [19] gives for this full-scale model a heat transfer of 4450 BTU/hr per disc, which is very close to the heat transfer requirement of 4720 BTU/hr per disc in the economic analysis of the periodic cooling tower for a 1000 megawatts electric power plant (4). Also with the NTU* of that analysis (4), based on the heat transfer coefficient measured in the experiment of Section II.1.1.2.3, it is predicted that the air side effectiveness is 46.5%, as compared to the experimental value of 48.5%

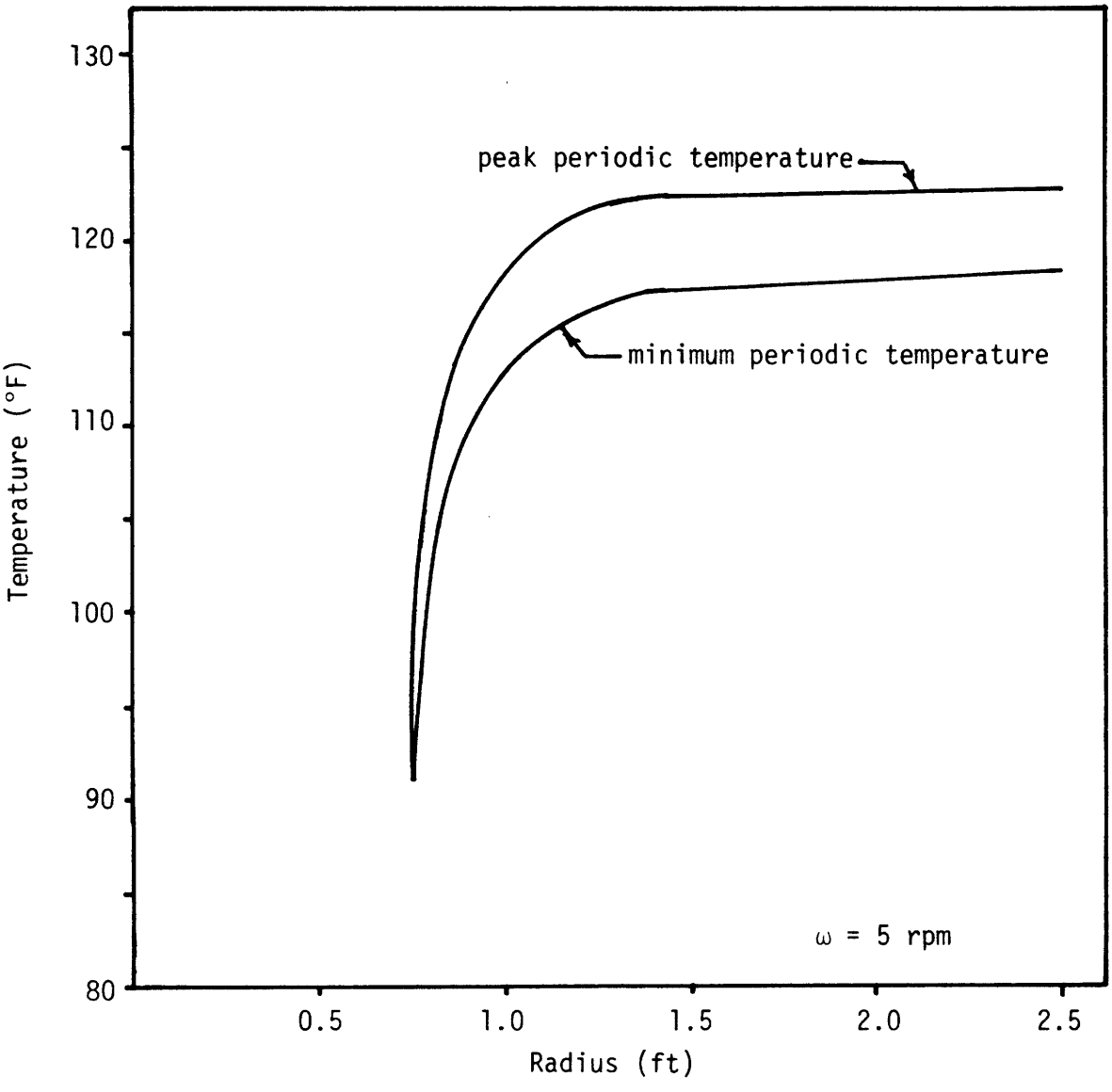

THEORETICAL DISC TEMPERATURE PROFILE
of Full Scale Periodic Cooling Tower

Figure 16

II.1.2 Suggestions for Improvement

The most significant factors that determine the heat transfer performance of the periodic cooling tower are the heat transfer coefficients on both the air and the water side. Improvement in these two heat transfer coefficients can reduce the heat transfer area for a given heat transfer requirement. Since more than half of the total cost of a dry cooling tower is the cost of the heat transfer surface, a reduction of the heat transfer area means a significant savings of the capital cost.

It was learned that on the air side, the air film is the dominant heat transfer resistance. It is well known this heat transfer resistance can be reduced by roughening the heat transfer surface. The roughness on the heat transfer surface breaks up the laminar sub-layer into a turbulent flow, inducing more flow turbulence on the heat transfer surface and thereby increasing the heat transfer coefficient. For this scheme to work, one point needs to be emphasized: Since the rotating discs of the periodic cooling tower are always coated with an oil film, the surface roughness must protrude through the smooth oil film to break up the laminar sub-layer.

On the water side, the oil film is the dominant heat transfer resistance. The water side heat transfer coefficient can be significantly increased by reducing the oil film thickness. One apparent scheme to increase this water side heat transfer coefficient is to use wipers to wipe the oil film off the rotating discs. But considering the high cost and complexity of fabrication and maintenance this scheme is considered impractical. In the experiments on testing the effects of rotating discs on oil churning, it was observed that when the disc rotated into the air side, the disc edge and a small region around it brought up a much thicker film of oil than other part of the disc (Figure 17). As the disc rotated further, this thick oil film sticking around the disc edge began to fall down due to gravity, covering the whole disc surface that was exposed to the air side. It thus appeared the amount of oil brought up by the disc edge and the small region around it contributed significantly to the overall oil film thickness. When a piece of 1/8 inch thick hard rubber was held against the disc edge as shown in Figure 17, a considerable amount of oil was wiped off the disc edge, reducing significantly the thickness of the oil

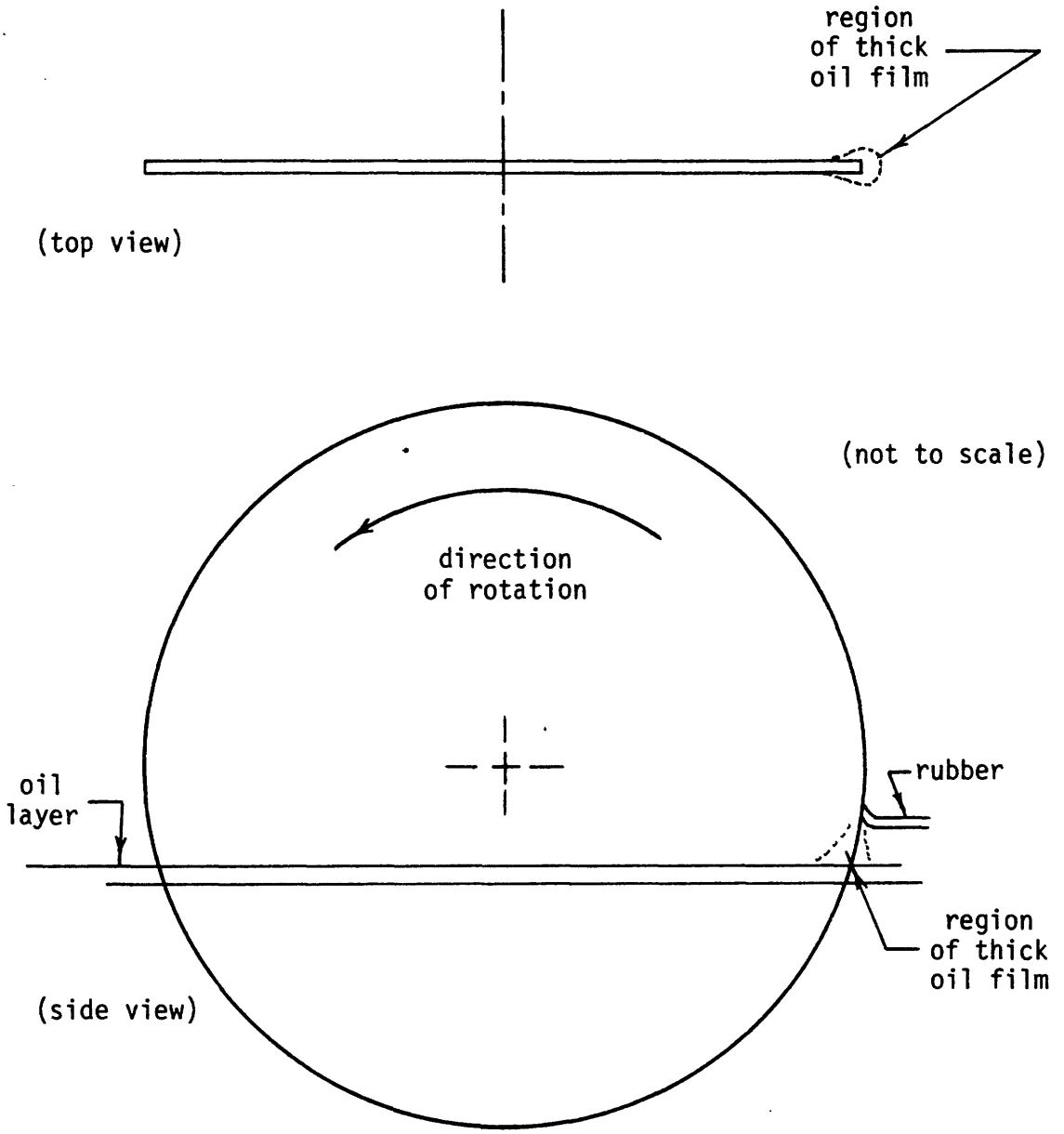

USE OF HARD RUBBER TO REMOVE SOME EXCESS OIL

Figure 17

film on the rotating disc. Observations of oil film thickness on the water side were hard to make, but it was expected phenomenon similar to the air side existed on the water side. The only difference was that instead of gravity pulling down the oil film on the air side, there was a buoyancy force pulling up the oil film on the water side. All those observations just described above suggest that the oil film heat transfer resistance can be considerably reduced simply by holding a piece of hard rubber against the disc edge at two locations; one just above the oil layer on the side where the discs rotate into the air stream, and one just below the oil layer on the side where the discs rotate into the water. Better results can be expected if small rollers that can cover a little around the disc edge are used to remove the oil film.

II.2 Full Scale Model

II.2.1 Test Facility

Much of the large scale test facility was described in last year's annual report (5). The following is a brief summary of that report.

After a study of the utility and facility needs, available locations, potential apparatus designs, and their costs, it was decided to construct an open circuit test loop in the Experimental Project Laboratory. Figures 18 & 19 illustrate the apparatus and the site location.

Much effort was made in the construction of a inlet contraction cone. The contraction cone and its flow straighteners provide a uniform air velocity profile at the entrance to the test section. Hence, during parametric testing of the disc, performance abnormalities will not result because of irregularities in the entering air flow.

A hot water supply system and test section trough was designed and constructed. The hot water system (Figure 20) simulates a power plant condenser, and provides a continuous supply of constant temperature water to the test section. Both the flow rates and inlet water temperature can be varied and accurately controlled. The water trough was constructed such that the inlet and outlet water ports could be varied for experimental purposes. Further, one side of the test section was fabricated out of plexiglas so that flow conditions could be visually observed.

Finally, a fan for the air delivery system was obtained and installed, along with its associated ducting.

For further details on the above, consult last years' annual report (5).

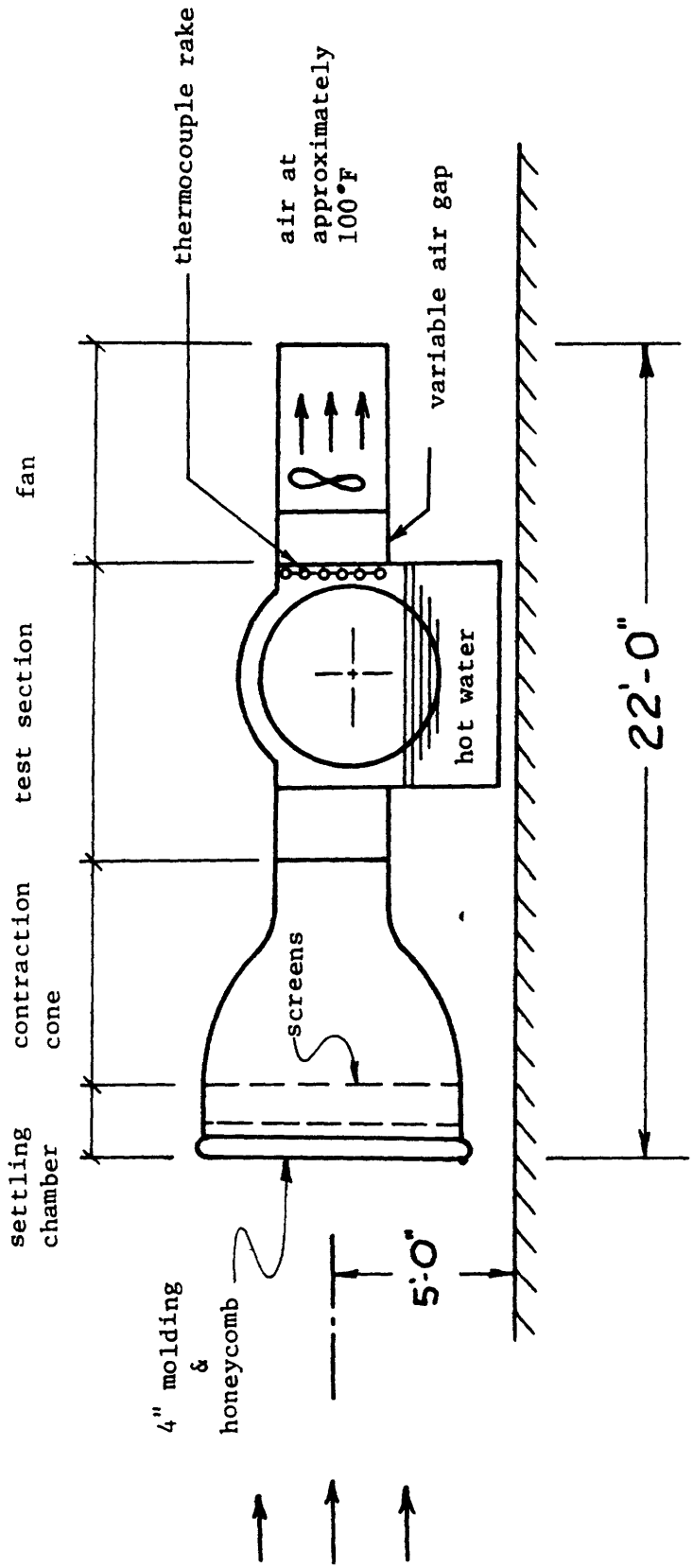

FULL SCALE PERIODIC HEAT EXCHANGER

Figure 18

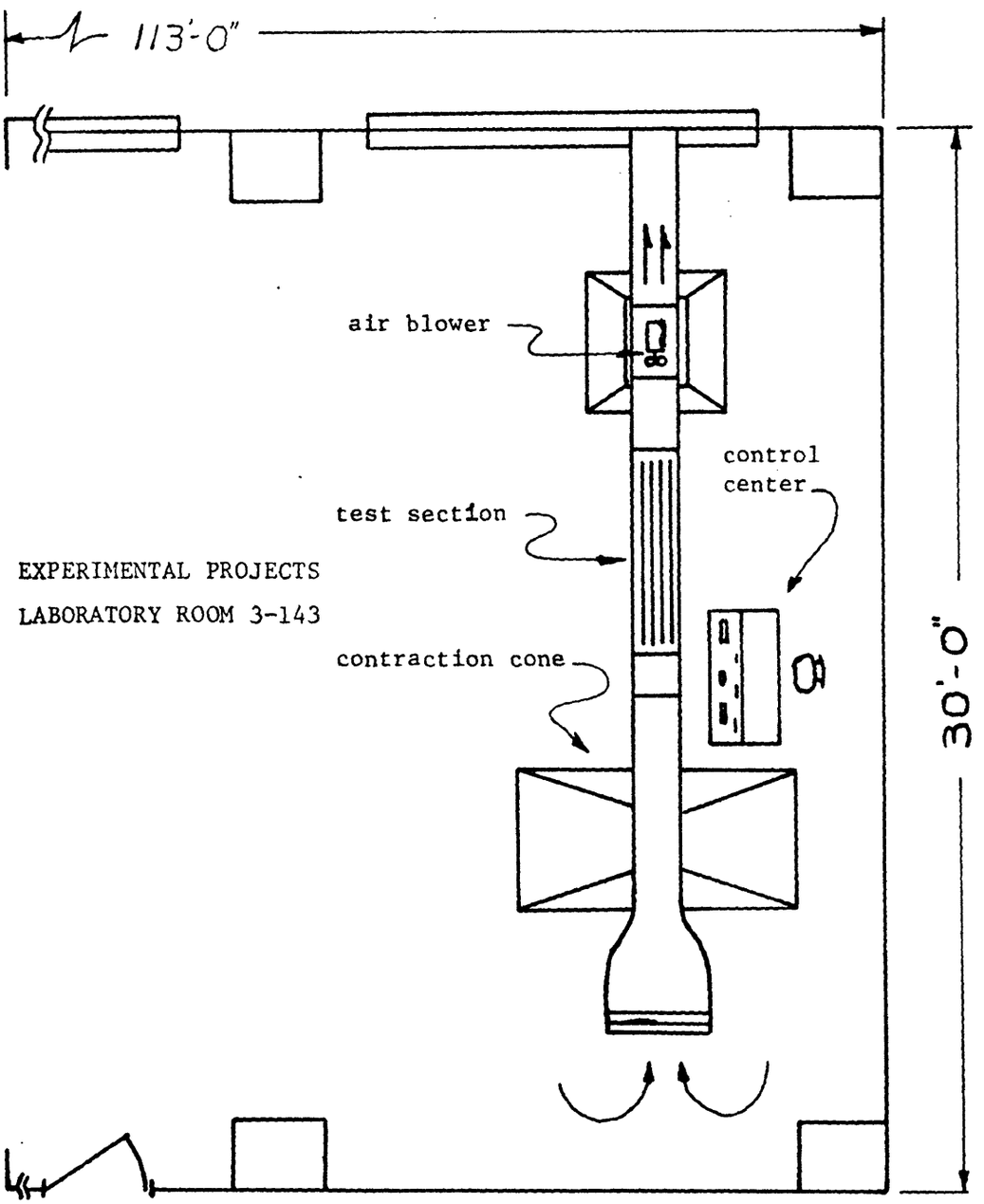

Site location - full scale model

Figure 19

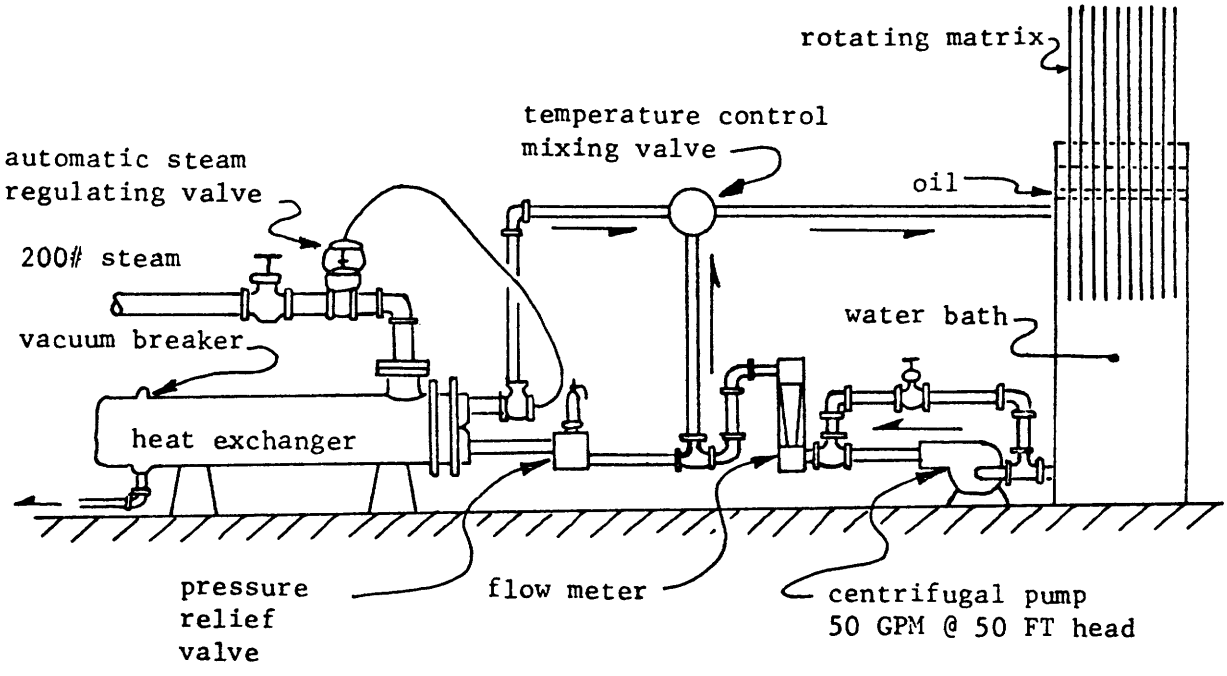

Hot water system - elevation view

Figure 20

II.2.1.1 Disc Construction

The size of the full scale rotating discs to be used in the Periodic Cooling Tower is limited to 5 feet, since that is the width of the largest strip of sheetmetal commercially available. Preliminary test runs with a small, 20 inch diameter disc in a model Periodic Heat Exchanger (5) had shown that the oil-water interface became mixed when the discs were rotated at 15-20 rpm. Assuming this mixing to be directly related to the circumferential disc velocity relative to the oil-water interface, the maximum rotational velocity at which a 5 foot diameter disc could be rotated through the same interface would be 5 rpm.

Five foot diameter test discs of 22 gauge sheetmetal were obtained and structural tests conducted to determine the rigidity of such a disc. A flat disc was not sufficiently rigid, and could not be used for a disc in the full scale model, as it buckled under its own weight when supported as it would be in the Periodic Heat Exchanger.

A one-sixth scale model of the 5 foot diameter disc was used to determine the necessary stiffness required to make the disc suitable for use in the Periodic Heat Exchanger. Scaling factors were obtained which would allow a 10 inch diameter disc to model the structural performance of the full scale disc (10). A systematic test program was developed to determine the best way of stiffening this sheetmetal disc so that it could withstand the stresses applied to it when used.

The previous method used in the 20 inch diameter disc model (5) had been to fasten a series of flat discs together in such a way as to form a rigid matrix. This method had been found to be unsatisfactory. The discs had been connected by drilling matching holes in each disc and inserting threaded rods and spacers through these holes. The main disadvantage was that the threaded rods disturbed the oil-water interface each time they passed through it. Also, immediately after passing through the oil layer the oil flowing off the spacers would bridge the gap between the discs and form a thin film between the discs similar to that observed in a child's bubble blowing ring. The bursting of this thin film could result in oil entrainment in the air stream. Due to these test results, it was decided to make each

disc structurally independent from the adjacent discs, and supported solely from a center shaft. The following paragraphs describe the various shapes that were pressed into 10 and 20 inch diameter discs in an attempt to provide structural rigidity. The thickness of these discs was selected by applying Roark's (10) scaling factors to a 5 foot, 22 gauge (B.W.G.) sheetmetal disc. According to Roark, for two discs with thicknesses scaled in proportion to the diameter and uniformly loaded with the same pressure, the ratio of deflections will be proportional to the ratio of diameters.

Radial Ribs (Figure 21)

A series of radial ribs were constructed to see if this method of stiffening devices could be used. They were formed by pressing a male, steel die into the disc which was backed by a 10 inch thick piece of hard rubber (80 durometer). Four ribbed 20 inch diameter discs were pressed and tested on the small scale model. Each disc had 6 equally spaced ribs that were approximately one quarter of an inch high. Tests showed that these discs broke down the oil-water interface at approximately 80% of the rotational velocity where breakdown had occurred using smooth discs bolted together. Each rib in itself was effective at eliminating buckling perpendicular to the rib. However, the overall stiffness of the disc was poor, with buckling occurring parallel to the ribs (Figure 21).

Single Circumferential Rib (Figure 22)

A one eighth inch high circular circumferential rib was pressed into the periphery of the disc. Although no buckling was noticed, large deflections were observed when this disc was subjected to slight edge loadings and it was concluded that additional stiffening was required.

Series of Four Circular Ribs (Figure 23)

Four circular, one sixteenth inch diameter, ribs were pressed into this 10 inch diameter disc. These ribs did not significantly increase the rigidity of the disc. Although buckling did not occur, the disc simply was not rigid. An increased rib height was tried but was not effective.

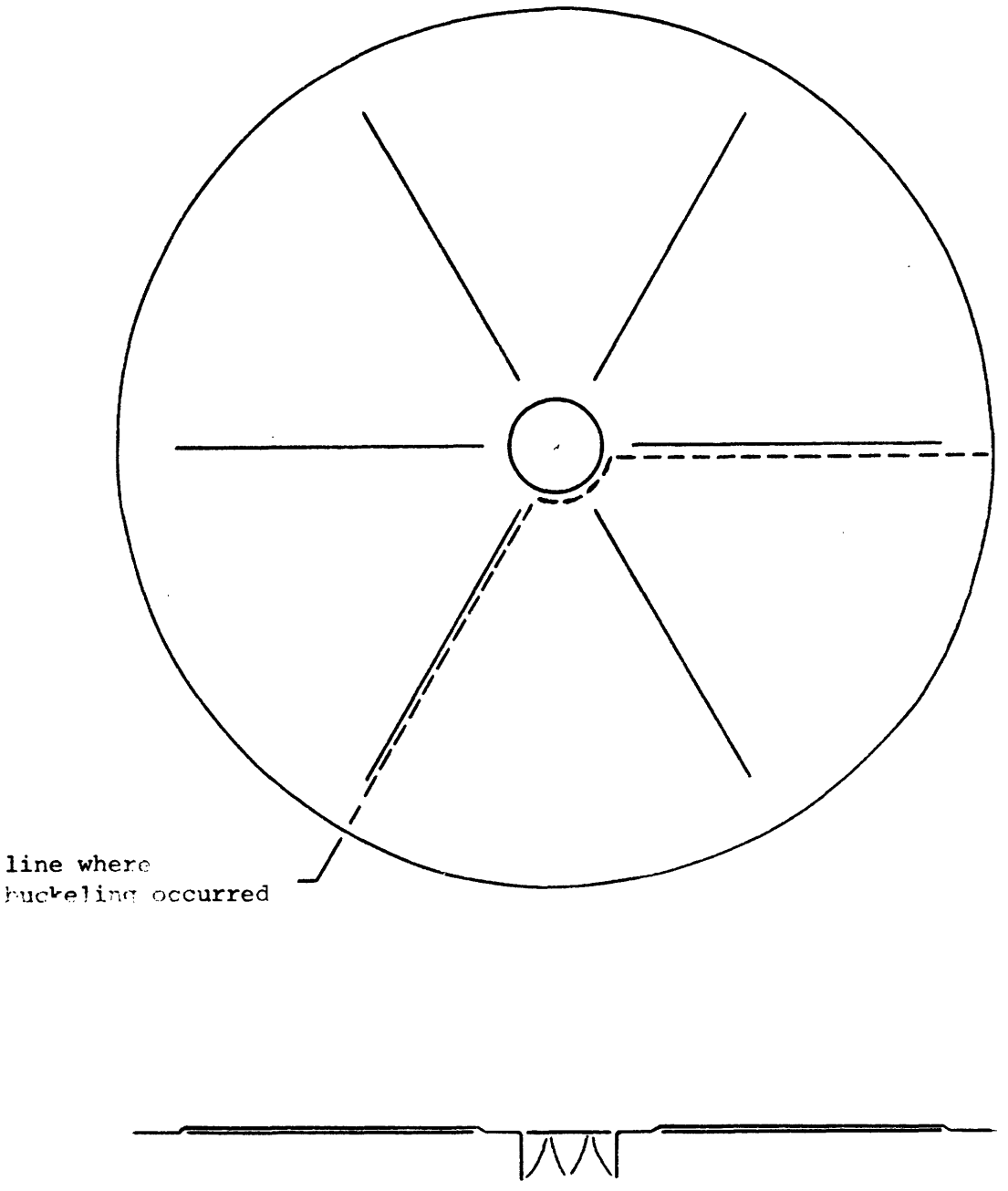

RADIAL RIBS IN MODEL DISC

Figure 21

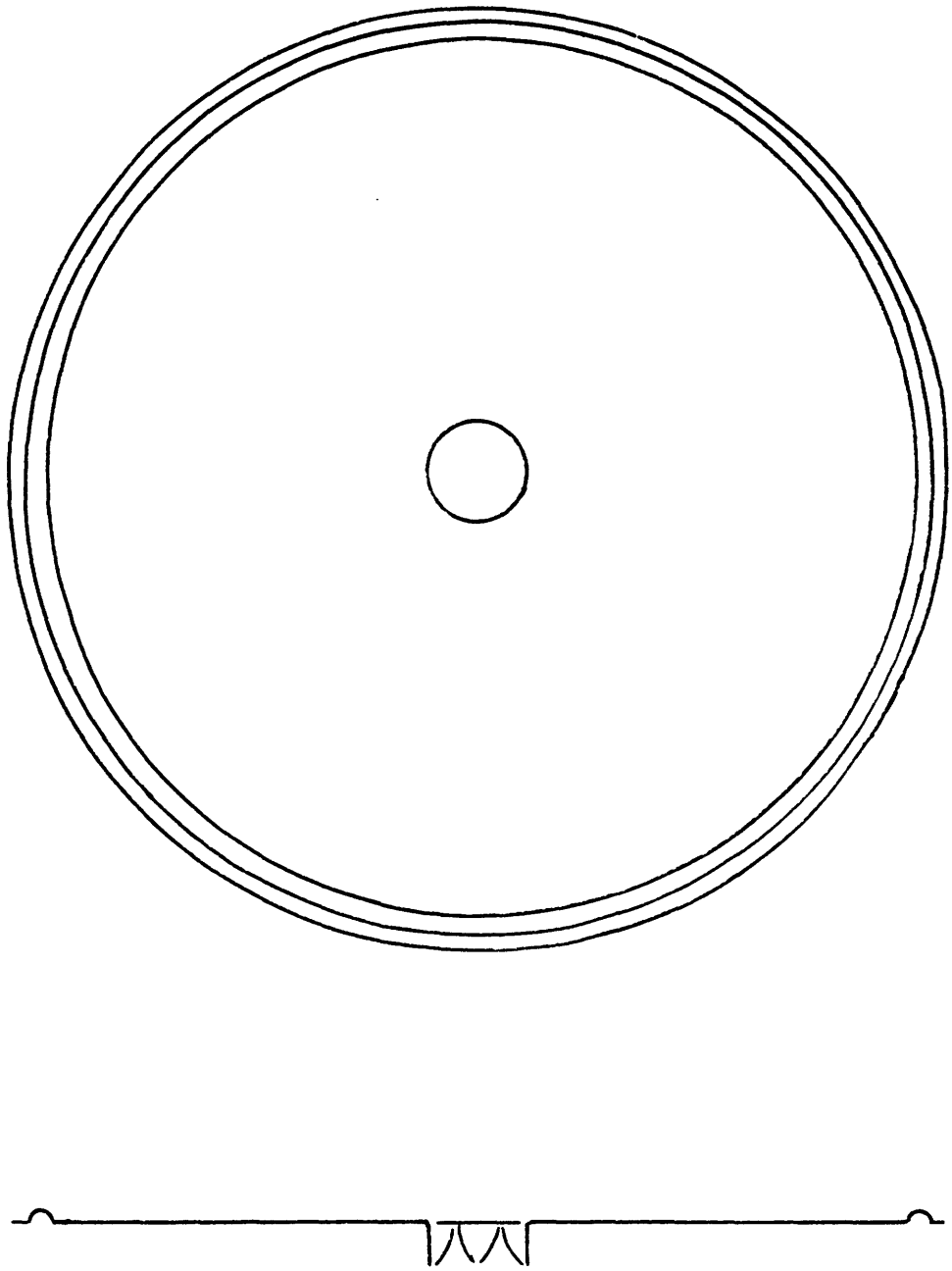

SINGLE CIRCUMFERENTIAL RIB

Figure 22

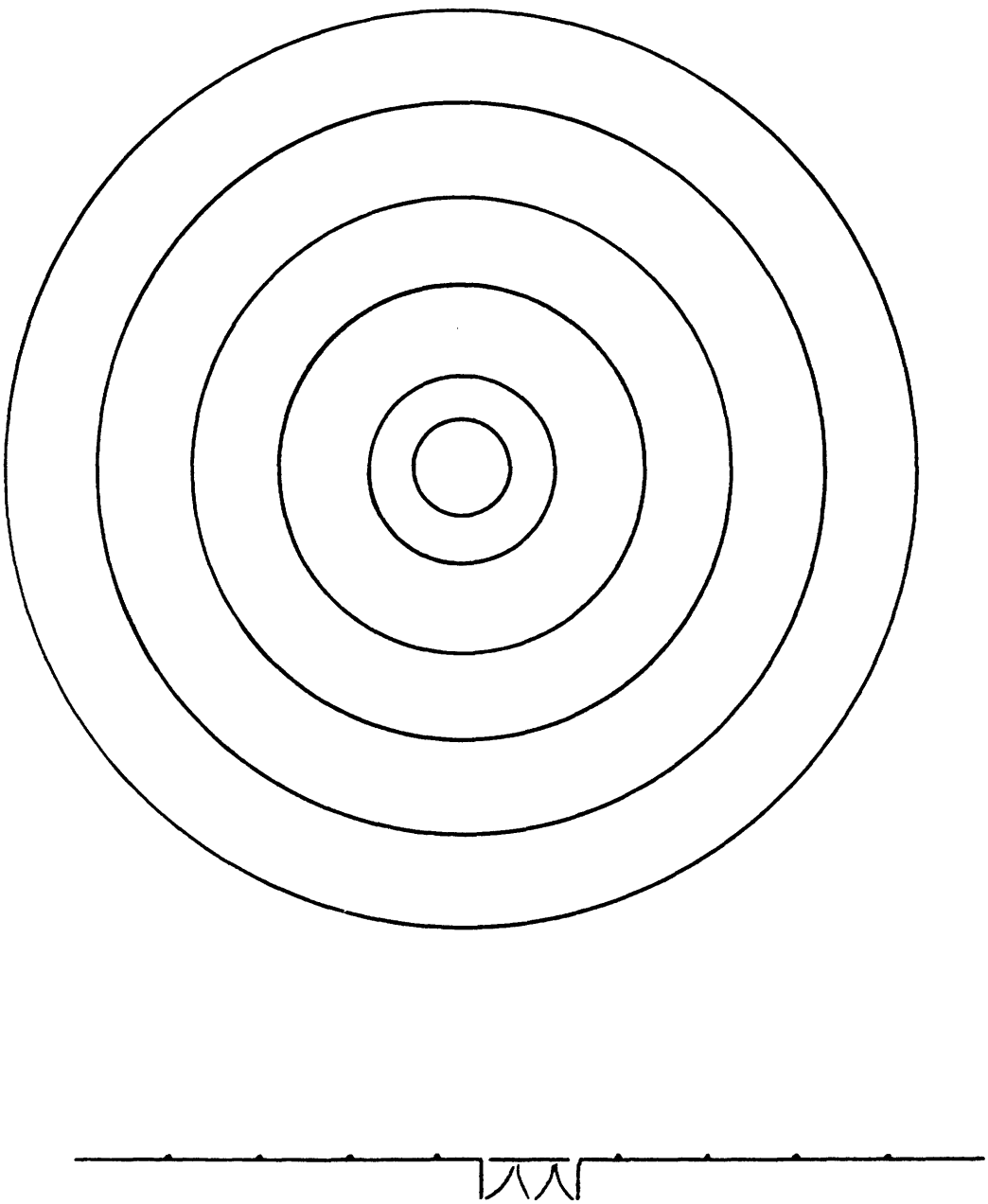

FOUR CIRCULAR RIBS

Figure 23

Waffled Disc (Figure 24)

This disc was waffled with small ridges one half inch apart. This created an unstable disc due to buckling which occurred along each rib. A single circumferential rib was added to this disc. Little improvement was noticed.

Dished Disc

The previous test results indicated that a slight, localized increase in the disc section modulus would be ineffective. The disc section modulus was next greatly increased by putting a slight dish into the disc. This was done by clamping a 10 inch test blank between two eight inch pipe flanges and pressing a slight dish shape into it (Figure 25). This dishing was done by pressing a smaller diameter one half inch steel ring down into the center of the disc while holding the periphery of the disc between the two flanges. It was noted that unless a high clamping pressure was used, wrinkles would occur in the disc due to slippage of the disc from between the two flanges. Slippage was eliminated by insuring that the product of the area of the disc. between the flanges per unit of circumference, the coefficient of friction, and the flange clamping pressure was greater than the product of the disc material's yield strength and the disc thickness per unit of circumference.

The optimum center ring diameter was found to be one third that of the larger disc. The best depth to dish the disc varied with the inside diameter used. The smaller the diameter of the inner ring, the greater the draw required. For a center ring diameter one third that of the larger disc, it was found that a dish depth one thirtieth that of the outer disc diameter would give the disc sufficient rigidity to support its own weight under the loading conditions used in the Periodic Heat Exchanger. Bouma analytically optimized these parameters in his study of Shell Research (11).

After the disc had been removed from the flanges, residual stress gradients remained in the periphery of the discs. This caused the edge of the disc to be slightly wavy. This was eliminated by pressing a single circular circumferential rib in the disc. This disc, shown in figure 25, was selected for

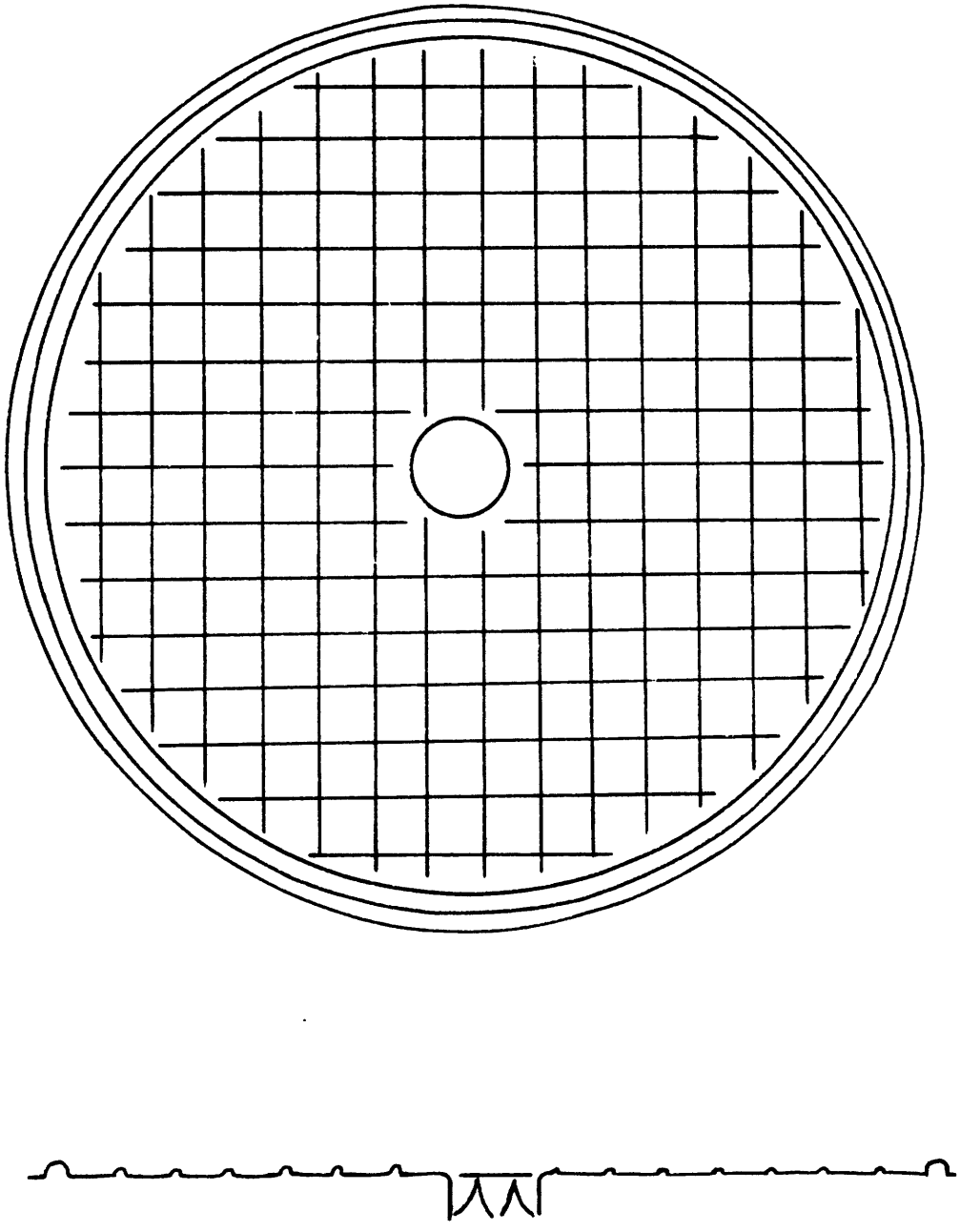

WAFFLED DISC

Figure 24

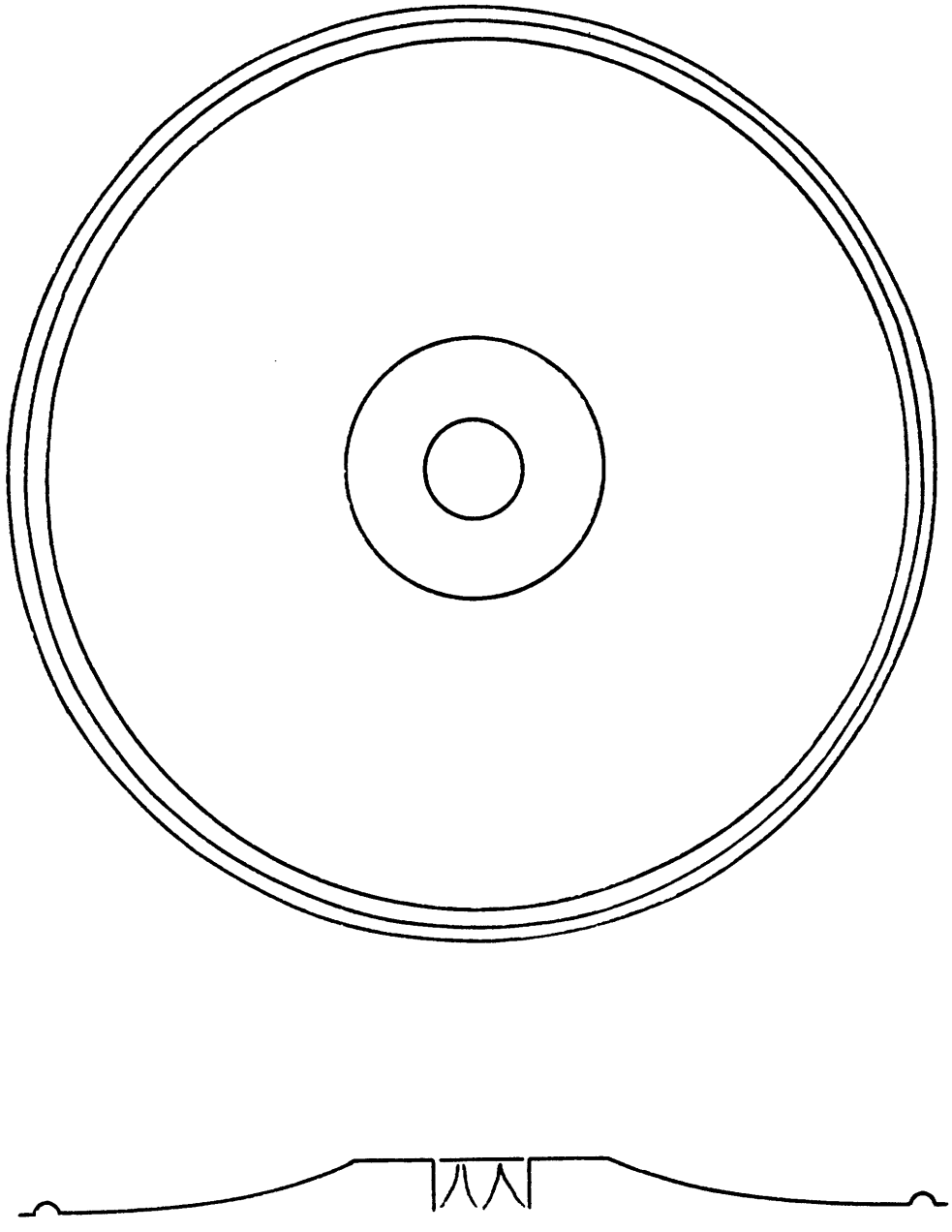

DISHED DISC

Figure 25

use in the full scale Periodic Heat Exchanger.

To fabricate a series of full scale discs, two large 5 foot diameter ring flanges were obtained from a local supplier. To insure that no slippage occurred between the sheetmetal disc and the flanges, calculations showed that a bolt spacing of two inches was necessary if three quarter inch bolts were used to clamp the flanges together. A pneumatic impact wrench was used to reduce the labor involved in tightening down the one hundred, three-quarter inch, bolts prior to pressing each disc.

Bouma's formulations (11) show that a press capacity of approximately 8 tons would be required for the dishing operation. Also, the throat of the press would have to accomodate the 5 foot flanges. A steel truss and frame were constructed on a six foot cast iron bed to serve as a press (Figure 26). Dishing was accomplished by placing the large flanges and sheetmetal blank on the bed beneath the steel truss with an electric fork lift, setting a 2 inch thick, 20 inch diameter ring in the center of the sheetmetal blank, and applying pressure on the ring with a 12 ton hydraulic jack. The flanges were removed and the circumferential rib was stamped into the sheetmetal disc using a steel male disc and a 1 inch thick rubber backing pad. This was done on the same cast iron bed plate. Eight discs were formed in this manner (Figure 27). The discs were attached to the center shaft of the Periodic Heat Exchanger by cutting and bending small sheetmetal tabs into the disc at the point where it slipped over the center shaft. These tabs were then clamped to the shaft using three quarter inch wide stainless steel hose clamps.

DISHING EQUIPMENT

Figure 26

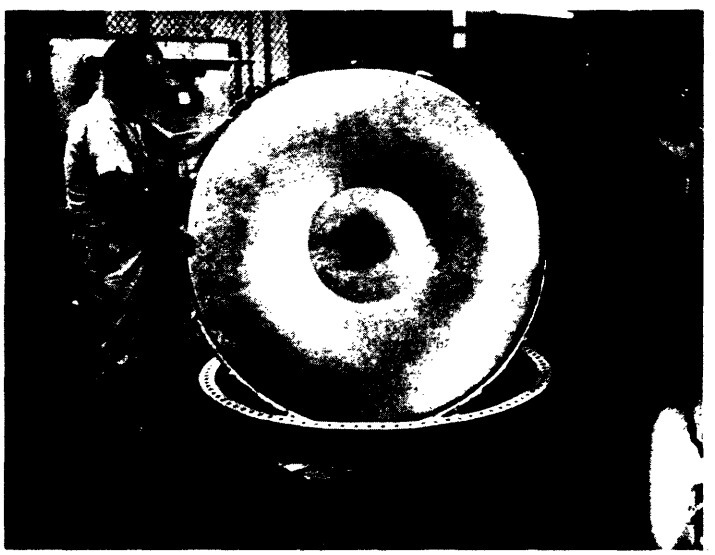

FINISHED DISC

Figure 27

II.2.1.2 Disc Instrumentation

Eight thermocouples were constructed from 0.005 inch diameter copper constantan thermocouple wire. Each thermocouple has a still water response time of 0.04 seconds (12). These thermocouples were radially spaced on the center 5 foot diameter disc to determine the radial disc temperature distribution. Two silver slip rings were installed on the disc shaft so that these readings can be taken under operating conditions. These cyclic temperature readings will be transferred to a chart recorder so that instantaneous disc temperature readings may be obtained for all locations of the disc.

II.2.1.3 Calibration of Waterside Flow Rate

The volume of water flowing through the water tank chamber of the heat exchanger is measured by either of two glass rotometers, one rated at 17.5 gpm, the other at 40 gpm. Each rotometer was calibrated in place using stop watches, barrels, and weighing scales.

The temperature drop of the water going through the heat exchanger is measured by two partial immersion thermometers located at the inlet and outlet of the water tank chamber. Knowing the water flow rate and the water temperature drop, an energy balance may be performed on both the water side of the unit and the air side to insure consistent data.

II.2.1.4 Center Shaft and Bearings

The center shaft which supports the 5 foot sheetmetal discs is a 4 foot long section of schedule 40 four inch pipe. This size was selected due to its availability and the fact that calculations show that for a disc spacing of 1 inch, this shaft could support a 10 foot long section of discs between supports. This allows the discs to be pre-assembled and installed in reasonably sized modulus in the field. The shaft in the test apparatus, however, is supported on ball bearings 27 inches on centers. The construction of the bearings is illustrated in Figure 28.

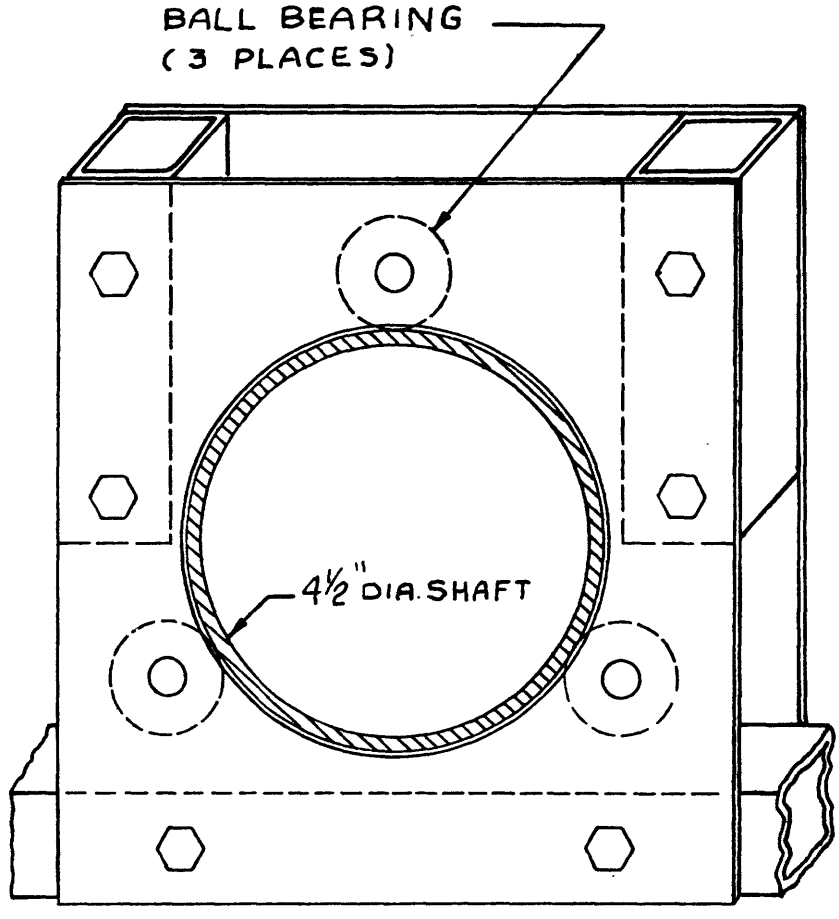

BEARINGS FOR FULL SCALE MODEL

Figure 28

II.2.1.5 Shaft Drive Assembly

The shaft is driven by a one quarter horsepower, 115 volt D.C., 1750 RPM, compound wound electric motor. A variable resistance coil is used to change the speed of this motor. A worm gear and pulley arrangement provides a 200 to 1 reduction drive mechanism between the motor and the disc shaft. This allows the shaft to be operated between 1/2 and 9 rpm.

II.2.1.6 Overhead Chain Hoist

Since the completed disc and shaft assembly weighs over 300 pounds, an aluminum I beam, steel trolley block, and one half ton chain hoist was installed over the Full Scale Apparatus (Figure 29). This permits the shaft assembly to be removed for inspection with a minimum of effort. This same chain hoist is used to remove and install the cover over the disc assembly (figure 29).

II.2.1.7 Cover and Air Baffle

A removable cover was constructed as shown in Figure 30. This cover controls the air side flow over the disc assembly. The entire front and part of the top of this cover is plexiglass which allows visual aerodynamic studies to be made of the discs in operation. A sheetmetal air baffle was formed over the top of the discs to prevent a significant amount of air from flowing over the top of the discs.

II.2.1.8 Calibration of the Air Side Flow Rate

The volume of air flowing through the test section is determined by two pair of static pressure taps in the walls of the contraction cone (Figure 18). A pitot tube traverse was first made at the outlet of the cone to determine the velocity profile at that point. The pitot tube was traversed horizontally across the outlet at five equally spaced vertical locations for five different air flow rates. The velocity profile measured was extremely flat (Figure 31). The velocity readings were identical across the cone outlet at the four lower air velocities measured. At the highest velocity measured, 27.6 ft./sec.,

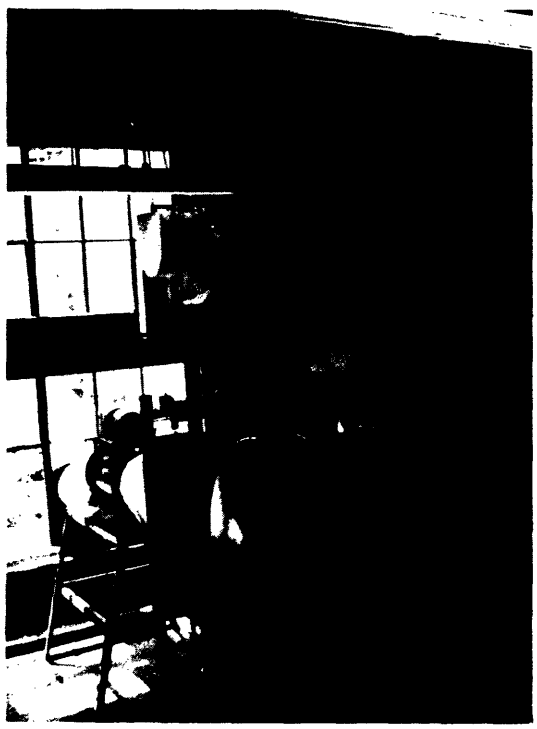

1/2 TON OVERHEAD CRANE WITH 'I' BEAM

Figure 29

REMOVABLE COVER (IN PLACE)

Figure 30

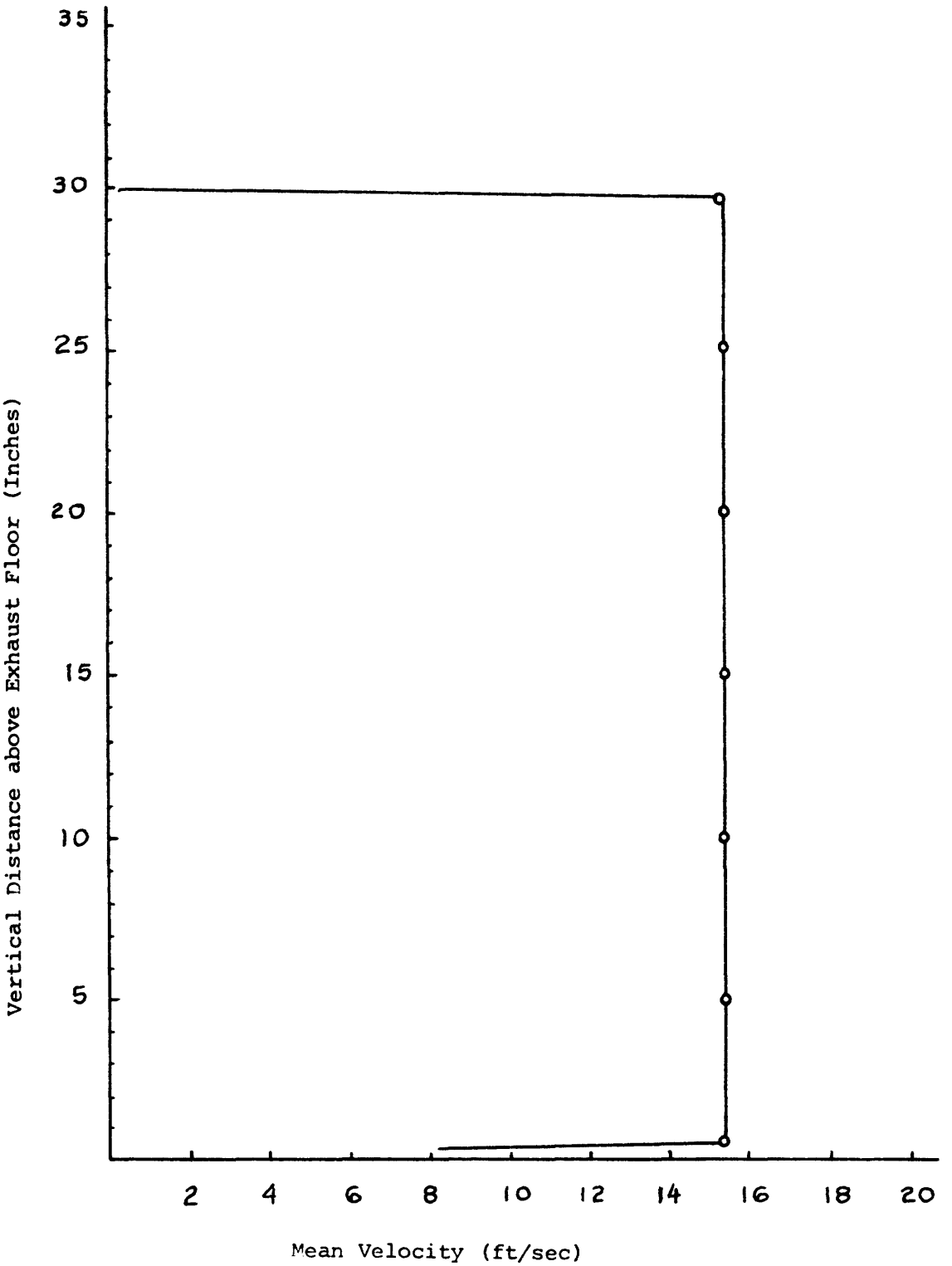

MEAN VELOCITY PROFILE IN CONTRACTION CONE OUTLET

Figure 31

a two percent deviation was noticed across several traverses. A calibration curve was constructed correlating pitot tube air velocities with static pressure tap velocities (Figure 32). The air mass flow rate used in future heat transfer experiments will be determined using this curve. The test section outlet air velocity profile will be made using standard pitot tube techniques. Air swirls created by the fan blades several feet downstream from this point will be prevented from traveling upstream and possibly affecting the pitot tube results by the installation of a 6 inch thick section of flow straighteners installed in the air stream.

II.2.1.9 Air Temperature Distribution

Air temperatures entering the contraction cone are measured with a mercury thermometer placed at the entrance to the contraction cone. Due to the low air velocities involved, no measurable air temperature increase has been detected through the contraction cone. Air temperature leaving the test section will be measured with a rake of 30 thermocouples which has been installed on the removable air cover just downstream of the test section (Figure 18). These temperatures will be used to determine an average temperature out of the test section, and to determine if the air baffle above the rotating discs is effective in equally distributing the air flow throughout the test section.

II.2.1.10 Fan Capacity

The fan capacity was controlled in two ways during these tests. Major air velocity changes were accomplished by partially blocking the fan suction with specially made sheetmetal baffles. Fine air velocity adjustments were made by using a variable air gap which allowed outside air to be drawn into the fan, thus reducing the air flow through the test section. This was done a sufficient distance downstream from the 30 thermocouples and the point of the pitot tube traverse to insure that this air flow did not affect these measurements.

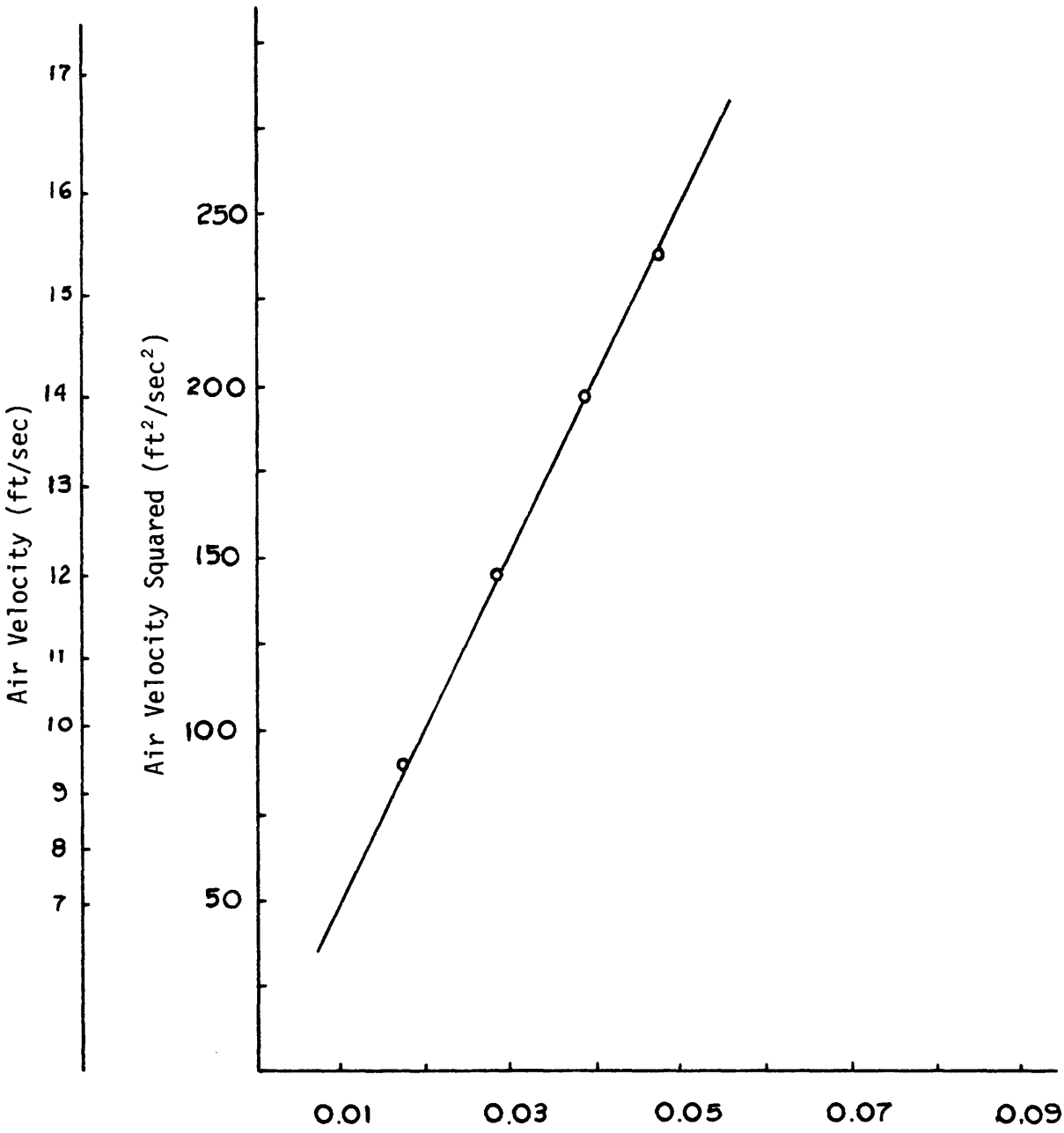

CONTRACTION CONE AIR VELOCITY CALIBRATION CURVE

Figure 32

II.2.2 Measurement of the Disc Oil Layer Thickness

The oil floated on the water surface eliminates water evaporation, but also coats the discs with a thin layer of oil. The thermal resistance of this layer decreases the overall heat transfer performance of the disc as the compared to a non-oiled surface. Depending upon the thickness of the oil layer, this decrease can be as much as 20-25%.

For the proper evaluation of the periodic surface and its optimization, it is imperative to know the oil layer thickness at given disc locations. This thickness is of course a function of disc size, RPM, oil viscosity, floating oil thickness, etc. Emperical and theoretical formulation for estimating the oil thickness exist (6, 13) but do not strictly apply to the periodic tower geometry. Thus it was decided to experimentally measure film thickness on the actual full sized disc.

Several methods of experimental thickness determination were considered. One of these was a capacitance method [14], which used the oil layer thickness as a dielectric of a capacitor. Here, the disc serves as one plate and a small plate fixed in space close to the disc, serves as the other. For a fixed plate to disc distance, the changing of thickness in between the disc and the small plate in theory would change the capacitance. The capacitance value could be determined by connecting it into an oscillator circuit and finding the resonant frequency. The major stumbling block with applying this technique to the oil thickness determination is the wobbling and fluctuations inherent in the rotating disc. The plate to disc distance is then not constant, and it seemed that large uncontrollable errors would be introduced because of this wobbling. Other methods [15,16] such as X-rays and absorption techniques were considered as too expensive and complicated and so were rejected as possible methods.

It was decided to measure the thickness mechanically by measuring the volume flow across small sections of the discs. Using a rubber wiper and a collection device, the oil flow across a small section could be picked off for an arbitrary time span and then measured in a graduated cylinder. The collector would be placed such that the wiper edge was perpendicular to the

velocity of the disc at the measuring points. This meant that the edge of the wiper lay along the disc radii. (Figure 33)

II.2.2.1 First Method of Thickness Calculation

Once the volume flow at a particular point was measured, the thickness could be calculated in several different ways. The first method used to calculate the thickness assumed that oil velocities relative to the disc were small. In other words, the oil was assumed to stick to the disc like glue, changing only its thickness as it rotates around. The oil thickness would have a uniform velocity equal to the tangential speed of the disc at the measured point. Also assumed was the fact that thickness was time independent, only varying with angular and radial position on the disc, parameters such as RPM, oil quantity, and temperature. With these assumptions, then

$$Q = \delta \ell \bar{v}_n \qquad [26]$$

where Q is measured in volume flow, δ is oil layer thickness, ℓ is length of wiper, and $\bar{v}_n$ is average speed of the oil film.

For no relative motion between the oil and the disc,

$$\bar{v} = \omega r \qquad [27]$$

where ω is the angular velocity of the disc and r is the radius of the measuring point. Then, substituting [27] into [26] and solving for oil thickness,

$$\delta = \frac{Q}{\ell \omega r} \qquad [28]$$

Thus, measuring the oil volume flow, and knowing ℓ, ω, and r , an approximate thickness can be determined.

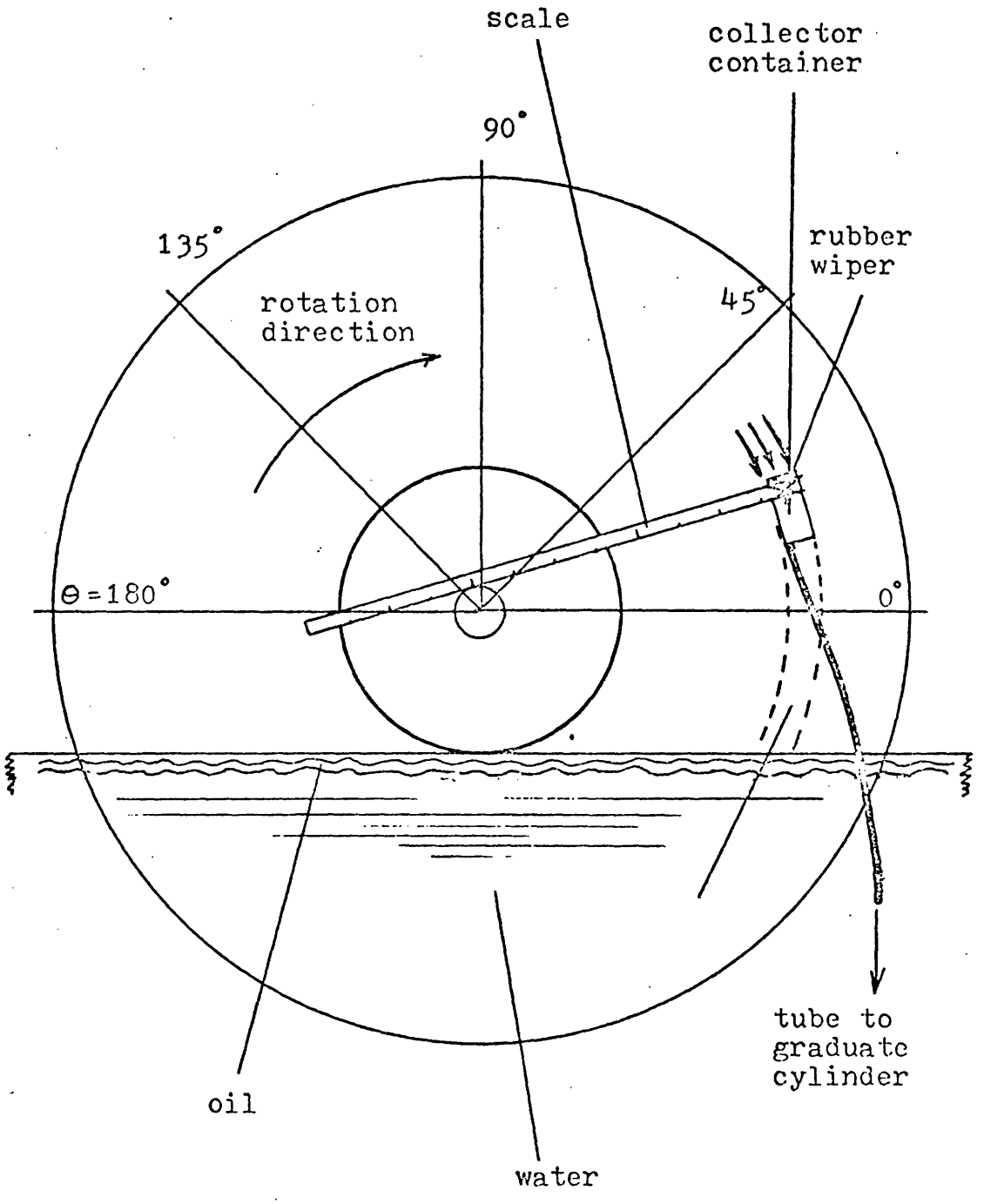

CONCEPTUAL DRAWING OF MEASUREMENT SCHEME

Figure 33

Dividing by dx dy dz and substituting for dm yields

$$\frac{d^2v_y}{dx^2} = \frac{\rho g}{\mu} \qquad [33]$$

Integrating twice, the general solution is

$$v_y = \frac{\rho g}{2\mu} x^2 + Ax + B \qquad [34]$$

which is the standard parabolic velocity profile [17]. To find the constants, use the boundary conditions

$$v_y = v_o \qquad @\ x = 0 \qquad [35]$$

and

$$\mu \frac{dv_y}{dx} = \tau_o = \frac{\text{Force}}{\text{Area}} = \rho g \delta \qquad @\ x=0$$

or

$$\frac{dv_y}{dx} = -\frac{\rho g \delta}{\mu} \qquad @\ x = 0 \qquad [36]$$

then

$$B = v_o \qquad [37]$$

$$A = -\frac{\rho g \delta}{\mu} \qquad [38]$$

giving

$$v_y = \frac{\rho g}{2 \mu} x^2 - \frac{\rho g \delta}{\mu} x + v_o \qquad [39]$$

To find the average velocity

$$\bar{v}_y = \frac{1}{\delta} \int_0^{\delta} v_y dx = \frac{1}{\delta} \left[\frac{\rho g}{6\mu} \delta^3 - \frac{\rho g}{2\mu} \delta^3 + v_o \delta \right]$$

II.2.2.2 Second Method of Calculation (Modified Thickness Calculation)

The above method was used as a first solution to the problem. However, the assumptions are not completely valid for certain portions of the disc, particularly for thick oil layers (>10 mil). As the oil layer becomes thicker, there is an appreciable oil velocity relative to disc due to gravity. This relative velocity becomes larger as the layer becomes thicker and must be accounted for in the thickness determination. This is especially true for thick oil at small radii. For these thick oil regions, the oil velocity down the disc is a significant fraction of the tangential speed (on the order of 30 to 40% at the smallest radius).

To account for these effects, a simplified view of the oil flow down the disc is taken. The vertical oil flow relative to the plate is assumed to reach a steady state balance between viscous and gravity forces. Horizontal speed is assumed to have no effect on the velocity profile as centrifugal effects are small. For oil of thickness δ running down the vertical moving plate, the following is true: For a mass element dm of fluid where acceleration is small

$$F_2 - F_1 = g\, dm \qquad [29]$$

where

$$F = \mu \frac{dv_y}{dx}\, dy\, dz \qquad [30]$$

and

$$dm = \rho\, dx\, dy\, dz \qquad [31]$$

See Figure 34.

then $F_2 - F_1 = \mu\, d\, (\frac{dv_y}{dx})$

or

$$\mu\, d\, (\frac{dv_y}{dx})\, dy\, dz = g\, dm \qquad [32]$$

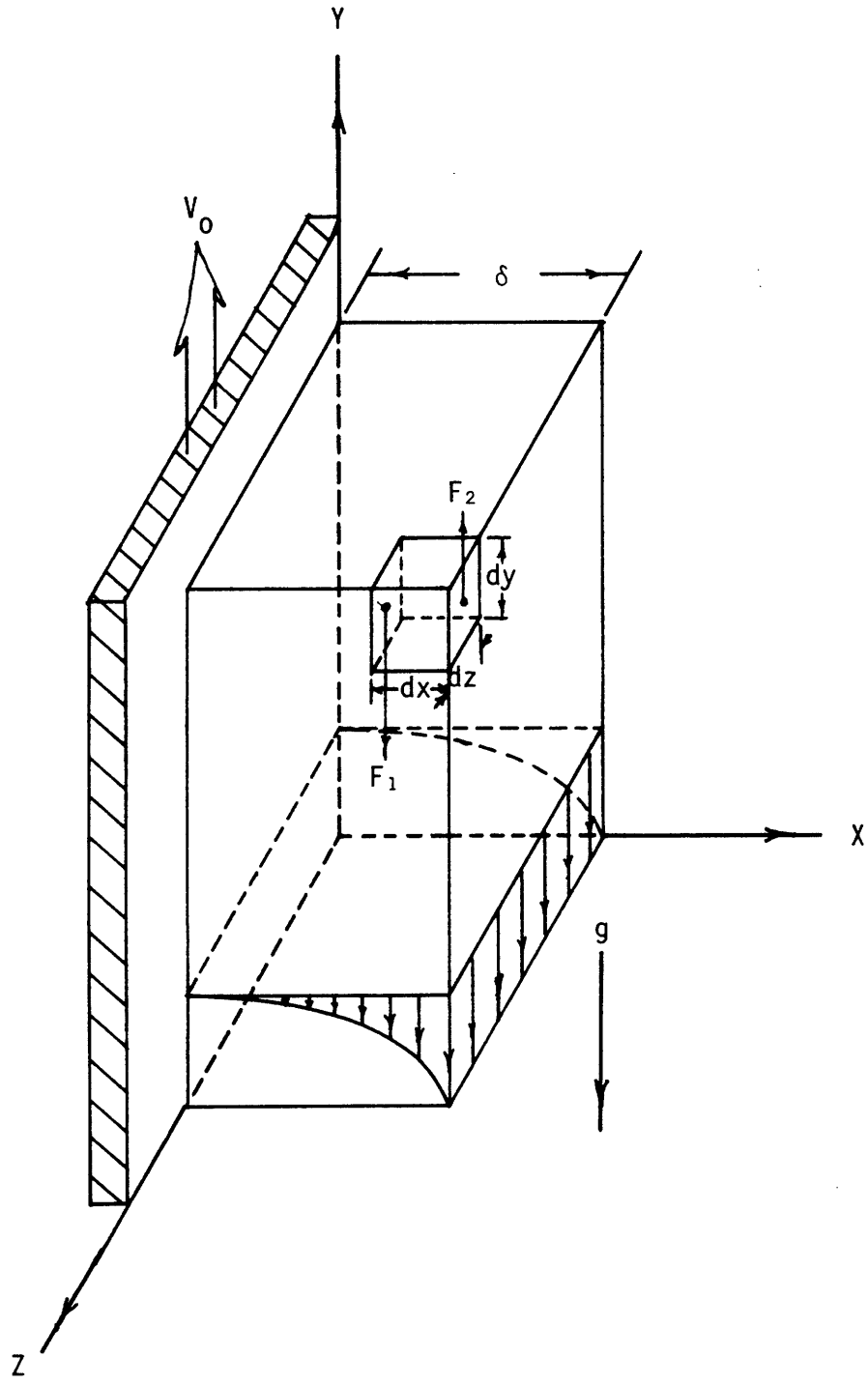

MODEL OF OIL FILM ON A FLAT PLATE

Figure 34

or

$$\bar{v}_y = v_o - \frac{\rho g}{3\mu}\delta^2 \qquad [40]$$

Now that we have an expression for the average velocity of fluid relative to ground, we can relate flow collected Q to thickness δ . For the configuration shown in Fig. 34 from the previous analysis, the average velocity of the oil relative to the disc is (using vector notation)

$$\bar{V}_r = V_{rx}\,\hat{i} + V_{ry}\,\hat{j} \qquad [41]$$

where

$$V_{rx} = 0 \qquad [42]$$

$$V_{ry} = -\frac{\rho g}{3\mu}\delta^2 \qquad [43]$$

The velocity of the disc at any point is

$$V_D = \omega r(\sin\theta\hat{i} - \cos\theta\hat{j}) \qquad [44]$$

Then the velocity of oil relative to ground $\bar{V}_o$ is

$$\bar{V}_o = V_D + \bar{V}_r \qquad [45]$$

$$V_o = (\omega r \sin\theta)\hat{i} - (\omega r \cos\theta + \frac{\rho g}{3\mu}\delta^2)\hat{j} \qquad [46]$$

The component of $\bar{V}_o$ normal to pickup, called $\bar{v}_n$, is responsible for flow collected. This is found by taking the dot product with the unit vector normal to pickup wiper blade.

$$\hat{n} = \sin\theta\,\hat{i} - \cos\theta\,\hat{j} \qquad [47]$$

$$\bar{v}_n = \bar{V}_o \cdot \hat{n} = \omega r \sin^2\theta + \omega r\cos^2\theta + \cos\theta\,\frac{\rho g}{3\mu}\delta^2$$

or

$$\bar{v}_n = \omega r + \cos\theta\,\frac{\rho g}{3\mu}\delta^2 \qquad [48]$$

Using [48] instead of [27] and substituting in [26], we arrive at

$$Q = \omega r \ell \delta + \cos\theta \frac{\rho g}{3\mu} \ell \delta^3 \qquad [49]$$

which is a cubic equation relating flow measured to oil thickness and known parameters.

The cubic equation can be solved by dividing [49] through by $\cos\theta \frac{\rho g \ell}{3\mu}$ (for $\cos\theta \neq 0$) giving the equation

$$\delta^3 + a\delta + b = 0 \qquad [50]$$

where

$$a = \frac{3\omega r \mu}{\rho g \cos\theta} \qquad [51]$$

$$b = -\frac{3\mu Q}{\rho g \ell \cos\theta} \qquad [52]$$

For $\cos\theta = 0$, equation [49] reduces to [26]. Equation [50] has standard solutions which are given in Appendix D along with data.

Thus, we have two equations which can be used to determine the thickness δ at a measuring point. If relative motions of oil on discs are small compared to its tangential speed, then we can use [28]. If this assumption is not valid as is the case for small radii with a thick oil layer at the horizontal positions (θ near 0^0 or 180^0), then modifications must be made which account for relative oil flow. This results in [50] which is solved in Appendix D.

II.2.2.3 Apparatus and Results

II.2.2.3.1 The First Apparatus

The first device constructed is shown in Fig. 35. It is simply a 2 inch section of an automobile wiper attached to a small sheet metal collector box. The collector box has a bulkhead fitting with a 1/4 inch tubing that drains into a graduated cylinder. The collector box is attached to the end of a yardstick which serves as the radius indicator and keeps the wiper perpendicular to the tangential velocity.

To use the device, the collector box is held such that the rubber wiper scrapes a clean layer of oil off the disc. The yardstick is held tangent to the disc center-shaft at the desired radius. The flow was collected over a minute interval, long enough to get a good average flow measurement for all positions. Because of the limitations of the device, measurements were taken only along the down rotation side at $\theta = 0^{o}$ of the front side of a disc. At that time, only one disc was used in the rig. Other discs were not put on until the second device was used. The thicknesses are in mils ($1x10^{-3}$ inches) and are plotted in Fig. 36 as a function of radius. Thicknesses have been calculated using both equations [28] and [50] (calculated results are in Appendix B). Those using equation [50] are named "modified" results in the graph. The tests were taken at oil temperatures of $67^{o}F$ and $129^{o}F$, and an RPM of 5.0. 1 gallon of GE Silicone Fluid SF-96 whose properties are in Appendix C was used. The effect of extra oil was demonstrated by adding an extra gallon. The results are also in Fig. 36.

For these tests, thickness values range from an average of 19 mils at an inner radius of 11 inches to 6.5 mils at a 27 inch radius. When results are obtained using the solution to equation [50], the average thickness at an 11 inch radius is somewhat less at about 14 mils. At the outer radius, both results are nearly the same as expected. From observations, the oil layer in this region is very thin and as a result, the relative velocity of oil in this region is small.

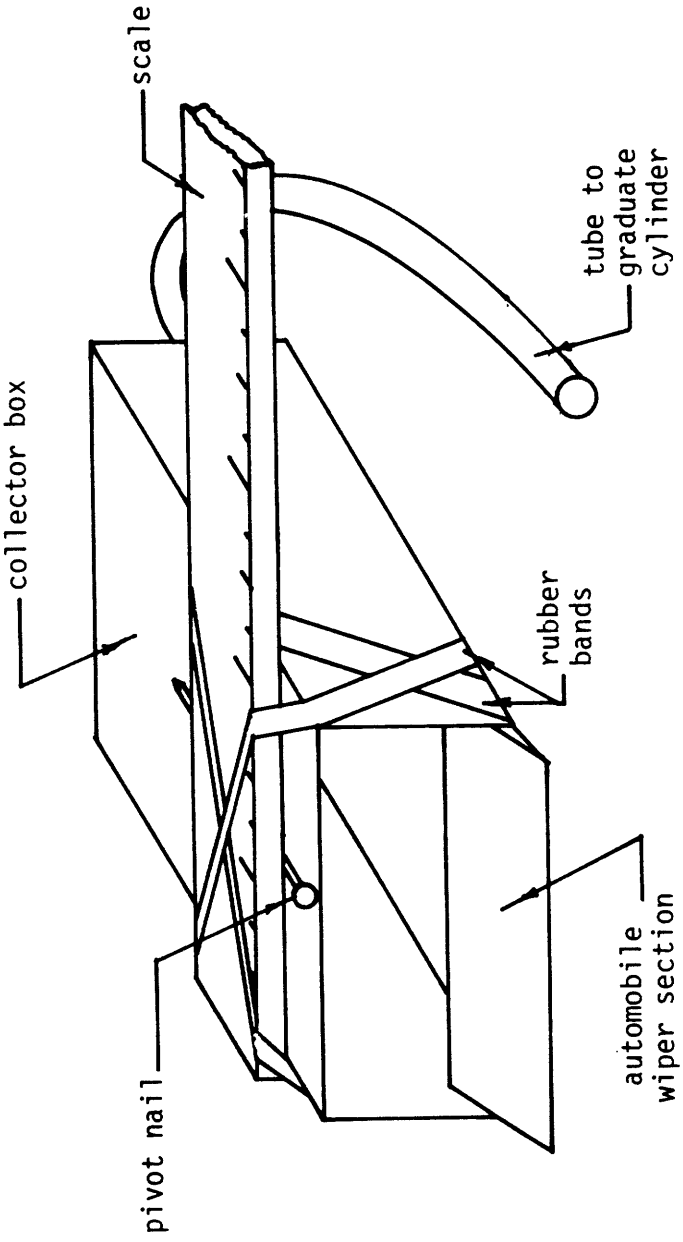

THE FIRST APPARATUS
FOR OIL FILM COLLECTION

Figure 35

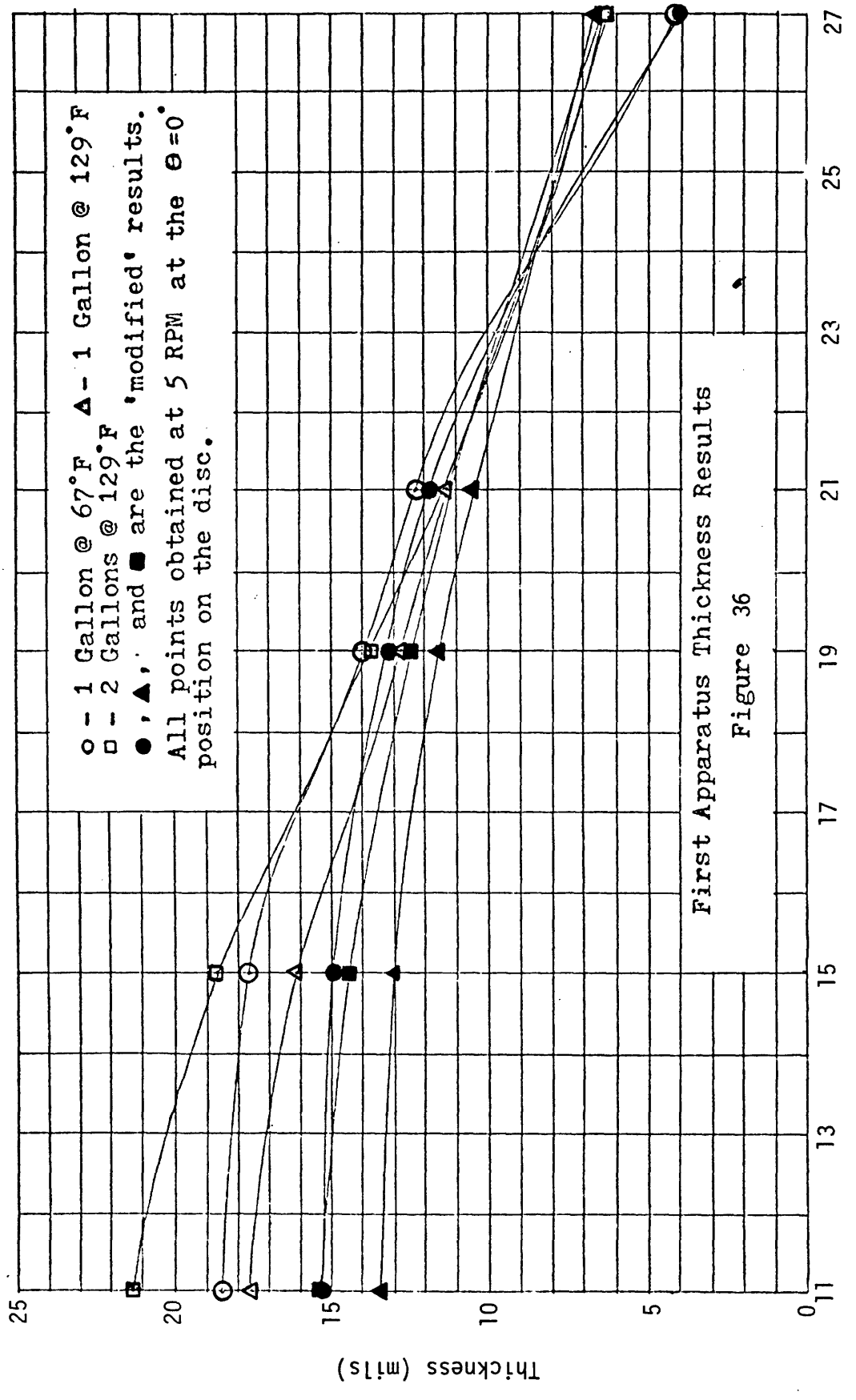
o - 1 Gallon @ 67°F Δ - 1 Gallon @ 129°F
□ - 2 Gallons @ 129°F
●, ▲, and ■ are the 'modified' results.
All points obtained at 5 RPM at the θ=0° position on the disc.
First Apparatus Thickness Results
Figure 36
Thickness (mils)
Radius (in)
0
5
10
15
20
25
11
13
15
17
19
21
23
25
27

The effect of doubling the amount of oil in the trough from one to two gallons @129^{o}F increased the average thickness (using eq. [50]) 12% at the inner radius of 11 inches (from 12.3 mils to 15.3 mils). At the outer radius of 27 inches, the thickness remained at 6.4 mils.

The effect of RPM on the oil layer region is shown in Fig. 37. As shown in the graph, RPM is a significant parameter for the amount of oil drawn up on the disc. Modified thicknesses are plotted as a function of radius for 2.75, 5, and 8 RPM.

From the preceeding, one can conclude that some useful information was obtained from measurements taken with the first device. But this device is extremely limited; only on the downside section for small values of θ can a flow be measured and a thickness calculated. For other areas, (as when $90^{o} < \theta < 180^{o}$), some device not relying on gravity must be used to draw the oil off the rubber wiper and into a collector for measurement.

II.2.2.3.2 The Second Apparatus (Vacuum Pickup)

The second device was a simple vacuum system which would draw oil off the disc by suction. The pickup and apparatus are shown in Fig. 38. The pickup was made using thirty plastic straws 3/64 inches in diameter, cut to 6 inch lengths. These lengths were lined up parallel to each other for a 2 inch width and placed on a 2 inch long piece of rubber cut into a wiper. The straws were clamped down on the blade with a small plexiglass bracket held together with small bolts and nuts. It was clamped so that the ends of all the tubes nearly lined up with the leading edge of the wiper blade. The other ends were broken up into 4 bundles and each of these bundles was inserted into 1/4 inch rubber tubing. RTV silicone rubber sealed up the connections. By the use of T-joints, a manifold was made which connected the 4 bundles to a single vacuum line.

The vacuum line connects the pickup to a 1000 ml aspirator bottle. The aspirator bottle acts as a trap preventing collected oil from going into the vacuum pump which is attached to the fitting in the aspirator neck. A right angle glass tube, which passes through a rubber stopper, connects the pickup hose to the aspirator bottle. Oil collects in the aspirator, being drawn in by the vacuum created by a Cenco vacuum pump.

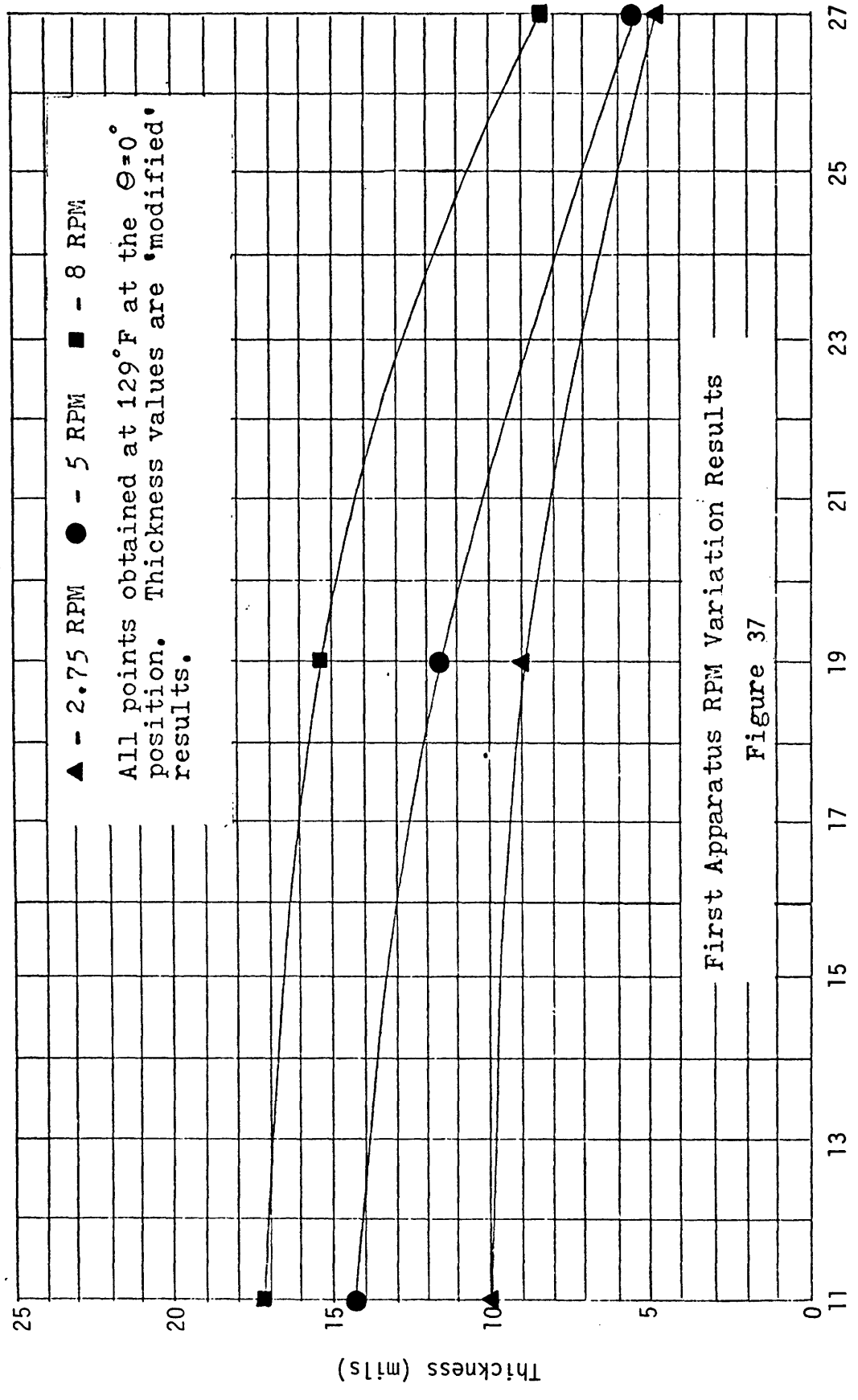
▲ - 2.75 RPM ● - 5 RPM ■ - 8 RPM
All points obtained at 129°F at the Θ=0° position. Thickness values are 'modified' results.
First Apparatus RPM Variation Results
Figure 37
Thickness (mils)
Radius (in)
25
20
15
10
5
0
11
13
15
17
19
21
23
25
27

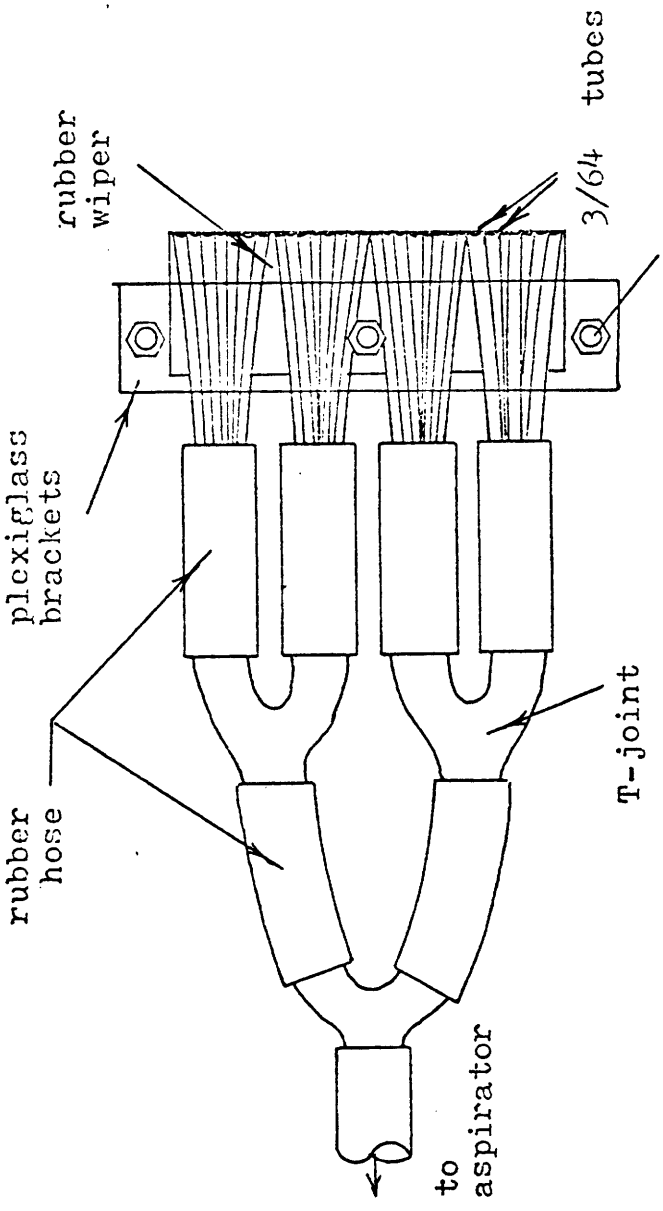

THE SECOND APPARATUS
FOR OIL FILM COLLECTION

Figure 38

The operation of the device is similar to the first device. To make a measurement, the device is held at the desired radius and angle θ with the aid of a yardstick that is clamped to a fixed piece surrounding the axle shaft of the heat exchanger. It is held there for a one minute interval and then removed. The volume of oil collected in the aspirator bottle is measured in a graduated cylinder and recorded along with the appropriate r and θ. This process was repeated for many positions over the entire disc, both the front and backside.

Measurements were taken for various operating conditions. The first set of measurements were taken with the disc rotating at 4 RPM and a water temperature at 58^{o}F. In all the tests using the vacuum pickup, the total quantity of oil used was 3.5-4.0 gallons. Measurements were taken at 9 radial locations and at 8 angular stations on the front side of the disc. The resulting thickness distribution calculated using equation [50] is shown in Fig. 39. The thickness is proportional to $\sqrt{(RPM)(r)}$ for $\theta = 180^{o}$, which is close to that predicted in the Levich analysis, discussed in the next section. At angles of $\theta = 150^{o}$ and 135^{o}, it is significant to note the very thick layers (21-23 mils) that occur near the outer radius. The disc, having a somewhat irregular edge, retains oil on this edge until a sufficient angle above the horizontal is reached. When this occurs, the excess oil on the edge runs down the disc surface. This process is occurring at $\theta = 150^{o}$ and 135^{o}. At $\theta = 120^{o}$ the excess runoff at the edge is essentially complete. The excess oil from the edge shows itself as an increased oil thickness in the middle radii (thickness increases from 17 mils to 20 mils) of $\theta = 120^{o}$ and $\theta = 90^{o}$. By $\theta = 60^{o}$, the oil layer is diminishing at the outer radii (7 mils) and increasing from small radii (from 7 to 20 mils). By $\theta = 30^{o}$, the oil is thickest at the smallest radius (20 mils @ r = 11 inch) and tapers off to a 6 mil thickness at a 27 inch radius. The thickness distribution changes little at $\theta = 0^{o}$ from that at $\theta = 30^{o}$.

The second set of measurements was taken at 4 RPM at the assumed operating temperature of 130^{o}F utilizing 3.5 gallons of oil. The oil viscosity is reduced by a factor of roughly 2 and as a result, thinner layers of oil are lifted by the rotating disc. Fig. 40 shows the thickness distribution

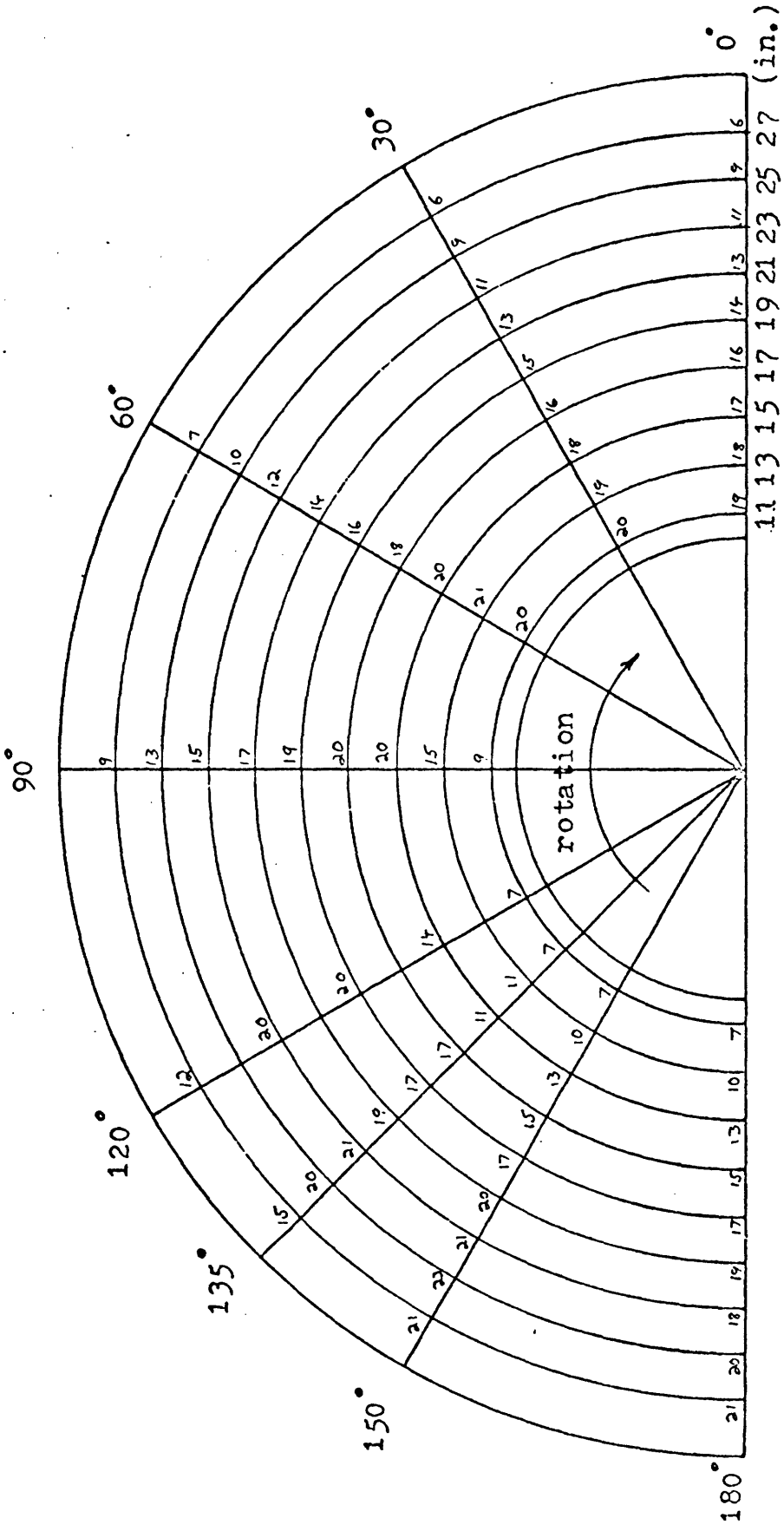

Modified Thicknesses of Disc Frontside at 58°F and 4 RPM

Figure 39

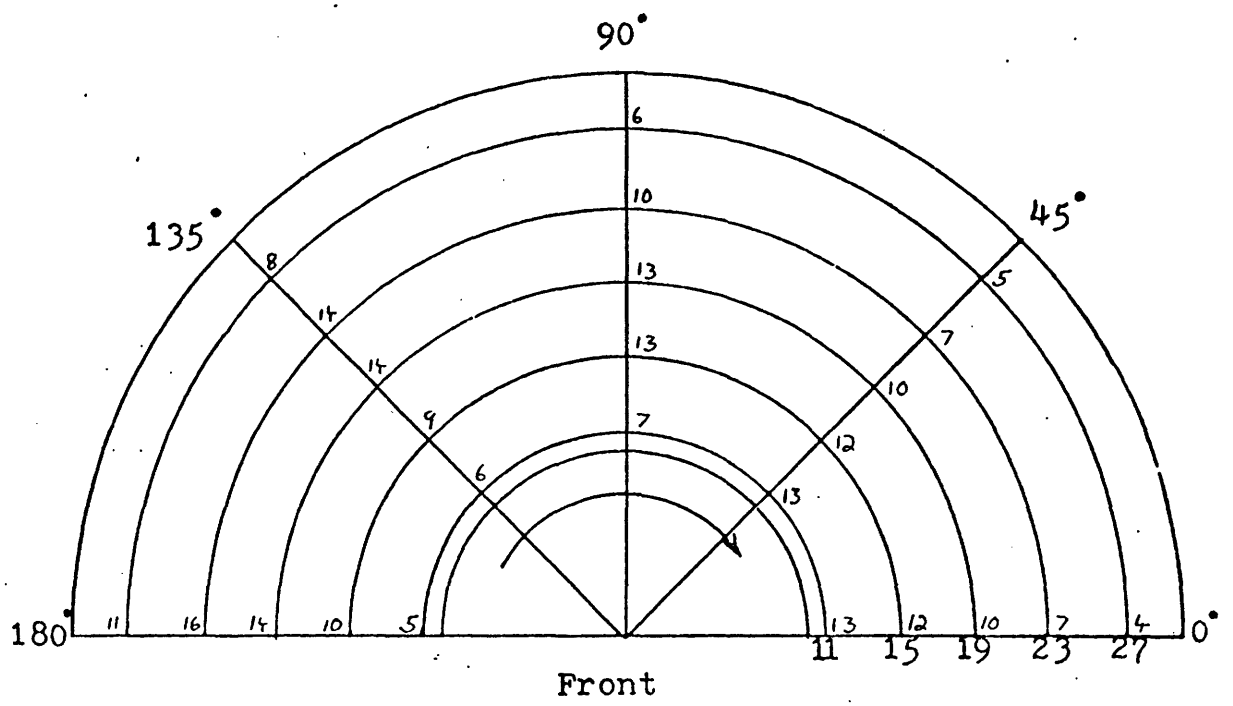

Front

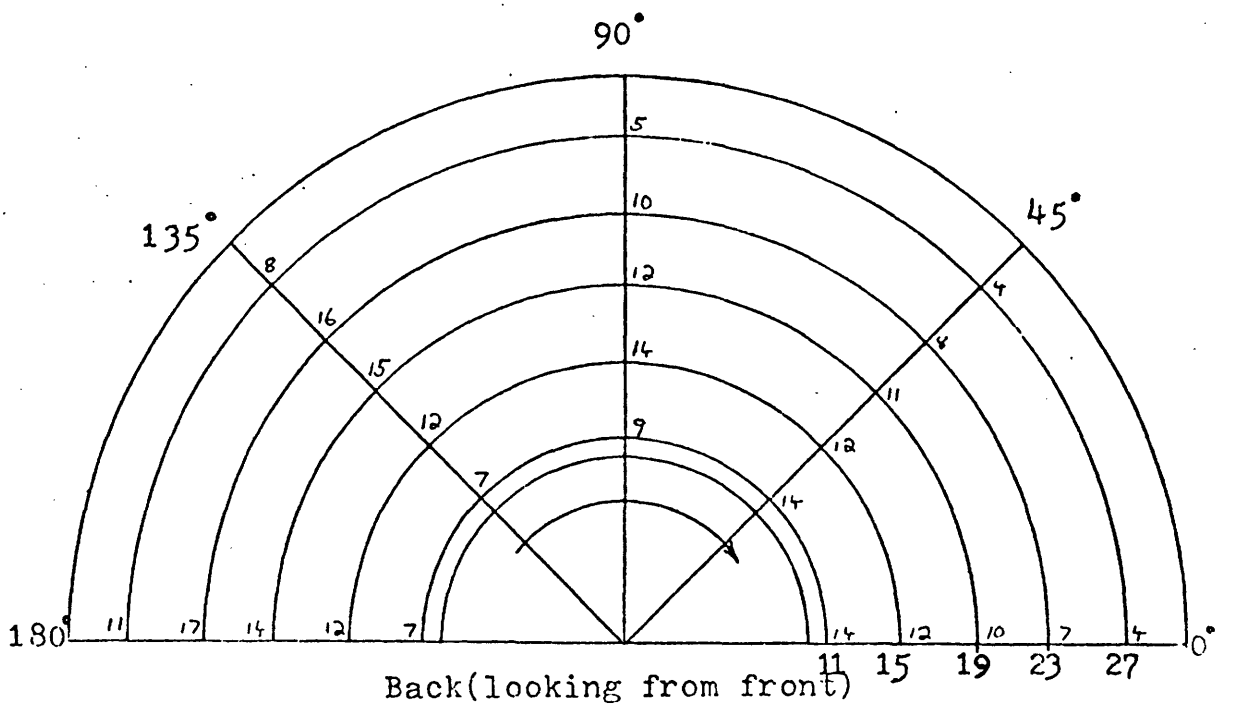

Back(looking from front)

Thickness Distribution at Operating Temperature
(130°F @ 4 RPM)

Figure 40

obtained for both the front and back side of the discs. The general thickness variation is similar to that obtained in previous sets of results, but at much reduced average thickness levels. The thickest layers are 17 mils rather than the previous 21 mils.

In the third set of measurements, the RPM was varied to determine its effect upon thickness. Oil was collected from four selected points; at θ = 180° and 90° for radii of 19 and 25 inches. The disc was run at speeds of 2, 4, and 6 RPM. For θ = 180°, the thickness is proportional to the square root of withdrawal speed ($\sim\sqrt{(RPM)(r)}$) at r=19 inches but not at r=25 inches. The relation is also approximately true at θ =90. To see the proportionality, $\delta/\sqrt{(RPM)(r)}$ has been plotted as a function of RPM for the four different positions measured in Fig. 41. The results of this can be used to approximate the thickness at any point for RPM's not measured in this study.

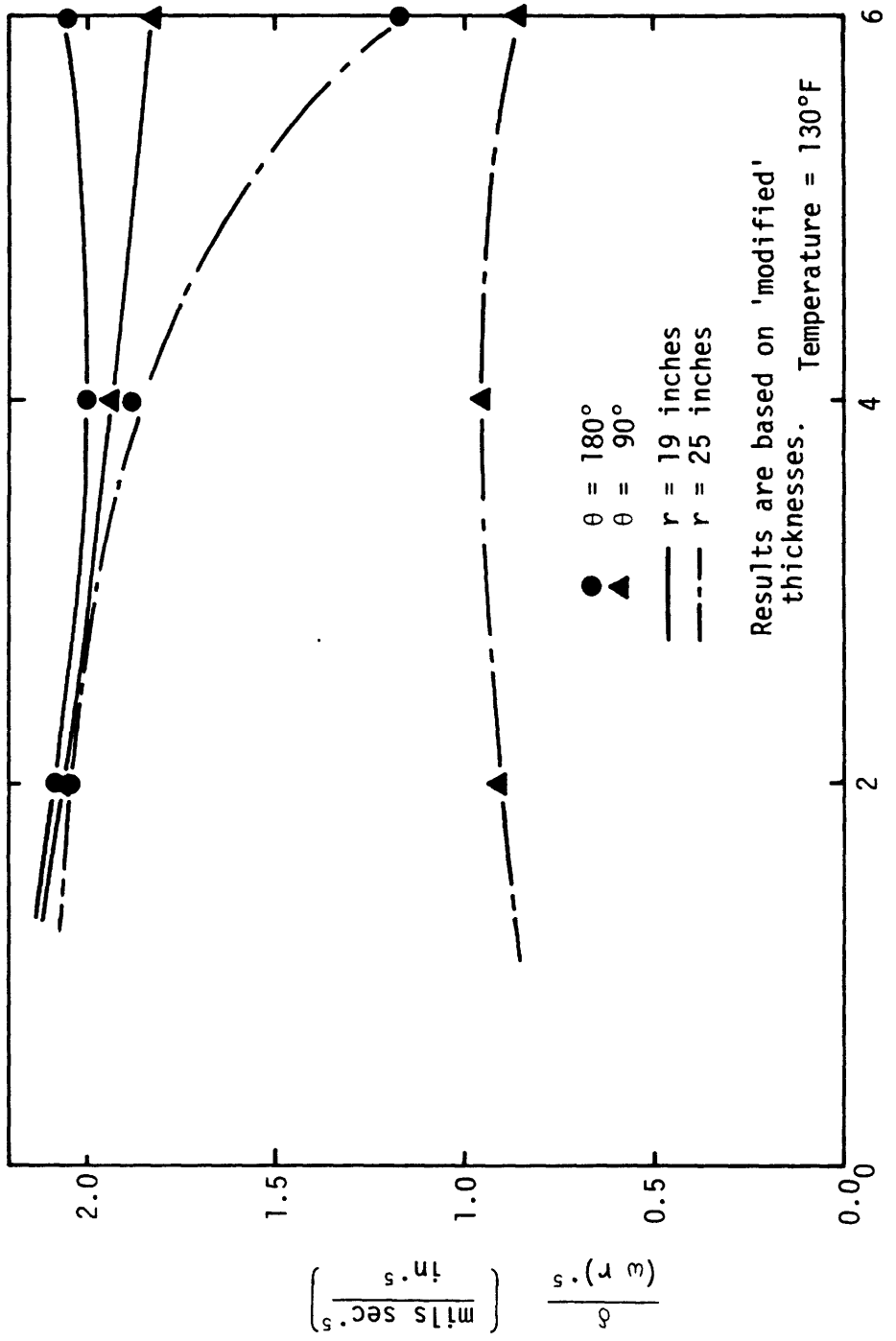

SECOND APPARATUS VARIATION WITH RPM

Figure 41

II.2.2.4 Comparison with Theory

While there was no means of calibrating the vacuum device to determine its accuracy, the results are compared for total flow at different θ's with the theory of Levich [6] and with an EPA study [13] to see if any degree of agreement existed.

In the Levich theory a solution was derived for an oil layer thickness on vertical plates being drawn at a uniform velocity out of an oil layer of infinite extent. Levich gives thickness as a funciton of V_o, the plate withdrawal rate, and the various oil parameters V, ρ, and σ. Using this thickness value, the disc velocities as the withdrawal rate, and integrating over the entire radius at $\theta = 180^o$, an upper bound was found for the amount of oil being picked up by the disc. For the analysis (Appendix E), the amount of oil picked up is 54.1 ml/sec. In the experimental case, the value was found by adding up the flows picked up. This value was 35 ml/sec which is considerably lower than the theoretical Levich value. However, the theoretical value is an upper bound because the integration was done under the assumption of no oil movement relative to the disc. The Levich thickness predicting the $\theta = 180^o$ radius has been plotted with the modified thickness values obtained by measurement with the second apparatus in Fig. 42.

Using the model in the EPA study [13], the calculated amount of oil picked up is 37.6 ml/sec; which is very close to the experimental value of 35 ml/sec (see Appendix F for calculation details).

As a check for consistancy of flow values recorded, all measurements at $\theta = 180^o$ position were performed twice in the first set of measurements using the vacuum pickup. In these cases, the variation in successive flow readings was in most cases less than 5%. At r = 13 inches, the variation from the average flow was 10%.

As a second check, the continuity of total flow was checked across different angular positions. The flows for a particular θ were summed and compared with the average value of total flow across all measured positions. In

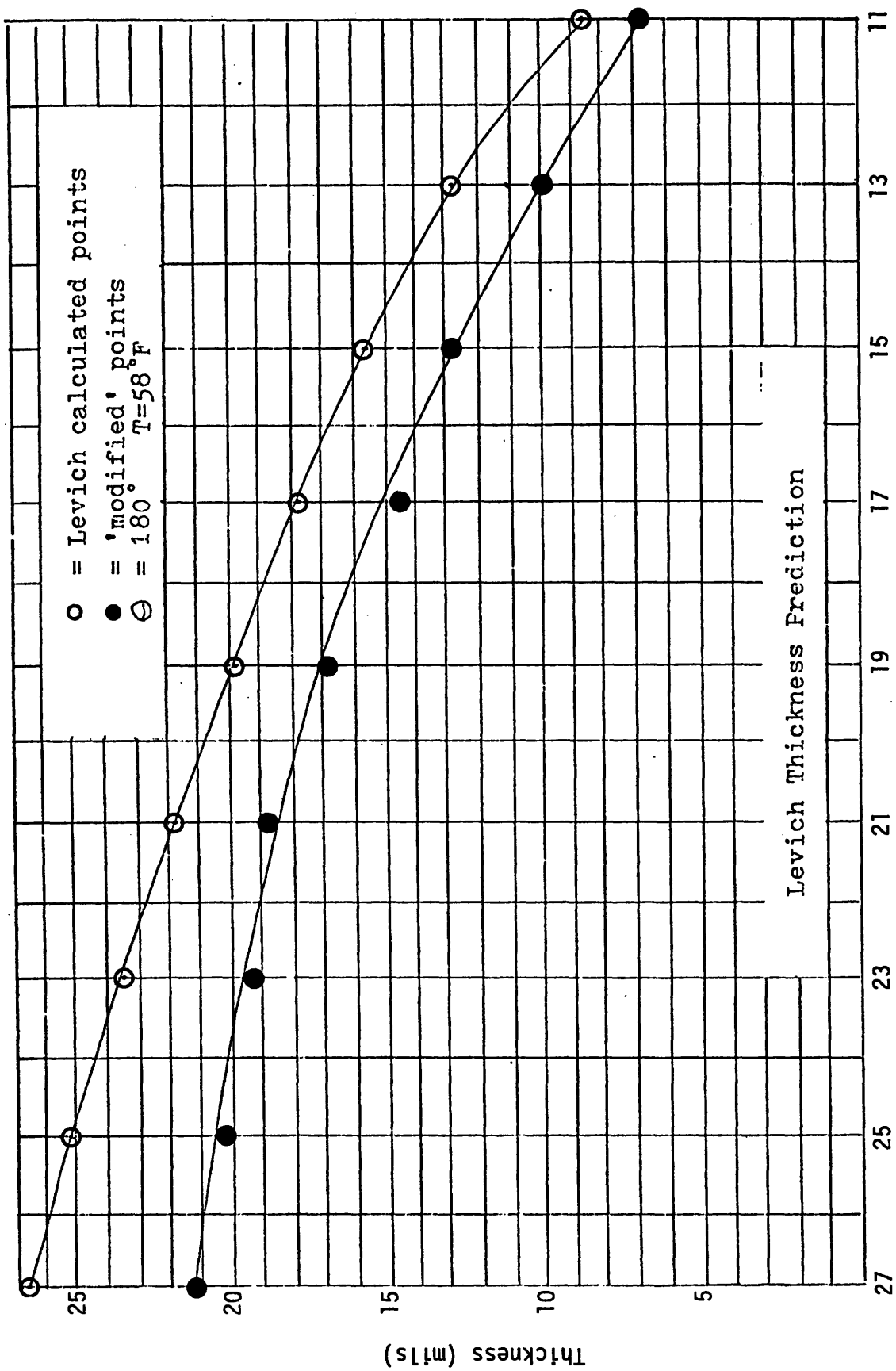
Levich Thickness Prediction
O = Levich calculated points
● = 'modified' points
Θ = 180° T=58°F
Thickness (mils)
25
20
15
10
5
11
13
15
17
19
21
23
25
27
Radius (inches)

Figure 42

the first case of measurements, the average total flow was 2090 ml/min. Most measured flows across sections varied from this average by less than 5% and in one case was low by 8%. This 8% variation was at $\theta=0^{o}$ where some oil flows down into the center section of the disc. This means that less oil flows in the measured region between r = 10 to r = 27 inches.

The accuracy of the thickness measurements is within 10% which is sufficient for numerical solution methods of heat transfer work. The pickup works very well, leaving negligible amounts of oil behind it and does not disturb to any great degree the oil immediately to either side of the 2 inch wiper.

II.3 Heat Transfer Augmentation by Surface Roughening

II.3.1 Introduction

As with all liquid-gas heat exchangers, the major resistance to heat transfer lies on the gas side. Any augmentation of the air side heat transfer coefficient will increase the performance of the heat exchanger.

As reported in last year's annual report (5), adding square-rib roughness elements to smooth surfaces will increase air side heat transfer coefficients. An economic optimization indicated that for a 1000 MW electric power plate, the use of such surface roughening elements would decrease the incremental and capital costs of the rotary heat exchanger by about 20%.

This previous ribbed surface study was based on existing correlations to predict the heat transfer coefficient and friction factor. However, the correlation was not based on the same geometry and flow conditions as exhibited by the rotary heat exchanger. For instance, the coating oil layer will change the square-rib profiles by rounding all sharp edges or corners and may affect the heat transfer coefficient and friction factor. Further, as the ribs are on a rotating disc, the angle between the rib and the flow direction is constantly changing from 0^{o} to 180^{o} and will affect the heat transfer coefficient and friction factor also.

To realistically evaluate disc ribbing, the functional dependence of heat transfer and friction on rib shape and angle of attack must be determined for the Reynold's flows that the discs will experience. This more detailed study is being examined both analytically and experimentally, and is discussed in the following sections.

II.3.2 Analysis

Virtually all prior heat transfer measurements for rib roughened surfaces have been made on internally roughened pipes. Although such experiments are by no means geometrically similar to the discs of the periodic heat exchanger, the results and analysis yield insights into the nature of the problem. For fully developed turbulent flow inside a smooth tube, the heat transfer coefficient depends on both the Prandtl number and Reynold's number, while friction factor depends solely on the Reynold's number [7].

$$f \simeq 0.0791/Re^{0.25} \qquad [53]$$

$$\frac{hD}{K} \simeq 0.023\ Re^{0.8} Pr^{0.4} \qquad [54]$$

where

f = friction factor
h = heat transfer coefficient
Re =Reynolds number (VD/ν)
D = hydraulic diameter
K = thermal conductivity
Pr = Prandtl number ($\mu C_p/K$)

For fully developed turbulent flow inside a tube internally roughened with rectangular ribs normal to the flow, the heat transfer coefficient depends not only on the Prandtl and Reynolds number, but also on the relative rib and tube dimensions. In this regime, the friction factor depends only on the roughness dimensions. Reference [18] yields the following correlations:

$$\sqrt{2/f} = 2.5\ \ln(D/2e) - 3.75 + 0.95\ (P/e)^{0.53} \qquad [55]$$

$$St = \frac{f/2}{1 + \sqrt{f/2}\ \left[4.5(e^+)^{0.28}\ Pr^{0.57} - 0.95\ (P/e)^{0.53}\right]} \qquad [56]$$

$$e^+ = \frac{e}{D} Re\sqrt{f/2} \geq 30, \text{ Defined as the fully roughened region} \qquad [57]$$

where

$$\frac{e}{D} = \frac{\text{transverse rib height}}{\text{tube diameter}}$$

$$\frac{P}{e} = \frac{\text{space between ribs}}{\text{transverse rib height}}$$

St = Stanton number $(h/C_p \bar{\rho} \bar{V})$

And the limits on the experimental variables are:

$$0.01 \leq \frac{e}{D} \leq 0.04$$

$$10 \leq \frac{P}{e} \leq 40$$

$$10^4 \leq Re \leq 2 \times 10^5$$

II.3.2.1 The effect of the Rib Profile

Equations [55], [56] and [57] were based on rectangular rib profiles with sharp edges in pipe flow. In the rotary heat exchanger, the flow is essentially that between parallel plates, and the oil layer coating the discs will change the rib profile by rounding all sharp edges and corners. Since the actual profiles of the oil coated rib are difficult to measure, several different shapes of rib profiles (square, trapezoidal and triangular) will be machined on aluminum surfaces to simulate the oil coated ribs (figure 43).

The major contribution to transfer augmentation (the friction factor increases also) is the continual breaking down of the laminar sublayer by the ribs. Thus, the relative magnitude of the laminar sublayer thickness and the rib height is an important factor in this mechanism. In order to understand the impact of the rib profile in heat transfer augmentation by surface roughening, consider more closely equations [55] and [57] and the pipe flow for which they are relevant.

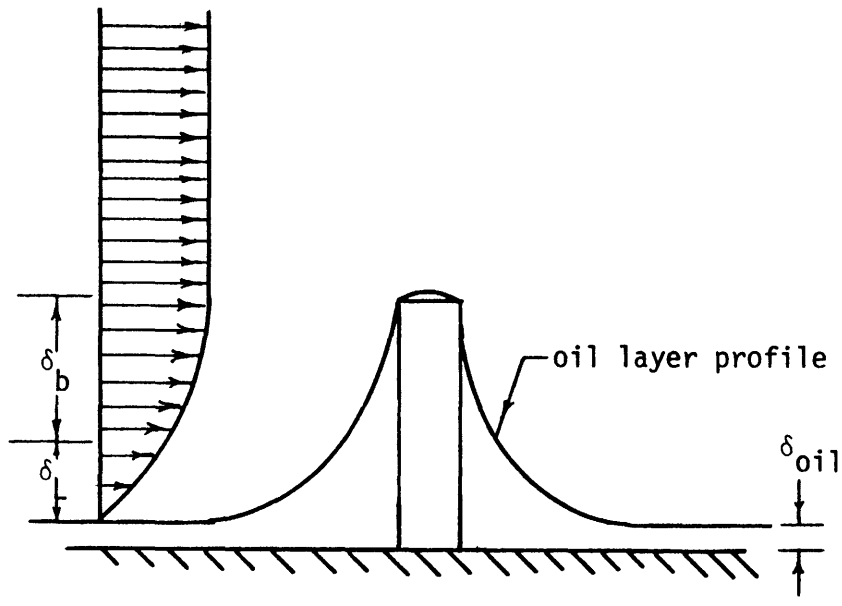

Imagined rib shapes with coating oil layer

e ≃ 0.1"

δ_{oil} ≃ 0.01" - 0.02"

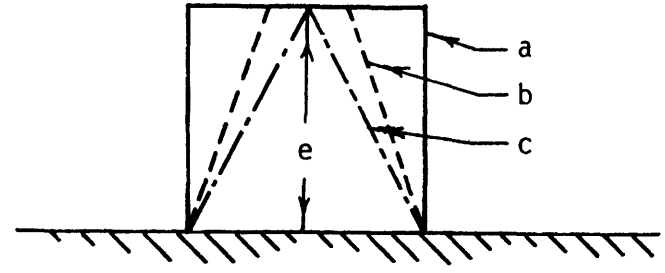

a - rectangular rib shape

b - trapezoidal rib shape

c - triangular rib shape

δ_b - buffer layer

δ_L - laminar sub layer

RIB SHAPE SIMULATION

Figure 43

A simple way to calculate the laminar sublayer thickness in pipes with varying Reynolds number is to use the "universal velocity distribution in smooth pipes" [7]. The universal velocity distribution considers 3 regimes, which are defined as:

$$
\begin{aligned}
&1 \leq y^+ \leq 5, && v^+ = y^+ && \text{laminar sublayer}\\
&5 \leq y^+ \leq 30, && v^+ = -3.05 + 5.0 \ln y^+ && \text{buffer layer}\\
&30 \leq y^+ && v^+ = 5.5 + 2.5 \ln y^+ && \text{turbulent core}
\end{aligned}
\qquad [58]
$$

where

$$y^+ = \frac{y}{\nu}\sqrt{\frac{\tau_o\, g_c}{\rho}} = \frac{y}{D}\,\mathrm{Re}\,\sqrt{f/2}$$

$$v^+ = V/\sqrt{\tau_o/\rho}$$

Assuming repeated ribs don't affect the laminar sublayer thickness, equation [58] could be used to calculate the laminar sublayer thickness and buffer layer thickness by using this three zone velocity distribution. (i.e., calculate the maximum laminar sublayer thickness, using $y^+ = 5$, and the maximum buffer layer thickness with $y^+ = 30$). Figure 44 shows the relative dimensions of the laminar sublayer thickness and rib height for two typical Reynolds number (10^4, 10^6).

Defining

e = rib height

δ_L = laminar sublayer thickness

δ_B = buffer layer thickness

A literature survey (19) yielded the following results:

if $e < \delta_L$ there is no effect on h and f

$e < 2\delta_L$ there is significant change on h and f

$e < \delta_B$ there is a very strong change in h and f. However this change is not a strong function of e, as h and f are relatively constant for

$$\delta_B < e < 8\delta_B.$$

It is important to point out that with $e \simeq \delta_B$, it is expected that h and

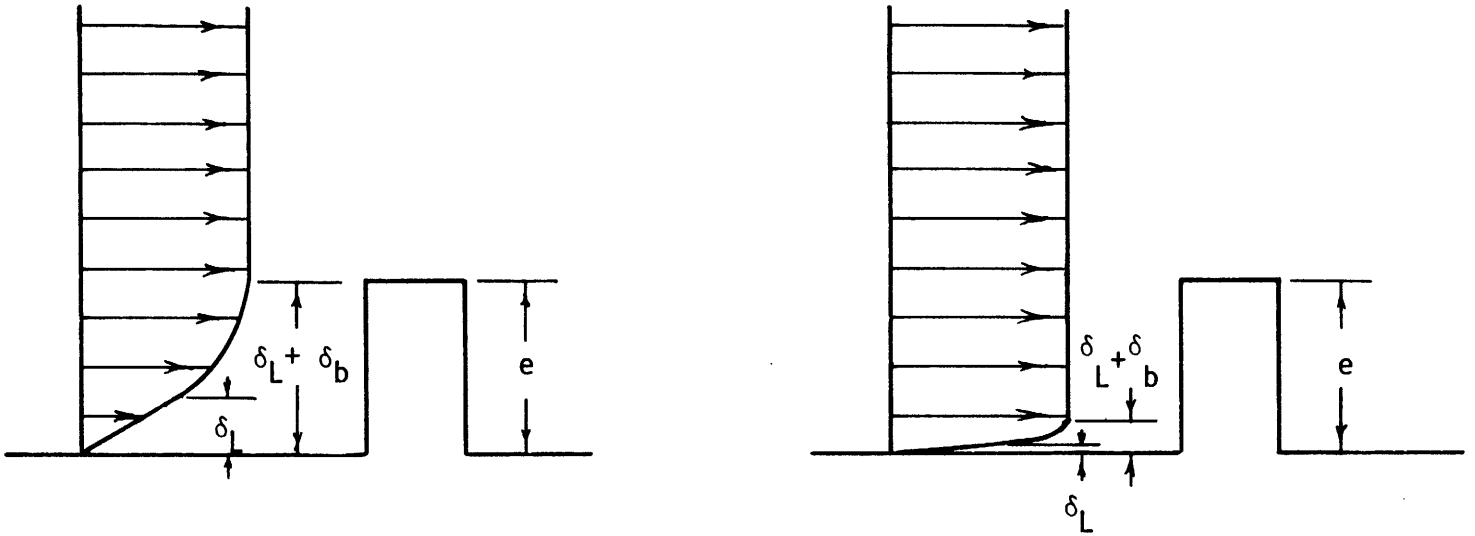

[A] $Re \simeq 10^4$

$\delta_L \simeq 1.6 \times 10^{-2}$ "

$\delta_b \simeq 6\delta_L \simeq 0.1$"

$e \simeq 0.1$"

[B] $Re \simeq 10^6$

$\delta_L \simeq 2.6 \times 10^{-4}$ "

$\delta_b \simeq 0.15 \times 10^{-2}$ "

$e \simeq 0.01$ "

when:

$e < \delta_L$	e has no effect on heat transfer and friction
$e > 2\delta_b$	e has a moderate effect on heat transfer and friction
$e > \delta_b$	e has a significant effect on heat transfer and friction
$\delta_b < e < 8\delta_b$	no significant difference from $e > \delta_b$

in case [A], where $e \simeq \delta_b$, the rib shape may have an effect on both heat transfer and friction

LAMINAR SUB-LAYER THICKNESS

Figure 44

f will be affected by different rib profiles. When $e < \delta_L$ or $e >> \delta_B$, it is not expected that rib shapes will affect h and f, since under these conditions e itself has little effect on h or f [19, 20].

This can also be shown by noting that the formulation of e^+ (equ. 57) and y^+ (equ. 58) are identical, and that equations 55, 56, and 57 hold for $e^+ \geq 30$. From the universal velocity distribution, it can be seen that this is tantamount to saying that this rib extends up into the turbulent core.

From equation [55], if $e^+ \geq 30$ (complete roughness or where the rib height extends beyond the buffer layer thickness), f is independent of Re. This means f is independent of rib profiles too. (The same case may be made for h.) But, if $e^+ < 30$ (which is the incomplete roughness region, or the height of rib is between δ_L and δ_B), f is dependent upon Re, and the degree to which the laminar boundary layer is disturbed is undoubtedly a function of the rib profiles (again, the same case may be made for h).

The real question is whether the optimum design of the rotary heat exchanger will require $e^+ > 30$, or $e^+ < 30$. If $e^+ > 30$ then it is expected that the rib profiles will not have a great affect on h and f. If $e^+ < 30$ then the rib profiles will have an affect on h and f. As reported in last year's report (5), a rib height (e) of about 0.1" and Re of about 10^4 yielded the economic optimum condition. Figure 44 shows that the thickness of the buffer layer (with $Re \simeq 10^4$) is the same order of magnitude as the height of the rib ($e \simeq 0.1$") This indicates that the rib profile is a concern, and that the dependance of h and f on the profile must be determined.

11.3.2.2 The Effect of Flow Attack Angle

A literature survey (21) provided the effect of flow attack angle on heat transfer coefficient and friction factor at very high Reynolds number flows ($Re = 10^5 \simeq 10^6$). However, there are no general correlations which correlate the functional relation between both f, and the angle between rib and flow direction (α).

Its also expected that the effect of α on h and f could be observed at lower turbulent flows ($3 \times 10^3 < Re < 3 \times 10^4$). A test facility has been constructed to experimentally measure heat transfer coefficients as a function of the rib geometry, the various shape parameters, and the angle of attack.

The final correlations of h and f will be expected as the following form:

$f = f(Re, e/D, P/e, \text{Rib shape}, \alpha)$

$h = h(Pr, Re, e/D, P/e, \text{Rib shape}, \alpha)$

II.3.3 Experimental Apparatus

Figure 45 shows the schematic drawing of the experimental apparatus. A blower will drive air at room temperature and pressure through a 4" diameter tube equipped with an ASME square-edge orifice plate to measure flow rates. The next section gradually changes its cross section so that the air entering the test section has a uniform velocity distribution. After the test section, a plexiglass section ducts the air into the atmosphere.

The test section consists of two parallel aluminum plates (60" x 12" x 1/4") that are either smooth (used for calibration) or have ribs machined in the surface. At present, the ribs are square in shape, but trapezoidal and triangular ribs will be tested. Aluminum was used as the test surface because of its high thermal conductivity and good machineability. The dimensions of the plates were chosed for the following reasons: 1/4" thickness to reduce the axial heat conduction to a negligible level, 12" wide so that the opposing plates appear as a pair of infinite parallel plates, and 60" long so that the flow is fully developed in the last half of the test section. Refer to fig. 46 for detailed test section dimensions.

Woven heaters embedded in silicone rubber provide a constant heat flux for the entire test surface. Each aluminum plate has 4 woven heaters (each heater is 6" x 30") with each heater providing a maximum energy of 5 watts/in^2. 4 variacs control the voltage across the heaters. See Figure 47 for details of the heating system.

The blower is capable of providing a range of air velocities through the test channel such that Re can vary between 3×10^3 and 3×10^4. An ASME orifice plate is used to measure the mass flow rate. The pressure drop across the test section is measured using a micromanometer. A potentiometer is used

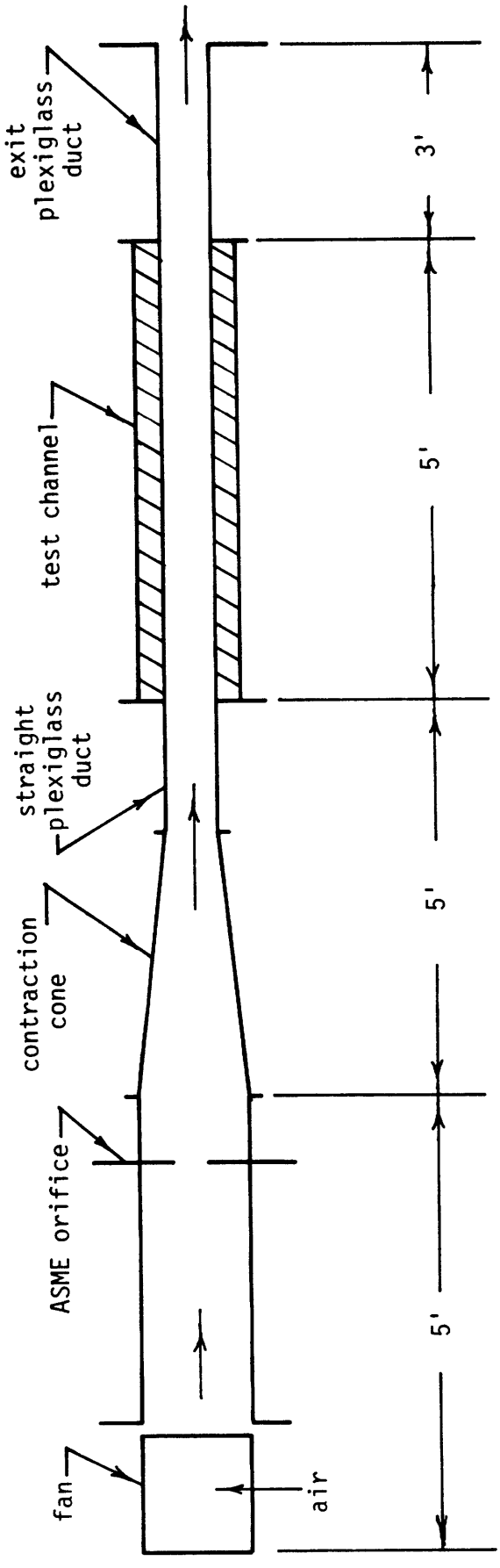

SCHEMATIC OF EXPERIMENTAL APPARATUS
FOR SURFACE ROUGHNESS TESTS

Figure 45

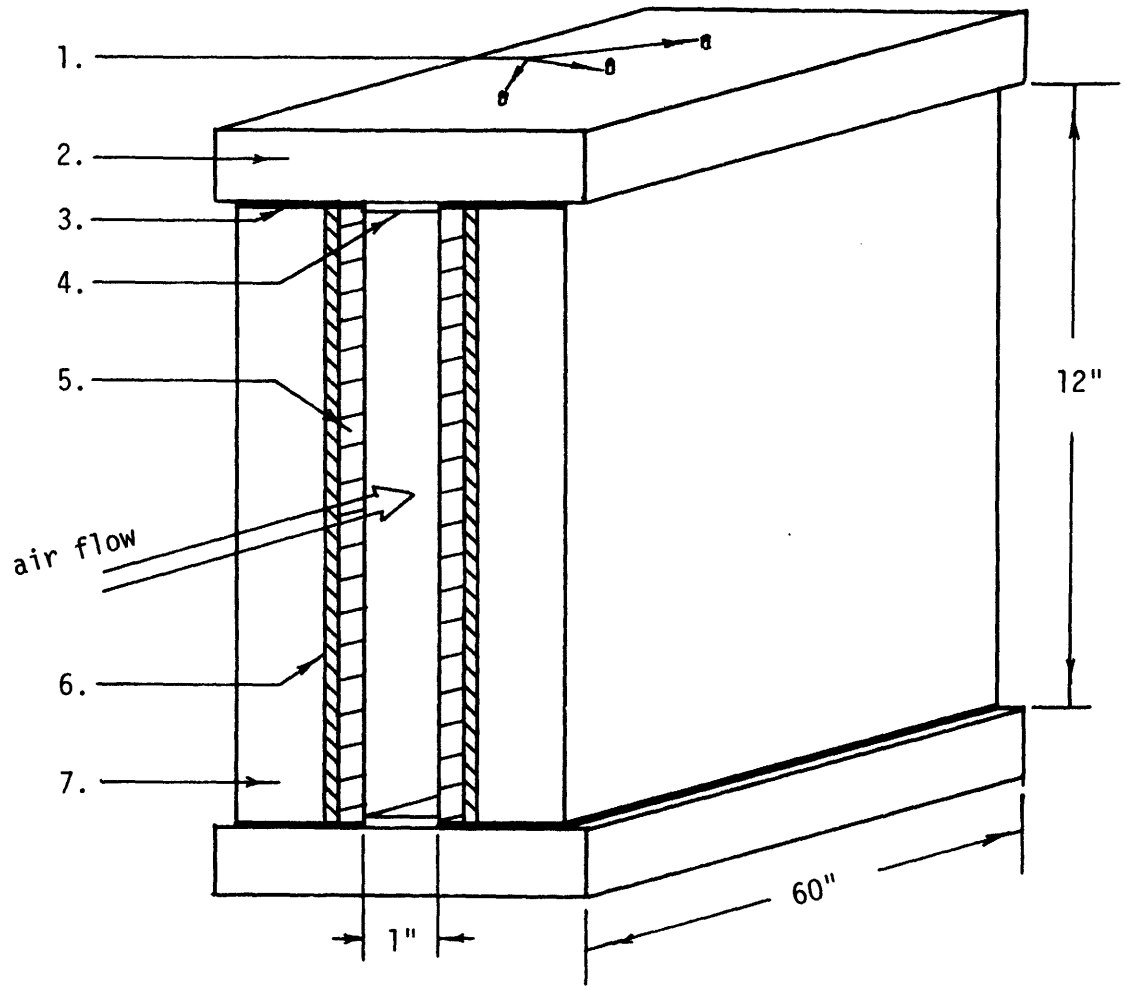

1. pressure taps
2. wood (1"x3"x60")
3. gaskets
4. metal spacer
   (1/4" x 1" x 60")
5. aluminum test surfaces
   (1/4" x 12" x 60")
6. electric heating mats
   (12" x 60")
7. wood (1/2" x 12" x 60")

(after assembly, entire test section is wrapped with insulation)

TEST SECTION CROSS-SECTIONAL VIEW

Figure 46

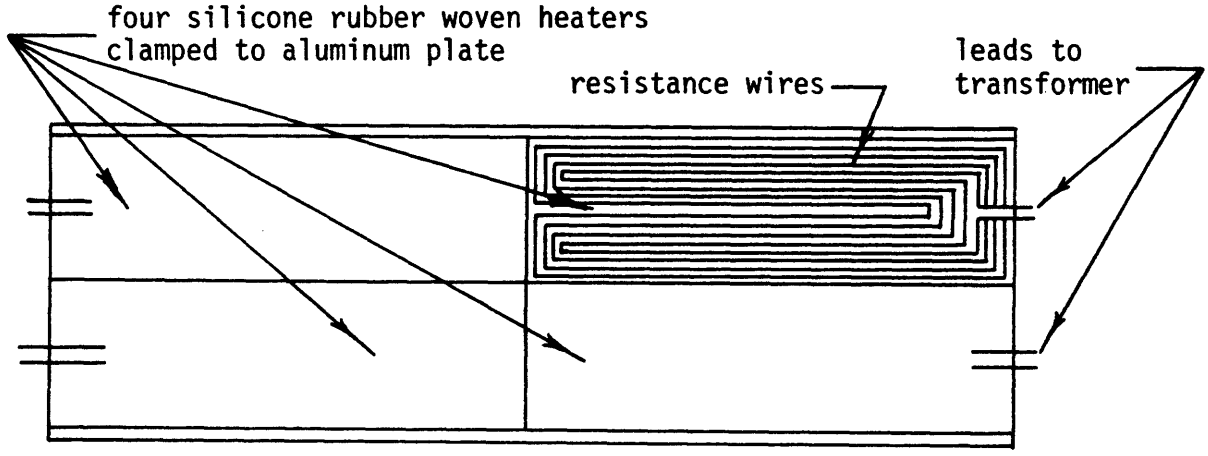

Section A-A

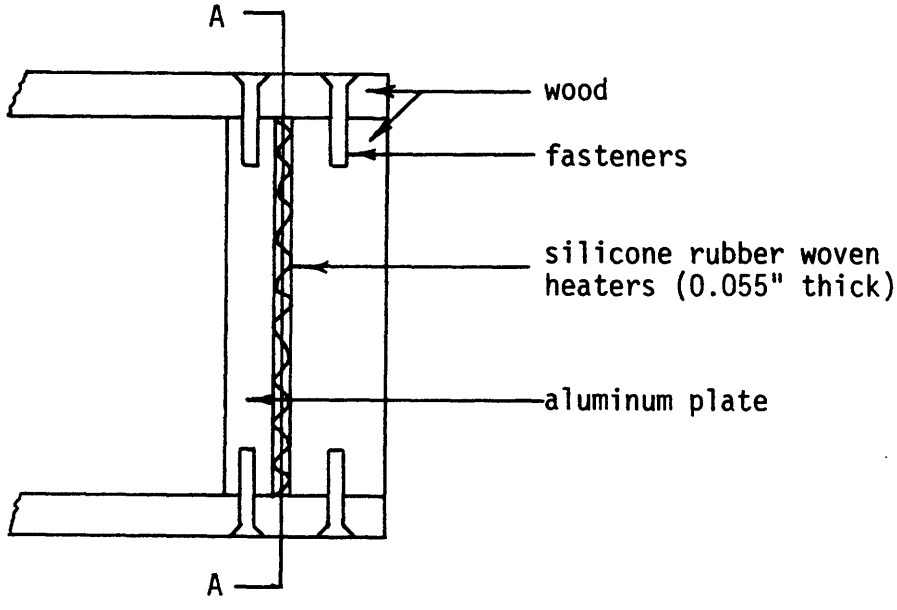

DETAIL OF SILICONE RUBBER WOVEN HEATERS

Figure 47

to measure the EMF of the thermocouples buried in the aluminum plates.

Thermocouples are also used to measure the bulk mean air temperatures entering and leaving the test section. See Figure 48 for the pressure tape and thermocouple locations.

II.3.4 Initial Tests

II.3.4.1 Means of determining the friction factor and heat transfer coefficient.

(a) Friction Factor can be determined by measuring the pressure drop across the flow channel and measuring the mass flow rate of the air ($\dot{m}$). With this data, the friction factor can be calculated as

$$f = \frac{\Delta P}{4 \frac{L}{D} (\bar{\rho}\, \bar{v}^{\,2} / 2g_c)} \qquad [59]$$

where ΔP = Pressure drop across flow channel (psf.)

L = flow channel length (in.)

D = hydraulic diameter of flow channel (in.)

$\bar{\rho}$ = average air density across flow channel (lbm/ft^3)

$\bar{V}$ = average velocity inside flow channel (ft/sec) = $\frac{\dot{m}}{\rho A}$

A = cross section area of test section (Ft^2)

$g_c = 32.2 \ \frac{lbm - ft}{lbf - sec^2}$

(b) heat transfer coefficient can be calculated from:

$$h = \frac{\dot{q}}{A\,(Tw - T_f)} \qquad [60]$$

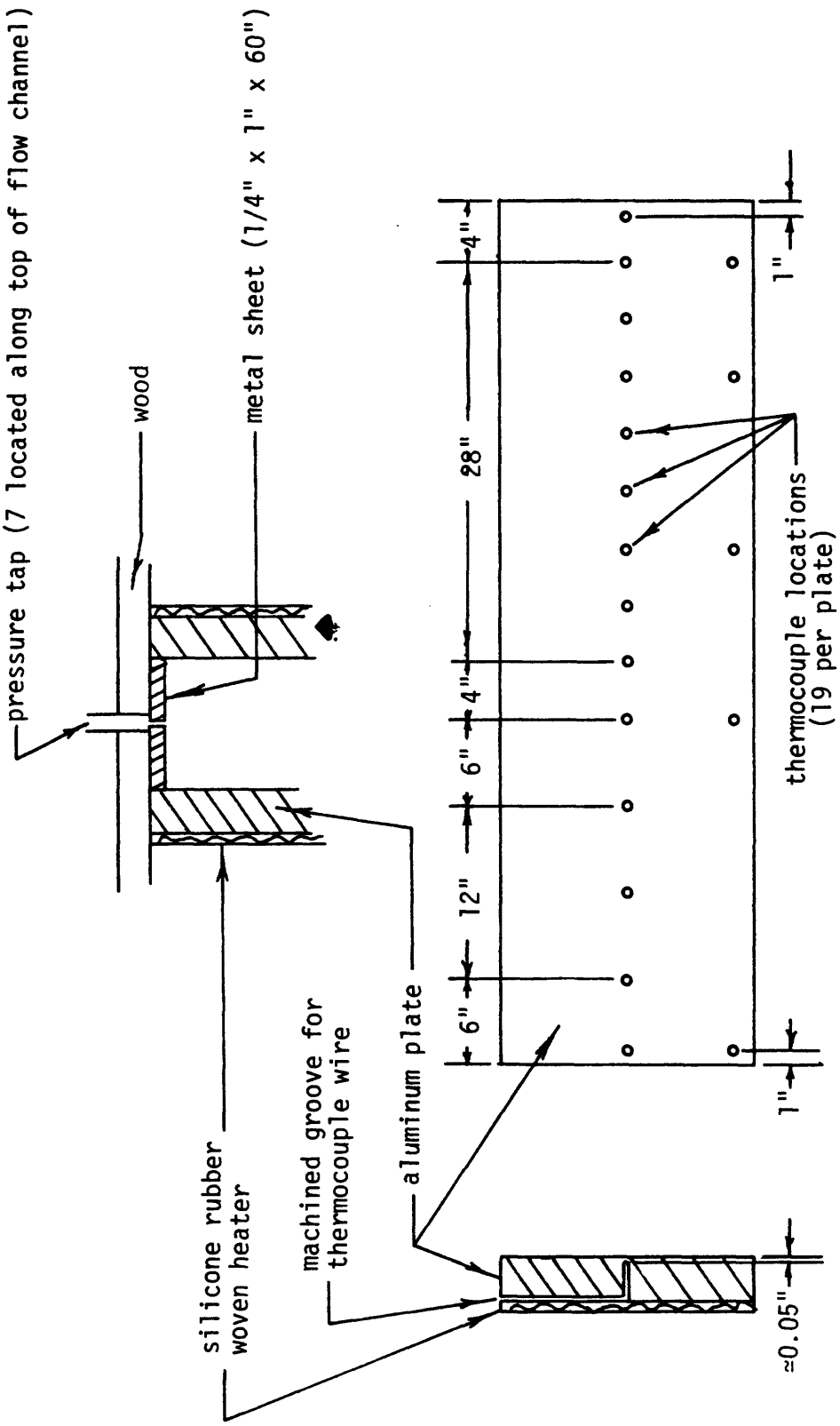

PRESSURE TAPS & THERMOCOUPLE LOCATIONS

Figure 48

where h = heat transfer coefficient, Btu/hr.ft^2°F

$\dot{q}$ = heat transfer rate, (wattage or Btu/hr.)

A = heat transfer surface area, (ft^2)

T_w = wall temperature (°F)

T_f = fluid bulk mean temperature (°F)

There are two ways to establish a value of $\dot{q}$: the heat input equals the wattage dissipated in the heater less the heat losses.

or $\dot{q}$ = (voltage) x (current) - (heat losses) [61]

As the external walls of the heaters are insulated, it is assumed that the heat losses are small. Secondly, a Heat Balance may be performed on the air passing through the test section. Here $\dot{q} = \dot{m} C_p (T_{bo} - T_{bi})$ [62]

where $\dot{m}$ = mass flow rate of air (lbm/hr.)

C_p = specific heat(Btu/lbm °F)

T_{bo} = Outlet bulk mean temperature of air(°F)

T_{bi} = inlet bulk mean temperature of air(°F)

$\dot{q}$ = heat input(Btu/hr.)

Theoretically, equation [61] will equal equation [62].

With a determination of the values of $\dot{q}$, T_w, T_t, A, the heat transfer coefficient can be calculated from equation [60].

II.3.4.2 Initial experimental results

Before initiating a series of experiments with ribbed roughened surfaces, it was important to calibrate and to test the accuracy of the apparatus. This was accomplished by measuring the friction factor and heat transfer coefficient for a smooth plate and comparing the results to accepted correlations for turbulent smooth walled tube flow.

The static pressure distribution was measured by using seven pressure taps along the top flow channel. The typical data were plotted in figure 49 for Re = 7×10^3 to 3×10^4.

The wall temperature distribution was measured by using the 19 thermocouples buried in the aluminum plate. Both plates have identical thermocouple locations to test the symmetric conditions of the flow channel. The typical data is plotted in figure 50 for different Re and $\dot{q}$.

By using equation [59] and figure 49, the friction factor can be calculated. Typical results are shown in figure 51.

By using equation [60] and figure 50, the heat transfer coefficient can be calculated. Typical results are shown in figure 51.

As seen by figure 51, there is good correlation between accepted correlation and experiment results for the smooth plate case.

II.3.4.3 Experimental error and accuracy of measurements.

There is always a certain degree of experimental error resulting from the accuracy of the measuring devices. Following is a brief discussion of the achieved accuracy of measurements and their affect on the experimental results.

(a) Measurement of the air mass flow rate (22)

$$\dot{m} = 0.1145\ D_2^2\ KY\sqrt{\frac{P_1}{T_1}\ Gy\ \Delta p}$$

where

$\dot{m}$ = mass flow rate, lbm/sec

D_2 = orifice diameter, in.

K = Flow coefficient, dimensionless.

Y = expansion factor, dimensionless

P_1 = static pressure before orifice, in Hg absolute.

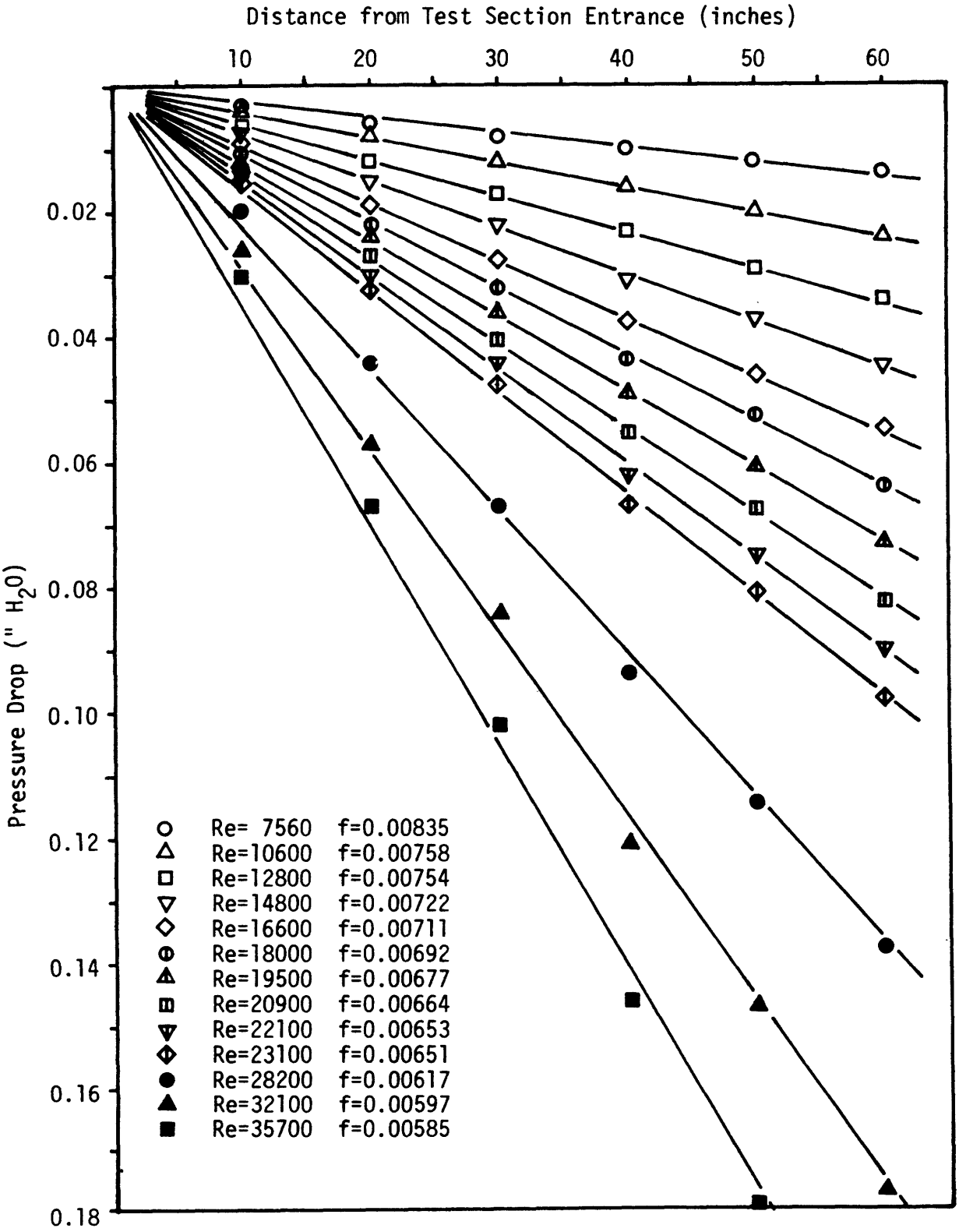

PRESSURE DROP ACROSS TEST SECTION

Figure 49

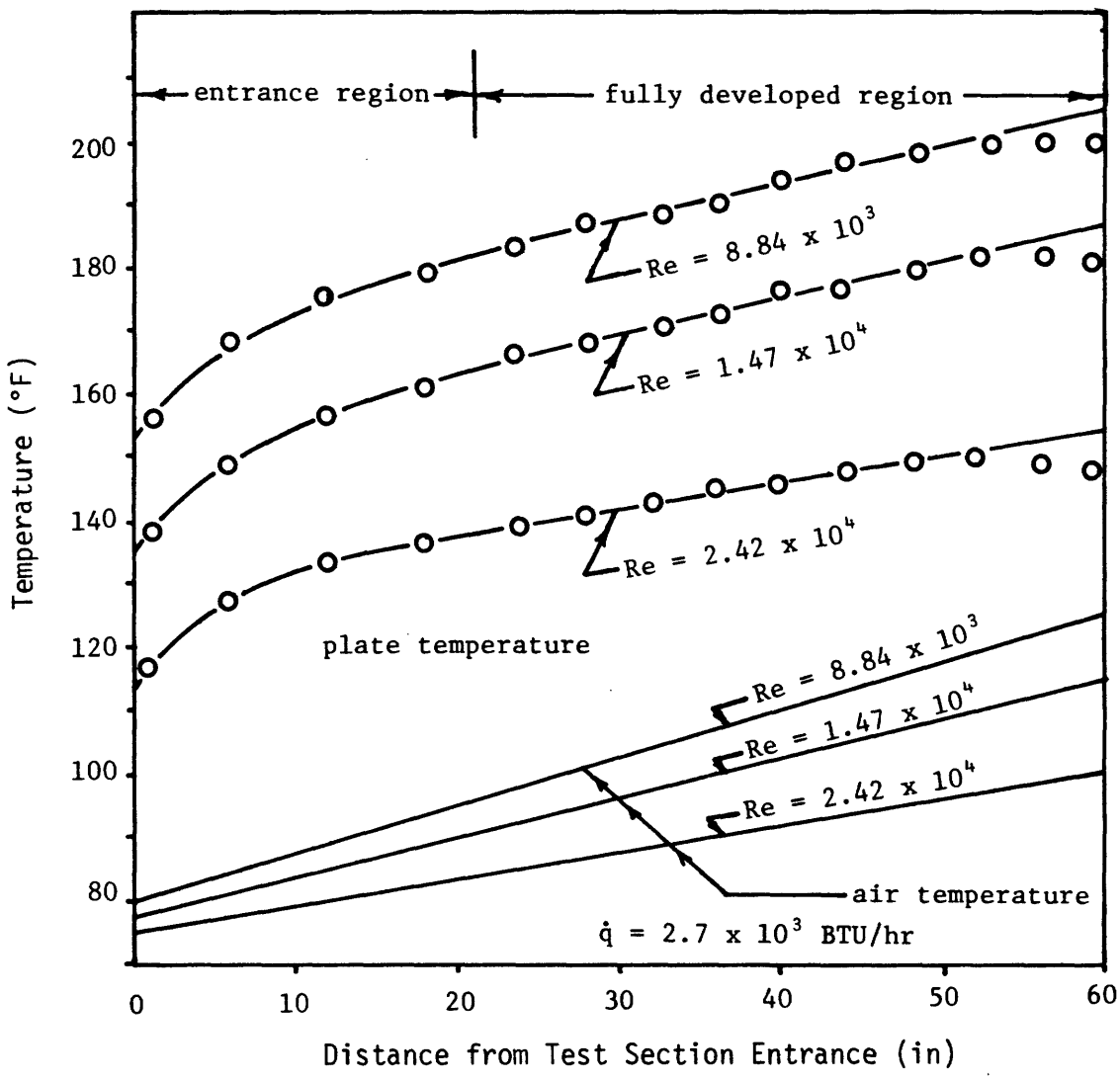

TEMPERATURE DISTRIBUTION ALONG ALUMINUM SURFACE

Figure 50

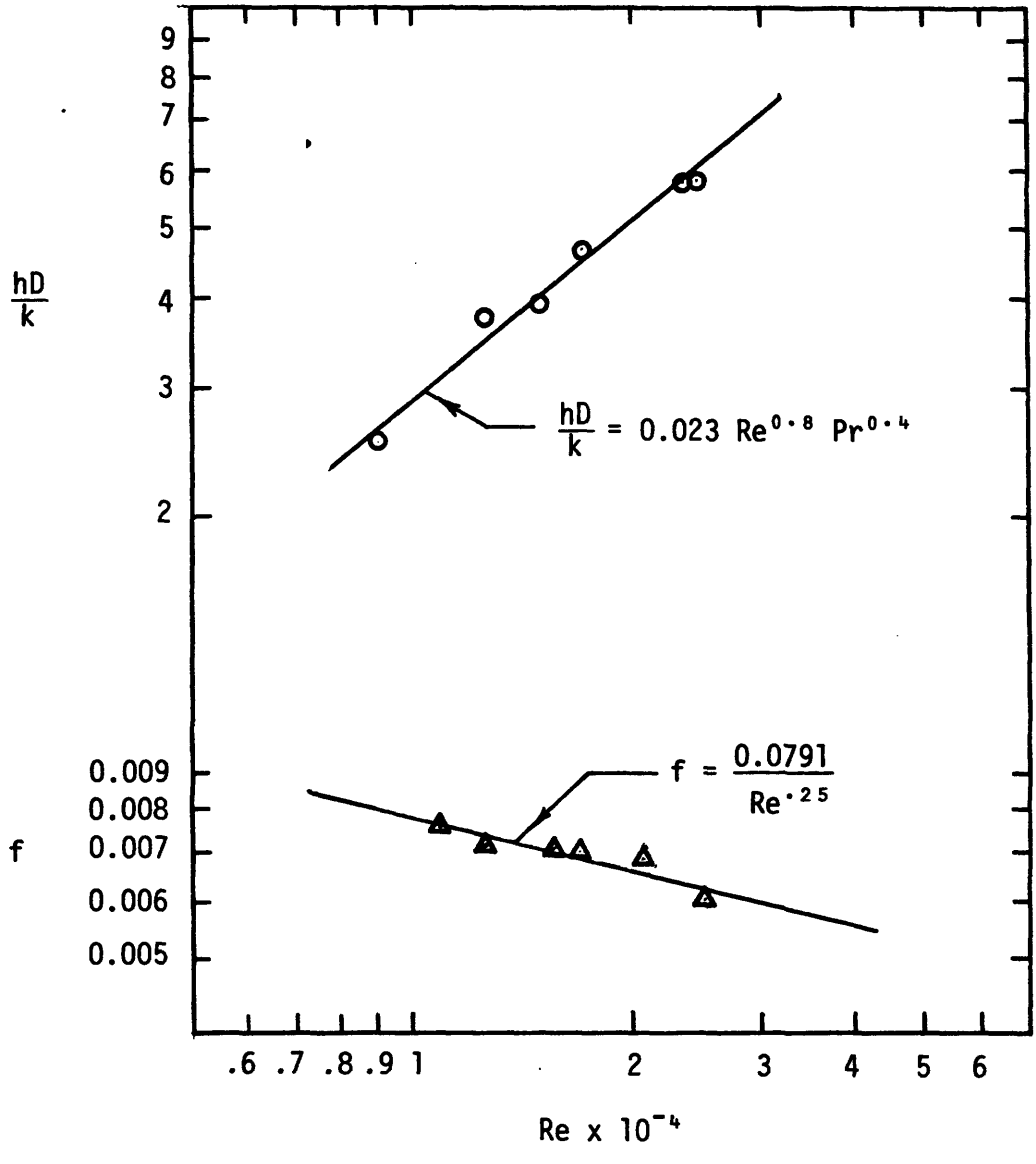

RESULTS OF SMOOTH SURFACE CALIBRATION TESTS
Comparison of Data with Accepted Correlations

Figure 51

T_1 = Temperature before orifice, °R

G = specific gravity of gas, for air G = 1

y = supercompressibility factor, dimensionless.

ΔP = pressure drop across orifice, in inches H_2O. Measured by inclined monometer accurate to within $\pm$ 0.001" H_2O

According to [22], if $\frac{\Delta P}{P_1} \leq 0.2$, the uncertainty will be about $\pm$ 0.5%.

In our case, $\frac{\Delta P}{P_1} \sim 0.01$ or less. Therefore, the uncertainty is exceedingly small. With an accurate reading of ΔP the air mass flow rate is used in determining the local Reynold's number. The Reynolds number is also a function of the flow area, and the local flow area is known if the aluminum plates are indeed parallel and flat. In order to prevent the plates from bending when they are heated up, the heat flux is limited such that $\dot{q} \leq 300$ watts/heater

(b) Pressure drop across test section

Because the friction factor is proportional to the pressure drop across the test section, the accurate measurement of pressure drop is very important.

The data in figure 49 was measured using an inclined manometer with an accuracy of $\pm$ 0.001" H_2O. By using a micromanometer this accuracy can be increased to $\pm$ 0.0001" H_2O.

(c) Temperature measurements.

Temperature measurements by thermocouples are accurate to within $\pm$.5°F. Because the heat transfer coefficient is inversely proportional to $(T_w - T_f)$, it is important to maintain the temperature difference between the wall and fluid sufficiently high (~ 50°F) so as to not have the thermocouple accuracy strongly affect the calculated heat transfer coefficient.

(d) Minimization of Heat Losses.

As previously noted, an accurate determination of h necessitates that q be accurately measured. This meakes it important to minimize or numerically account for all heat losses. The method employed on the present apparatus is to minimize heat losses by heavily insulating the test apparatus.

(e) Overall Accuracy of f & h

- friction factor

The friction factor is determined using equation [59]

where V is determined from $V = \frac{\dot{m}}{\rho A}$

therefore
$$f = \frac{\Delta P}{4 \frac{L}{De} \frac{\dot{m}^2}{2\rho g_c A^2}} \qquad [63]$$

It is the accuracy of the measured components which determines the overall accuracy. From the preceeding sections, and assuming that linear measurements are accurate to within .01 inch, the percent error of each measured component of eq. [63] is listed in Table 3.

Table 3

Component		Max % Error
ΔP		5
m		.5
L		.05
D_e		1
A:	length	.1
	width	1

Therefore, in accordance with the method of ref. 27 the maximum error in the friction factor is:

$$\% \text{ error} = [5^2 + 2(.5^2) + .05^2 + 1^2 + 2\,(.1^2 + 1^2)]^{\frac{1}{2}} = 5.34\%$$

- Heat Transfer Coefficient

The heat transfer coefficient is determined using either equation [61] or [62] in equation [60].

Table 4 lists the percent errors of the measured quantities used in the determination of h. These values assume: (1) volt meter and ammeters are accurate to within 2%; (2) temperature differences can be measured to within 1°F; (3) linear measurements are accurate to within .01", and (4) the losses in equation [61] are 4%.

Table 4

Component	Max % Error
q: (eq. 61) V	2
I	2
losses	4
q: (eq. 62) m	.5
$T_{bo} - T_{bi}$	5
A: length	.02
width	.1
$T_w - T_f$	2

Again, using the method of reference 27, the overall error in h using equation [60] & [61] is:

$$\% \text{ error} = [2^2 + 2^2 + 4^2 + .02^2 + .1^2 + 2^2]^{\frac{1}{2}} = 5.29\%$$

and the total error in using equation [60] and [62] is:

$$\% \text{ error} = [.5^2 + 5^2 + .02^2 + .1^2 + 2^2]^{\frac{1}{2}} = 5.41\%$$

II.3.5 Program for testing rib roughened surfaces.

The initial experimental test results for smooth surface have shown that the experimental apparatus is accurate and can reproduce accepted data. The apparatus is now to be used in a series of tests on rib roughened surfaces. The following are the parameter variations to be made in the series of tests. In all tests, the Re will be varied between 3×10^3 and 3×10^4.

a. Similarity tests:

with $\alpha=90°$, square rib shape, & $\frac{P}{E}=5$

vary $\frac{e}{D}$: $\frac{e}{D}$ = 0.1, 0.05, 0.025

b. Non-similarity tests:

with $\alpha=90°$, square rib shape, & $\frac{e}{D}$ = 0.05

vary $\frac{P}{E}$: $\frac{P}{E}$ = 5, 10, 20

c. Non-similarity tests:

with $\alpha=90°$, $\frac{e}{D}$ = 0.05, $\frac{P}{E}$ = 10

vary rib shape: rib shape = square, trapezoidal, triangular

d. Non-similarity tests:

with square rib shapes, $\frac{e}{D}$ = 0.05, & $\frac{P}{E}$ = 10

vary α: α = 90°, 45°, 0°

II.4 Contacts with other Utilities and Architects/Engineers

A series of meetings was held in April, 1975 with architect-engineering firms engaged in the design or study of dry cooling towers and with a utility building a large plant with a dry cooling tower. The meetings were set up by Air Preheater representatives who attended along with L.R. Glicksman from MIT. The purpose of the meetings was to get opinions on the rotary concept as a viable design for large dry towers and to judge when dry cooling towers would be needed for large power plants. The architect/engineers visited were: Stone and Webster in Boston, responsible for the design of the 330 MgW plant with dry cooling at Wyodak, Wyoming; Sterns - Roger in Denver, responsible for the small (20 MgW) dry cooled plant in Wyoming; R. W. Beck in Denver, author of a number of studies on dry cooling towers sponsored by the AEC, ERDA and the utilities; Bechtel Power Corp. in San Francisco; and Pacific Power and Light in Portland, Oregon, part owner of the Wyodak plant.

A list of atendees at the meeting is included in appendix A and a list of detailed comments is also given there. A summary of the comments is presented below.

On the use of dry towers in general, all of the participants felt that the choice of dry versus wet towers was strictly a matter of water availability and overall costs. All groups except Bechtel felt that dry towers were economically justifiable for some sites in the west now or within the next decade. The combination of wet and dry towers looks like a good intermediate design which saves water consumption while not penalizing plant performance as much as a totally dry tower. A combined system might actually use physically separated wet and dry towers.

All participants stressed the need for dry towers with good reliability, maintainability, long life in utility applications and which occupied as little land area as possible. There was an uncertainty whether any of the present designs would meet these dry tower requirements.

Confidence will not be developed in any of the designs until a reasonable amount of utility operating experience is accumulated.

Key problems with dry towers are freeze-up during starting at very low ambient temperatures and longevity of finned heat exchanger surfaces.

Specifically on the rotary concept, no one rejected it out of hand. Rather, they felt that as with all concepts there is a need to demonstrate reliability and performance. If it is less expensive and reliable, as demonstrated by a full scale cell test, it would be a preferred choice. The ability of the rotary tower to run as a dry or wet tower, when the oil film is removed, was appealing. General questions which must be resolved are: dust entrainment in the oil and oil cleanup, complications of disc rotational drives, oil entrainment in very high winds, and rotary arrangement to minimize land use while allowing easy access for rotar maintenance and removal.

III. Conclusions and Recommendations

Based on the results of the small scale testing, the following four conclusions and recommendations can be made:

1. Silicone oil, having a very low vapor pressure, has a negligible evaporation rate under the operating conditions of the periodic tower. However, silicones have three potentially detrimental aspects: (1) high capital costs, (2) potentially high damage to the turbine blading if they are leaked into boiler feed water loop, and (3) the unknown ecological effect of admitting silicones to the atmosphere, even at relatively low rates. Consequently, it is recommended that further hydrocarbon oils be investigated to ascertain their applicability to the periodic cooling tower. The use of hydrocarbon oils would mean a higher operating cost (due to their higher evaporation rate) but their costs are significantly lower, and the ecological impact of unburned hydrocarbons in the atmosphere is fairly well understood and can be delt with.

2. The operation of the full-scale periodic cooling tower at 5 rpm is not anticipated to have oil churning problems.

3. Equation 6 gives a good estimate of the oil film heat transfer resistance for the 20 inch model. This is verified by the good agreement between the water side heat transfer coefficient given by equation 6 and the experimental value.

4. The theoretical analysis in Section II.1.1.2 gives fair predictions of the heat transfer coefficients and heat transfer. Improvements in the theory are expected to yield more accurate predictions.

The full scale test apparatus is completed and fully instrumented. Full sized discs that are structurally self supporting and cause minimal turbulence with the floating oil layer can be made by 'dishing' flat discs. Eight such discs have been fabricated and assembled into a test module. This module is also fully instrumented with thermocouples.

The oil thickness distribution on the full sized discs has been determined for the operating temperature of the heat exchanger at 4 RPM. The effects of different RPM on thickness have also been examined and it is now possible, from data at 4 RPM, to approximate the oil layer distribution at other RPM values by extrapolation. Heat transfer performance calculations should now be able to proceed.

As for thickness distributions on interior discs, it would be appropriate to assume that it is nearly the same as on the outer discs measured. This is

a good assumption provided that enough oil is used in the tank. The way it is designed now, the inner discs seem starved of oil on the down rotation side especially if a large enough quantity ($\cong$ 5 gallons) of oil is not used. A baffle system could be designed which would channel oil to all the discs more evenly. As it is presently designed, oil piles up in great quantities on the $\theta = 180°$ position and because of the proximity of the tank wall to the disc, the oil works against the motion of the disc as it flows back to the $\theta = 0°$ position. The narrowness of this channel restricts the backflow greatly. In fact, the amount of oil covering the water at $\theta = 0°$ is 1/4 inch or less at 4 RPM with 4.5 gallons of oil in the tank. A baffle system would greatly increase the oil supply in this $\theta = 0°$ region and eliminate the backing up of oil at the $\theta = 180°$ position. Also, since the best performance of the exchanger requires as thin a layer of oil on the water that can be maintained unbroken, a more even distribution of oil by baffle would mean a smaller quantity of oil could be used.

For high Reynolds' flows and particular geometries, the augmentation of heat transfer by surface roughening has been experimentally verified and correlated by various investigators. To evaluate the augmentation for Reynolds' flows and geometries representative of the periodic tower, an experimental apparatus has been constructed, instrumented, and calibrated. It is expected that for the operational conditions of the periodic tower, augmentation will depend not only upon rib height, disc spacing, and rib spacing, but also upon rib shape and the angle at which the air approaches the rib. The test apparatus has been designed to allow a parametric study of these variables.

The architect engineers who were contracted this year felt the rotary concept has merit if reliability and cost advantages over a conventional design could be established. No one expressed the attitude that since the design is new and unusual the industry will not accept it. This is in part due to the fact that doubts are held concerning so called conventional designs.

REFERENCES

1. Jones, W. J., "Natural Draft Cooling Towers", Hamon-Cottell, Inc., 1968.

2. Dickey, J. B. Jr., and R. E. Cates, "Managing Waste Heat with the Water Cooling Tower", The Marley Company, 1970.

3. Glicksman, L. R., "Thermal Discharge from Power Plants", ASME Paper No. 72-WA/Ener-2, 1972.

4. Robertson, M. W., Glicksman, L. R., and Rhosenow, W. M., "Improvement of the Environmental and Economic Characteristics of Cooling Towers, Part II: Periodic Cooling Towers", MIT, Heat Transfer Lab report number 80047-82, June, 1973.

5. Hon, P. C., Han, Je-Chin, Pilger, P. F., Glicksman, L. R., and Rohsenow, W. M., "Improvement of the Environmental and Economic Characteristics of Cooling Towers Part II of II: The Periodic Cooling Tower- Flow Visualization, Surface Roughening, and Full Scale Model", Energy Lab report number MIT-EL 74-008, MIT, June, 1974.

6. Levich, V. G., Physiocochemical Hydrodynamics, Prentice-Hall, Englewood Cliffs, New Jersey, 1967.

7. Rohsenow, W. M., and Choi, H. Y., Heat, Mass and Momentum Transfer, Prentice-Hall, New Jersey, 1961.

8. Noll, W., Chemistry and Technology of Silicones, Academic Press, New York, 1968.

9. Kays, W. M., Convective Heat and Mass Transfer, McGraw-Hill, New York, 1966.

10. Roark, R. J., Formulas for Stress and Strain, McGraw-Hill, New York, 1965.

11. Bouma, A. L., Hass, A. M., Shell Research, Interscience Publishers, New York, 1961.

12. Temperature Measurement Handbook, Omega Engineering, Inc., Stamford, Conn., 1974.

13. Atlantic Research Systems Division (A Division of the Susquehanna Corporation), Recovery of Floating Oil by Rotating Disc Type Skimmer, for the Water Quality Office, EPA 15080 FWM. July 1971.

14. Sward, C. G. and Gardner, Paing Testing Manual, ASTM Technical Publication 500, ASTM, Philadelphia, PA, 1972.

15. Murt, E. M. and Guldner, W. G., Physical Measurement and Analysis of Thin Films, Plenum Press, New York, 1969.

16. Francon, M., Modern Applications of Physical Optics, Interscience Publishers, New York, 1963.

17. Sabersky, R. H., Acosta, A. J., Haptmann, E. G., Fluid Flow, The MacMillan Co., New York, 1971.

18. R. L. Webb, E. R. Eckert and R. J. Goldstein, "Heat Transfer and Friction in Tubes with Repeated-Rib Roughness", Int. J. Heat Mass Transfer, Vol. 14, pp. 601-617, 1971.

19. A. Bhattacharyya, "Heat Transfer and Pressure Drop with Rough Surfaces, a Literature Survey", Engineering Library Qc323.B575, May 1964.

20. W. J. White and L. White, "The Effect of Rib Profile on Heat Transfer and Pressure Loss Properties of Transversely Ribbed Roughened Surfaces", papers collected by A. E. Bergles, "Augmentations of Convective Heat, Mass Transfer", 1970.

21. L. White and D. Wilkie, "The Heat Transfer and Pressure Loss Characteristics of some Multi-Start Ribbed Surfaces", papers collected by A. E. Bergles, "Augmentations of Convective Heat, Mass Transfer", 1970.

22. W. A. Leary and D. H. Tsai, "Metering of Gases by Means of the ASME Square-edged Orifice with Flange Taps", Sloan Lab. for Automotive and Aircraft Engines, MIT, July 1951.

23. General Electric, "Silicones", Technical Data Book S-9D, Silicone Products Department, Waterford, New York, 1970.

24. General Electric, "Silicones", Technical Data Book S-10B, Silicone Products Department, Waterford, New York, 1970.

25. Burington, Richard Stevens, Handbook of Mathematical Tables and Formulae, Handbook Publishers, Inc., Sandusky, Ohio, 1955.

26. Pilger, Paul Fred, "Design and Construction of a Periodic Heat Exchanger", Master of Science Thesis, MIT Department of Mechanical Engineering, 1974.

27. Holman, J. P., Experimental Methods for Engineers, McGraw-Hill, New York, 1971.

Appendix A

Summary of Utility and A/E Contacts - Trip of April 16, 17, 18 Accompanying Air Preheater Representatives Written by Leon R. Glicksman

Stearns-Rodger, Denver

Jerry Mounts (Supervisor System & Equipment Group)
Joe Parce (Responsible for small (20 MgW) Black Hills Dry Tower)
S.T. Shary
W.H. George
J.L. Winter
R.J. Holland
S.A. Zambolla
Hank Osborne (Air Preheater)
Gene Krumm (Air Preheater)
Leon Glicksman

General on Dry Towers:

Choice of towers - strictly a matter of water availability
Projected future costs of water in West up to $1000/acre foot. *Alternatively water may not be available at any price.
Capital costs of dry tower twice wet tower
Direct Condensing Dry - Size Limited
There are problems with direct contact condensors, although conventional condensors surfaces sacrifice ΔT.
Currently looking at (designing with?) wet/dry towers which reduce water consumption 60 to 80% over wet towers.
Wet/Dry costs more than straight dry and has problem of tube corrosion etc., but eleviates summer capacity loss of pure dry tower.
Severe problem with dry start up during very cold conditions.
General impression: in the West dry towers seem inevitable in next decade or two.

Comments on our design: General Questions

Put towers in round configuration instead of linear
Problem of dirt, large debris caught on oil surface
Temperature effect of oil viscosity, especially at low temperatures
Key-reliability, put in duplicate drives rather than a few contralized drives.
Possible metal imbrittlement at low temperatures
Concentrate on building one test cell as a standard.

General - open minded about new concept; need to demonstrate reliability and performance. If it is cheaper and reliable it will be chosen before the others.

---

*For a Fossil Fuel Plant with a Conventional Wet Tower using water at $1000/acre foot, makeup water for the tower would cost 1.5 mils/KW hr.

R.W. Beck and Co.

John Rossie
Bob Mitchell
Hank Osborne
Gene Krumm
Leon Glicksman

General - They don't seem to have a good feel on equipment design details; more experience in general simulation, general trends, etc.

By 1980 dry towers will be included in some power plant designs at arid sites or for new additions to power parks where no more water is available. Key question is the longevity and reliability of finned surfaces, the best looks like GEA galvanized.
For wet/dry towers they suggested physically separating the two to reduce surface corrosion, etc.
No detailed comments on rotary. If it works and is cheaper it may be the way to go.
Suggest demonstration on small existing plant. Get ERDA to support the new concept, possibly a plant in N.Y. state.

Bechtel Power Corporation, San Francisco

R.M. Jensen
Tom Hamilton (Cooling Tower Expert)
J.W. Brown
J.P. Dieden
B. Bornstein
Ron Gibson
Hank Osborne (Air Preheater)
Gene Krumm (Air Preheater)
Bob Hinton (Air Preheater)
Leon Glicksman

Hamilton feels that air cooled towers are a ways off - the cost is too excessive - four to five times the capital cost of wet (he says). It is still cheaper for utilities in the West to bring water to the plant than use dry towers.

A very frank discussion of the rotary tower was held with the understanding that they were going out of their way to point out possible problems. There was no concensus that the design in general will not work or is at first look unacceptable. However, there was the stress on reliability, maintainability, and long life for utility applications.

Possible Problems:

Head loss of air through entries to rotors
Dirt entrainment in oil, cleaning of basins
Seismic design problems (not necessarily important)
Oil scum formation after disc stopped
Dirt buildup on oil layer
Methods of rotor removal to replace or service

Possible Problems (continued):

Oil entrainment in very high winds, up to 60 MPH say
Possible costs versus conventional dry towers; Hamilton has costs on letter he will send me. He claims these costs are rather low.

Other comments:

Direct condensing dry towers are limited to 200 Mg or less.
Proposed coal gasification plants will use air cooling.
Land area for fossil fuel dry tower 8 acres for 800 MgW plant,
11 acres 1200 MgW nuclear plant.

Many people voiced strong concern if this concept needed more land area than other dry towers.

Pacific Power & Light, Portland, Oregon

P.G. Humphreys (V.P., Key decision maker)
Gary Larson (Project Leader on Wyodak Plant)
Ed Anderson
Jack Stitis
Marvin S. Lang
Thomas M. Ashton
Hank Osborne (A.P.)
Gene Krumm (A.P.)
Bob Hinton (A.P.)
Leon Glicksman

They gave general comments, referred to Stone and Webster for detailed technical comments. They feel West (e.g. Upper Colorado) has very restrictive water supplies and in the future utilities may have great troubles getting water rights. In the past utilities purchased ranches or farmlands to obtain their water rights; this will be prohibited in the future. Humphreys also suggested that in 20 to 25 years the utilities may even be forced to retrofit older plants with dry towers to conserve water.

If the economics justify it, as at Wyodak, they will use dry towers. They were not concerned about high back pressure turbines - they felt this was not a major problem, rather Westinghouse and others overplayed it.

Key problems of dry towers were summer loss of capacity, freeze up, general economics.

They feel air coolers developed and used in the petrochemical industry has too short a life (5 to 10 years) for their needs (30 years). Did not feel confident to say that present designs (e.g. Hudson) had the required life.

On the rotary design they stressed reliability, maintainability, and l[illegible] ea problems. They suggested a demonstration model (at least one full [illegible]zed cell) on a power plant should be run. They don't feel ten years of operating experience is needed but that a few years of demonstration without any significant operating problems would be required. Again they didn't give any negative reaction to the concept per se and indicated that if the total costs (including maintainance) were less than conventional dry towers, that the rotary would be preferred choice.

They along with others seemed to like the idea that the tower could be run wet in the summer by removing the oil layer. They suggested test data on the wet operation would be helpful.

Appendix B

Data from Full Sized Disc Film Thickness Measurements

First Apparatus Results

	r (in)	Q (ml/min)	δ (mils)	$\delta_{modified}$ (mils)
Run 1:	5 RPM, 67°F, θ = 0°, 1 gallon oil			
	27	110	4.0	3.94
	27	147	5.3	5.25
	27	90	3.2	3.23
	27	110	4.0	3.94
	27	130	4.7	4.65
	21	265	12.3	11.72
	21	270	12.5	11.93
	21	260	12.0	11.52
	19	280	14.3	13.43
	19	267	13.6	12.87
	15	250	17.3	14.71
	15	260	18.0	15.21
	11	200	18.5	15.37
	27	100	3.6	3.59
Run 2:	5 RPM, 129°F, θ = 0°, 1 gallon oil			
	27	190	6.8	6.67
	27	180	6.1	6.33
	21	240	11.1	10.32
	21	250	11.6	10.69
	19	240	12.3	11.17
	19	260	13.3	11.95
	15	230	15.6	12.80
	15	240	16.6	13.23
	11	190	17.6	13.46
Run 3:	5 RPM, 129°F, θ = 0°, 2 gallons oil			
	27	170	6.1	6.00
	27	190	6.8	6.67
	11	230	21.3	15.37
	19	270	13.8	12.33
	19	275	14.1	12.51
	15	270	18.7	14.47

r (in)	Q (ml/min)	δ (mils)	$\delta_{modified}$ (mils)
Run 4: 5 RPM, 129°F, θ = 0°, 2 gallons oil			
27	155	5.6	5.48
27	160	5.8	5.66
19	250	12.8	11.56
11	210	18.5	14.44
11	205	18.1	14.20
Run 5: 8 RPM, 129°F, θ = 0°, 2 gallons oil			
27	385	8.7	8.45
19	540	17.2	15.44
11	390	21.5	17.20
Run 6: 2.75 RPM, 129°F, θ = 0°, 2 gallons oil			
27	75	4.9	4.79
19	105	9.8	8.79
19	110	10.2	9.13
11	75	12.0	9.75
11	80	12.8	10.21

Second Apparatus Results

r (in)	Q (ml/min)	δ (mils)	$\delta_{modified}$ (mils)	δ_{Levich} (mils)
Run 1: 4 RPM, 58°F, θ = 180°, 4 gallons oil				
11	60	6.62	6.84	8.57
13	110	10.27	11.03	12.74
13	90	8.40	8.79	12.74
15	140	11.33	12.23	15.54
15	150	12.14	13.29	15.54'
17	180	12.85	14.05	17.84
17	190	13.57	15.04	17.84
19	235	15.01	16.88	19.86
21	290	16.76	19.27	21.72
21	280	16.19	18.35	21.72
23	325	17.15	19.54	23.44
23	320	16.89	19.13	23.44
25	365	17.72	20.12	25.07
27	410	18.43	20.93	26.71
27	415	18.66	21.29	26.71

	r (in)	Q (ml/min)	δ (mils)	$\delta_{modified}$ (mils)
Run 2:	4 RPM, 58°F, θ = 150°, 4 gallons oil			
	11	65	7.17	7.41
	13	100	9.34	9.80
	15	145	11.74	12.58
	17	190	13.57	14.78
	19	235	15.02	16.53
	21	300	17.34	19.64
	23	335	17.68	19.85
	23	360	19.00	21.92
	25	405	19.70	22.61
	27	415	18.66	20.77
Run 3:	4 RPM, 58°F, θ = 135°, 4 gallons oil			
	11	65	7.17	7.36
	13	110	10.27	10.77
	15	140	11.92	11.33
	17	215	15.35	16.80
	19	245	15.65	17.00
	21	300	17.34	19.06
	23	360	19.00	21.14
	25	385	18.70	20.48
	27	325	14.61	15.30
Run 4:	4 RPM, 58°F, θ = 120°, 4 gallons oil			
	11	65	7.17	7.30
	15	165	13.35	14.03
	19	290	18.53	20.10
	23	350	18.47	19.69
	27	265	11.92	12.16
Run 5:	4 RPM, 58°F, θ = 90°, 4 gallons oil			
	11	80	8.83	8.83
	13	165	15.41	15.41
	15	250	20.23	20.23
	17	275	19.64	19.64
	19	305	19.49	19.49
	21	290	16.76	16.76
	23	285	15.04	15.04
	25	260	12.63	12.63
	27	200	8.99	8.99

r (in)	Q (ml/min)	δ (mils)	$\delta_{modified}$ (mils)
Run 6: 4 RPM, 58°F, θ = 60°, 4 gallons oil			
11	200	22.07	19.57
13	250	23.35	20.80
15	265	21.45	19.60
17	270	19.28	18.02
19	265	16.93	16.12
21	250	14.45	13.97
23	240	12.67	12.37
25	215	10.44	10.28
27	155	6.97	6.92
Run 7: 4 RPM, 58°F, θ = 30°, 4 gallons oil			
11	230	25.38	20.44
13	240	22.41	19.03
15	245	19.83	17.54
17	250	17.85	16.25
19	250	15.97	14.87
21	240	13.87	13.18
23	220	11.61	11.22
25	185	8.98	8.81
27	140	6.29	6.24
Run 8: 4 RPM, 58°F, θ = 0°, 4 gallons oil			
11	220	24.28	19.40
13	235	21.95	18.41
15	240	17.01	17.01
17	240	17.14	15.52
19	240	15.33	14.22
21	230	13.30	12.60
23	210	11.08	10.69
25	180	8.74	8.56
27	130	5.85	5.79

Runs at Operating Temperature (second apparatus)

Frontside

r (in)	Q (ml/min)	δ (mils)	$\delta_{modified}$ (mils)
Run 1: 4 RPM, 129°F, θ = 180°, 3.5 gallons oil			
11	45	4.97	5.21
15	110	8.90	10.24
19	175	11.18	13.72
23	240	12.67	15.99
27	230	10.34	11.35

	r (in)	Q (ml/min)	δ (mils)	$\delta_{modified}$ (mils)
Run 2:	4 RPM, 129°F, θ = 135°, 3.5 gallons oil			
	11	50	5.52	5.75
	15	105	8.50	9.18
	19	185	11.82	13.55
	23	240	12.67	14.37
	27	165	7.42	7.64
Run 3:	4 RPM, 129°F, θ = 90°, 3.5 gallons oil			
	11	60	6.62	6.62
	15	165	13.35	13.35
	19	200	12.78	12.78
	23	185	9.76	9.76
	27	130	5.85	5.85
Run 4:	4 RPM, 129°F, θ = 45°, 3.5 gallons oil			
	11	140	15.48	12.88
	15	175	14.16	12.46
	19	170	10.86	10.14
	23	145	7.65	7.42
	27	105	4.72	4.67
Run 5:	4 RPM, 129°F, θ = 0°, 3.5 gallons oil			
	11	150	16.55	12.90
	15	170	13.76	11.74
	19	170	10.86	9.91
	23	140	7.39	7.10
	27	100	4.50	4.44

Backside

Run 1:	4 RPM, 129°F, θ = 180°, 3.5 gallons oil			
	11	60	6.62	7.28
	15	120	9.71	11.71
	19	175	11.18	13.72
	23	245	12.93	16.75
	27	220	9.89	10.75
Run 2:	4 RPM, 129°F, θ = 135°, 3.5 gallons oil			
	11	60	6.62	7.04
	15	130	10.52	12.07
	19	195	12.46	14.53
	23	260	13.72	16.01
	27	165	7.42	7.63

r (in)	Q (ml/min)	δ (mils)	$\delta_{modified}$ (mils)
Run 3: 4 RPM, 129°F, θ = 90°, 3.5 gallons oil			
11	80	8.83	8.83
15	175	14.16	14.16
19	195	12.46	12.46
23	190	10.03	10.03
27	100	4.50	4.50
Run 4: 4 RPM, 129°F, θ = 45°, 3.5 gallons oil			
11	150	16.55	13.62
15	170	13.76	12.21
19	180	11.50	10.68
23	150	7.92	7.67
27	90	4.05	4.02
Run 5: 4 RPM, 129°F, θ = 0°, 3.5 gallons oil			
11	160	17.66	13.56
15	175	14.16	12.05
19	170	10.86	9.93
23	145	7.65	7.34
27	80	3.60	3.57

RPM Variation Runs

r (in)	Q (ml/min)	θ (degrees)	$\delta_{modified}$ (mils)	$\frac{\delta_{modified}}{\sqrt{RPM\ r}}$ $\left(\frac{mils\ sec^{.5}}{in^{.5}}\right)$
Run 1: 2 RPM, 58°F, 4.0 gallons oil				
19	90	180	13.34	2.160
25	130	180	14.38	2.030
19	100	90	12.78	2.070
25	60	90	5.83	0.824
Run 2: 4 RPM, 58°F, 4.0 gallons oil				
19	240	180	17.36	1.990
25	330	180	17.64	1.760
19	265	90	16.93	1.940
25	190	90	9.23	0.923
Run 3: 6 RPM, 58°F, 4.0 gallons oil				
19	450	180	21.74	2.040
25	430	180	14.50	1.180
19	455	90	19.38	1.820
25	320	90	10.36	0.846

Appendix C:

PROPERTIES OF SILICONE OIL

In CGS system units the properties of SF-96 oil are [23]:

surface tension σ= 20.8 dynes/cm

density ρ = .953grams/cm^3 @ 25°C

kinematic viscosity $\nu = 20x10^{-2}$ cm^2/sec = 20 centistokes

absolute viscosity $\mu = \rho\nu = (.953)(20x10^{-2})$ dyne-sec/cm^2

$= 19.06x10^{-2}$ poise @ 77°F

= 19.06 centipoise @ 77°F

The viscosity-temperature coefficient VTC is defined as the following:

$$VTC = 1 - \nu_{@210°F}/\nu_{@100°F} \qquad (C1)$$

For SF-96 the VTC = .58.

The Versilube fluids (a trademark of General Electric) in general the $\log_{10}$ of viscosity (kinematic) is roughly linear with the $\log_{10}$ of temperature (in °F) for small temperature ranges [24]. Then if VTC = .58, then $\nu_{@210°F}/\nu_{@100°F} = .42$ from equation C1. If we assume linearity, then the slope m of the graph plotting $\log_{10}\nu$ vs. $\log_{10}$ T(°F) is given by

$$m = (\log\nu_{@210°F} - \log\nu_{@100°F})/(\log 210°F - \log 100°F)$$

Then

$$m = (\log (\nu_{@210°F}/\nu_{@100°F}))/(\log(210/100))$$

$$= -1.169$$

Then ν is related to T in this temperature range by

$$\log(\nu_{@T}/\nu_{@77°F}) = -1.169\log(T/77°F) \qquad (C2)$$

Using this relation, then

$$\log(\nu_{@129°F}/\nu_{@77°F}) = -.2620$$

or

$$\nu_{@129°F}/\nu_{@77°F} = .547$$

Then

$$\nu_{@130°F} = (.547)(20\times10^{-2}) = 10.94\times10^{-2} \text{ stokes}$$

In a similar manner by solving equation C2, we obtain

$$\nu_{@58°F} = 27.85\times10^{-2} \text{ stokes}$$

Using $\mu = \rho\nu$

$$\mu_{@129°F} = 10.43\times10^{-2} \text{ poise}$$

$$\mu_{@58°F} = 26.54\times10^{-2} \text{ poise}$$

Appendix D:

CUBIC EQUATION SOLUTIONS

For the cubic equation

$$x^3 + ax + b = 0$$

real valued closed form solutions depend according to reference [25] on the value of the discriminant D defined as

$$D = b^2/4 + a^3/27$$

For $0° \leq \theta < 90°$ where θ is the angle of the measurement taken, D is always positive because a is positive. The real positive root for this case is given by

$$x = 2\sqrt{a/3}\ \text{ctn}\ 2\phi$$

where

$$\text{ctn}\ 2\psi = \sqrt{\frac{b^2}{4} / \frac{a^3}{27}}$$

and

$$\tan\phi = \sqrt[3]{\tan\psi}$$

When $90° < \theta \leq 180°$, D is negative for all the experimental measurement points and the real positive root is given by

$$x = 2\sqrt{-a/3}\ \cos(\phi/3 + 240°)$$

where

$$\cos\phi = -\sqrt{\frac{b^2}{4} / \frac{a^3}{27}}$$

Appendix E

OIL FLOW RATE & THICKNESS AS PREDICTED BY LEVICH'S ANALYSIS

By Levich's analysis [6], oil thickness on a plate that is being pulled with a velocity v_0 out of oil is given by

$$\delta = \frac{\sqrt{\mu v_0}}{\rho g} \quad f\left(\frac{\mu v_0}{\sigma}\right) \tag{E.1}$$

where

$$f\left(\frac{\mu v_0}{\sigma}\right) = .93\left(\frac{\mu v_0}{\sigma}\right)^{1/6} \quad \text{for} \quad \frac{\mu v_0}{\sigma} << 1$$

or

$$f\left(\frac{\mu v_0}{\sigma}\right) = 1 \quad \text{for} \quad \frac{\mu v_0}{\sigma} >> 1$$

For the rotary heat exchanger, the extreme value of $\frac{\mu v_0}{\sigma}$ occurs at the rim ($r = 2.5$ft.) where the withdrawal speed is highest. Then for 4 RPM at a temperature of 58°F

$$\frac{\mu v_0}{\sigma} = (26.54\times10^{-2})(4\times2\pi/60)(2.5\times12\times2.54)/(20.8)$$
$$= 4.07\times10^{-1}$$

which satisfies the conditions of $\frac{\mu v_0}{\sigma} << 1$. Then δ is given by

$$\delta = \frac{\sqrt{\mu v_0}}{\rho g} \quad (.93)\left(\frac{\mu v_0}{\sigma}\right)^{1/6} \tag{E.2}$$

Using equation E.2 a thickness distribution can be determined along the $\theta=180°$ position. For v_0, the vertical component of velocity at the oil level was used. This velocity is

$$v_0 = \omega r \cos\alpha \tag{E.3}$$

where

$$\cos\alpha = \sqrt{r^2 - 25.4^2/r} \tag{E.4}$$

α is the angle that each radius makes with the horizontal where the radius intersects the oil layer. Equation E.4 assumes that the oil level is 10 inches (25.4 cm.) below the axis of disc rotation. Substituting equations E.3 & E.4 into E.2 one obtains

$$\delta = \left(\frac{\mu}{\rho g}\right)^{1/2} (.93) \left(\frac{\mu}{\sigma}\right)^{1/6} \omega^{2/3} (r^2 - 25.4^2)^{1/3} \qquad \text{(E.5)}$$

which expresses δ as a function of radius. If the assumption is made that the thickness distribution changes by small amounts from the oil level to the θ=180° position, then equation E.5 expresses the thickness distribution at θ°=180 position. Equation E.5 is used in the calculation of Levich predicted values in Figure 42.

For the integration of δ to find total Q_T, α was assumed to be small on the average giving

$$v_o = \omega r \qquad \text{(E.6)}$$

Substituting equation E.6 into E.2 yields

$$\delta = \left(\frac{\mu}{\rho g}\right)^{1/2} (.93) \left(\frac{\mu}{\sigma}\right)^{1/6} (\omega r)^{2/3} \qquad \text{(E.7)}$$

To find Q_T integrate the product of the oil velocity and the thickness over the radius. This is

$$Q_T = \int_{r_1}^{r_2} v_o \, \delta \, dr \qquad \text{(E.8)}$$

Substituting equations E.7 and E.6 into E.8 yields

$$Q_T = \int_{r_1}^{r_2} (\omega r)^{5/3} \left(\frac{\mu}{\rho g}\right)^{1/2} (.93) \left(\frac{\mu}{\sigma}\right)^{1/6} dr \qquad \text{(E.9)}$$

Integrating E.9 yields

$$Q_T = K \, r^{8/3} \Big|_{r_1}^{r_2}$$

where

$$K = \frac{3}{8}\omega^{5/3}\,(.93)\left(\frac{\mu}{\sigma}\right)^{1/6}\left(\frac{\mu}{\rho g}\right)^{1/2}$$

Using oil properties in Appendix C for a temperature of 58°F,

$$K = 6.661\text{x}10^{-4}\ (\text{cm})^{9/8}(\text{sec})^{-1}$$

Then

$$Q_T = (6.661\text{x}10^{-4})r^{8/3} \qquad \begin{vmatrix} r_2 = (28)(2.54) \\ r_1 = (10)(2.54) \end{vmatrix}$$

$$Q_T = 5.41\text{x}10^{1}\ \text{cm}^3/\text{sec}$$

Appendix F:

OIL FLOW RATE PREDICTED BY EPA STUDY

From page 93 of the EPA study [13], the dimension-less oil depth is $\bar{d}$ defined as

$$\bar{d} = d\sqrt{\rho g/\sigma}$$

Using a depth of oil of about 1 in.

$$\bar{d} = (2.54)\sqrt{(.953)(981)/(20.8)} = 17.02$$

which is much greater than 1. Because $\bar{d} >> 1$, the curve on page 94 of reference 13 that corresponds to $\bar{d} = \infty$ can be used. As a limiting case, this is a good approximation of $\bar{d} = 17.1$.

Then calculating the dimensionless rotational speed, $\bar{\omega}$ using a chord length of 50 inches for the oil level, we obtain

$$\bar{\omega} = .679$$

For this small $\bar{\omega}$, the assumption of the limiting case where $\bar{d} = \infty$ proves to be a good one. This can be seen by observation of the graph on page 94 of reference 13. Then continuing

$$\log \bar{\omega} = 0.168$$

Using the graph, the $\bar{Q}$ corresponding to this $\bar{\omega}$ is

$$\bar{Q} = 2.238 \times 10^{-2}$$

From the definition of $\bar{Q}$ one can solve for Q_T obtaining

$$Q_T = \bar{Q}\, C(\sigma/\mu)/\sqrt{\rho g/\sigma}$$

Using oil properties at 58°F, we obtain

$$Q_T = 37.6 \text{ cm}^3/\text{sec}$$